



PONTIFICIA UNIVERSIDAD CATOLICA DE CHILE
ESCUELA DE INGENIERIA

ANALYSIS OF SOLAR TRACKING SYSTEMS FOR PHOTOVOLTAIC POWER PLANTS CONSIDERING EXPERIMENTAL AND COMPUTER MODELED RESULTS FOR MUNICH, GERMANY

HARALD FRINDT

Thesis submitted to the Office of Research and Graduate Studies in partial fulfillment of the requirements for the Degree of Master of Science in Engineering

Advisor:

RODRIGO ESCOBAR M.

Santiago de Chile, July 2009

© 2009, Harald Frindt



PONTIFICIA UNIVERSIDAD CATOLICA DE CHILE
ESCUELA DE INGENIERIA

ANALYSIS OF SOLAR TRACKING SYSTEMS FOR PHOTOVOLTAIC POWER PLANTS CONSIDERING EXPERIMENTAL AND COMPUTER MODELED RESULTS FOR MUNICH, GERMANY

HARALD FRINDT

Members of the Committee:

RODRIGO ESCOBAR

JUAN DIXON

AMADOR GUZMÁN

ANDRÉS GUESALAGA

Thesis submitted to the Office of Research and Graduate Studies in partial fulfillment of the requirements for the Degree of Master of Science in Engineering

Santiago de Chile, July 2009

ACKNOWLEDGMENTS

At this point I would like to acknowledge the support of both advisors who guided me throughout my work: Dr. Markus Spinnler of the Technical University of Munich and Dr. Rodrigo Escobar of the Pontific Catholic University of Chile.

I would like to thank Dr. Spinnler for letting me work with him in Germany as a foreign student in such an interesting topic and for guiding me throughout the complete research process of this thesis at the *Technische Universität München*.

My gratitude also goes to Dr. Rodrigo Escobar for supporting my stay in Munich and being my advisor at the *Pontificia Universidad Católica de Chile*.

Further, I would like to thank my parents for supporting me during the two years I spent in Germany, as well as for the whole education time which lead to this work.

I would also like to show my gratitude to the people who made it possible for me to go to Germany and supported me during my stay.

CONTENTS

Acknowledgments	iv
Contents	v
List of Tables	viii
List of Figures	x
List of Symbols and Acronyms	xiv
Abstract	xvii
Resumen	xviii
 1 Introduction	 1
1.1 Motivation	2
1.2 Investigation Outline	3
1.1.1 Hypothesis	3
1.1.2 Research Outline	3
1.1.3 Research Contribution	4
 2 Current State	 5
2.1 Solar Energy	5
2.1.1 Power Sources	5
2.1.2 Solar Energy at the Present Time	7
2.1.3 Concepts on solar radiation	9
2.2 Solar Tracking Systems	11
2.2.1 Solar Tracking Mechanisms	11
2.2.2 Performance Studies	13
2.2.3 Brief Review of the Solar Industry	16
2.3 Photovoltaic Plants at the Technical University of Munich	18
2.3.1 The Fixed Solar Plant MW-5	18
2.3.2 The 2-Axis tracked Plant VIAX	20
2.3.3 The Meteorological Center of the LMU at Garching	23

2.4	Present State of Computer Simulations.....	24
2.4.1	The Standard Reference Year	24
2.4.2	Computer Simulation Problems.....	25
2.5	The Climate at Munich.....	28
3	Methodology.....	31
3.1	Calibration of Sensors	31
3.2	Improvements made to the Power Plants	33
3.2.1	The MW-5 Plant	33
3.2.2	The VIAX Plant	33
3.3	Data Measurement.....	36
3.3.1	Calibration of the Power Plants	36
3.3.2	Measurement Period and Weather Conditions	36
3.3.3	The MW-5 Plant	37
3.3.4	The VIAX Plant	38
3.4	Computer Simulations.....	39
3.4.1	The INSEL Simulation Program.....	39
3.4.2	Simulation Models of the Existing Power Plants	40
3.4.2.1	FH Model - Fixed Plant with Horizontal Radiation as Input Data.....	47
3.4.2.2	FT Model - Fixed Plant with Tilted Radiation as Input Data	47
3.4.2.3	NH Model - Two Axis Tracking with Horizontal Radiation as Input Data.....	48
3.4.2.4	NT Model - Two Axis Tracking with Tilted Radiation as Input Data.....	49
3.4.3	Other Tracking Mechanisms.....	50
4	Results and Analysis.....	53
4.1	Measured Data with the power plants at Munich.....	53
4.2	Simulated Data for the plants at Munich.....	72
4.3	Comparison of Experimental and Simulated Data.....	77
4.4	More Solar Tracking Systems.....	89
4.5	More results related to the Simulations.....	96
4.5.1	The Batman Effect	96
4.6	Application Options in Chile.....	98

4.7	Economic Evaluation	100
5	Conclusions and Further Work	103
5.1	Main Conclusions.....	103
5.2	Additional Comments	105
5.3	Recommendations for Further Research	106
	References	109
	A P P E N D I X E S	111
	Appendix A: Data Sheet of the solar modules installed at the MW-5 and VIAX power plants	112
	Appendix B: Summary of the Radiation Data Used for the Simulations	116
	Appendix C: Sensors Description	119
	Appendix D: Simulation Description	121
	Appendix E: Experimental Assembly	128

LIST OF TABLES

Table 2-1: Energy gain estimations of the solar industry (kWh/kWp). Information by author	16
Table 3-1: Calibration results of the radiation and temperature sensors	32
Table 3-2: Input Range of the SB 700 inverters.....	34
Table 3-3: Weather Condition of the days during the measurement period from October 20 th until December 3 rd 2008	37
Table 3-4: Four simulation combinations, using two different approaches with two power plants each	41
Table 3-5: INSEL blocks represented by the flow chart on Figure 3-3	42
Table 4-1: Calibration information on a cloudy and a sunny day for the MW-5 and the VIAX power plants, and the parameters of the linear regression	54
Table 4-2: Measurement results of representative days for the measurement period (October 20 th to December 3 rd 2008) commented with the selected days	57
Table 4-3: Measurement results for November 5 th , 2008.....	64
Table 4-4: Measurement results for November 6 th , 2008.....	68
Table 4-5: Measurement results for October 25 th , 2008.....	70
Table 4-6: Irradiance measurement losses with photovoltaic detectors compared to pyranometers	71
Table 4-7: Measurement results for the simulated models.....	73
Table 4-8: Error comparing the simulated results to the experimental results, November 6 th , 2008	84
Table 4-9: Error comparing the simulated results to the experimental results, October 25 th , 2008	87
Table 4-10: Simulated irradiation and irradiance values for September 1 st	91
Table 4-11: Yields of the different tracking systems and gains on irradiation and AC energy.....	94
Table 4-12: Yields of the different tracking systems and gains on irradiation and AC energy, new STR	95

Table 4-13: Simulated yields of the different tracking systems and gains on irradiation and AC energy for Santiago and Punta Arenas, Chile. Data: 1995	99
Table 4-14: Economical Evaluation of the different power plants.....	101

LIST OF FIGURES

Figure 2-1: Evolution of world total primary energy supply (WBGU, 2003).....	6
Figure 2-2: Local solar irradiance averaged over three years from 1991 to 1994 (24 hours a day), taking into account the cloud coverage available from weather satellites (Loster, 2006)	7
Figure 2-3: Installed power capacity of Solar PV in the world (REN21, 2009)	8
Figure 2-4: Some tracking mechanisms (by Canova et al., 2007).....	11
Figure 2-5: Energy gain using tracking systems (Huld et al., 2008).....	13
Figure 2-6: Energy gain using tracking systems (Narvarte & Lorenzo, 2007)	15
Figure 2-7: West wing of the MW-5 solar power plant	18
Figure 2-8: East wing of the MW-5 solar power plant.....	18
Figure 2-9: Scheme of the MW-5 power plant	19
Figure 2-10: Sunny SensorBox at the MW-5 power plant	19
Figure 2-11: Schema of the VIAX tracking mechanism (Bauer et al., 2005)	21
Figure 2-12: VIAX power plant	21
Figure 2-13: VIAX power plant	21
Figure 2-14: Example of how the upper bars of the tracking mechanism generate shadow on the solar panels	22
Figure 2-15: Comparison of the diminished power generated by the VIAX and a conventional 2-Axis power plant without the shadow problem.....	23
Figure 2-16: Pyranometer	24
Figure 2-17: Global horizontal, diffused horizontal and global tilted with 2-axis tracking radiation for the 27th of May 2005 from measured values (Bernal, 2007, p.48).....	25
Figure 2-18: Extraterrestrial, global horizontal and simulated global tilted with 2-axis tracking radiation for the 1 st of September using the SRY (Bernal, 2007, p.50)	26
Figure 2-19: Two axis tracking mode simulated with INSEL and TRNSYS using as input data a fictitious day. (Bernal, 2007, p.53).....	27

Figure 2-20: Climate Chart for Munich	29
Figure 3-1: New electrical panel for the VIAX power plant.....	35
Figure 3-2: Power generated by each side of the VIAX and the ideal scenario without the shadow effect, calculated with the 2-inverter system	35
Figure 3-3: Flow Chart of the general case using the horizontal radiation, ambient temperature and wind speed as input data	42
Figure 3-4: Flow Chart of the general case using the global tilted radiation and the module temperature	46
Figure 3-5: Scheme of the FH model.....	47
Figure 3-6: Scheme of the FT model	48
Figure 3-7: Scheme of the NH model	49
Figure 3-8: Radiation sensors the VIAX power plant.....	49
Figure 3-9: Scheme of the NT model.....	50
Figure 3-10: Scheme of the simulation model for all tracking mechanisms using the TRY as input data	51
Figure 4-1: Power generated by each side of the VIAX during a sunny day (October 18 th , 2008) with no tracking operation, using the 2-inverter configuration	56
Figure 4-2: Irradiance levels measured at November 5 th , 2008 in Garching at Munich	59
Figure 4-3: Temperatures measured at November 5 th , 2008 in Garching at Munich.....	60
Figure 4-4: Wind speed measured at November 5 th , 2008 in Garching at Munich.....	61
Figure 4-5: Power generation measured at November 5 th , 2008 in Garching at Munich.....	61
Figure 4-6: Comparison factor (F) for both power plants measured at November 5 th , 2008 in Garching at Munich.	63
Figure 4-7: Irradiance levels measured at November 6 th , 2008 in Garching at Munich	66
Figure 4-8: Temperatures measured at November 6 th , 2008 in Garching at Munich.....	66
Figure 4-9: Power generation measured at November 6 th , 2008 in Garching at Munich.....	67
Figure 4-10: Irradiance levels measured at October 25 th , 2008 in Garching at Munich	68

Figure 4-11: Temperatures measured at October 25 th , 2008 in Garching at Munich	69
Figure 4-12: Power generation measured at October 25 th , 2008 in Garching at Munich	69
Figure 4-13: Simulation Results for November 5 th , 2008	74
Figure 4-14: Simulation Results for November 6 th , 2008	75
Figure 4-15: Simulation Results for October 25 th , 2008	76
Figure 4-16: Comparison of irradiance levels for measured data and simulation results on a tilted surface, November 5 th , 2008 in Garching at Munich.....	77
Figure 4-17: Comparison of irradiance levels for measured data and simulation results on a tracked surface, November 5 th , 2008 in Garching at Munich	78
Figure 4-18: Temperatures of measured data and simulation results, November 5 th , 2008 in Garching at Munich	79
Figure 4-19: Comparison of power generation levels for measured data and simulation results on tilted and tracked surfaces, November 5 th , 2008 in Garching at Munich.....	80
Figure 4-20: Comparison of irradiance levels for measured data and simulation results on a tilted surface, November 6 th , 2008 in Garching at Munich.....	82
Figure 4-21: Comparison of irradiance levels for measured data and simulation results on a tracked surface, November 6 th , 2008 in Garching at Munich	83
Figure 4-22: Temperatures of measured data and simulation results, November 6 th , 2008 in Garching at Munich	83
Figure 4-23: Comparison of power generation levels for measured data and simulation results on tilted and tracked surfaces, November 6 th , 2008 in Garching at Munich.....	84
Figure 4-24: Comparison of irradiance levels for measured data and simulation results on a tilted surface, October 25 th , 2008 in Garching at Munich.....	85
Figure 4-25: Comparison of irradiance levels for measured data and simulation results on a tracked surface, October 25 th , 2008 in Garching at Munich	86
Figure 4-26: Temperatures of measured data and simulation results, October 25 th	86
Figure 4-27: Comparison of power generation levels for measured data and simulation results on tilted and tracked surfaces, October 25 th , 2008 in Garching at Munich.....	87

Figure 4-28: Irradiance profiles for September 1 st using the SRY	90
Figure 4-29: Comparing irradiance profiles for September 1 st using the SRY	91
Figure 4-30: Monthly yields of the different tracking systems	92
Figure 4-31: Comparing the annual yield according to the seasonal tracking steps	93
Figure 4-32: Comparing the annual yield of different tracking systems.....	93
Figure 4-33: Comparing the annual yield of different tracking systems with the old and the new Standard Reference Years	95
Figure 4-34: Daily profile of the global irradiation on tracked surfaces with different time shifts causing the	96
Figure 4-35: Influence of the time shift on the annual yield	97
Figure 4-36: Comparison of the simulated annual yield of different solar tracking systems for Santiago and Punta Arenas, Chile. Data: 1995	98

LIST OF SYMBOLS AND ACRONYMS

α	[°]	Elevation of the sun
β	[°]	Tilted angle of surface
γ	[°]	Azimuth orientation of surface (north = 0°, west = 270°)
δ	[°]	Declination of the sun
η	[%/100]	Conversion efficiency of the photovoltaic cells
θ	[°]	Incidence angle of beam radiation
θ_z	[°]	Zenith angle ($\theta_z = 90^\circ - \alpha$)
ρ	[%/100]	Albedo or ground reflectance
ψ	[°]	Solar azimuth angle (north = 0°, west = 270°)
ω	[°]	Hour angle of the sun
β_0	[-]	Regression Parameter
β_1	[-]	Regression Parameter
G_h	[W/m ²]	Global radiation on a horizontal surface
$G_{h,beam}$	[W/m ²]	Beam or direct radiation on a horizontal surface
$G_{h,diff}$	[W/m ²]	Diffuse radiation on a horizontal surface
$G_{h,ref}$	[W/m ²]	Reflected radiation on a horizontal surface
G_t	[W/m ²]	Global radiation on a tilted surface
$G_{t,beam}$	[W/m ²]	Beam or direct radiation on a tilted surface
$G_{t,diff}$	[W/m ²]	Diffuse radiation on a tilted surface

$G_{t,ref}$	[W/m ²]	Reflected radiation on a tilted surface
G_{oh}	[W/m ²]	Extraterrestrial radiation on a horizontal surface
G_{sc}	[W/m ²]	Solar Constant. In this work $G_{sc} = 1367 \text{ W/m}^2$
h	[h]	Hour
I_{ac}	[A]	Current at alternating current side
I_{dc}	[A]	Current at direct current side
I_{mpp}	[A]	Current at MPP
k_p	[%/K]	Temperature coefficient of power
k_t	[%/100]	Clearness index
P_{ac}	[W]	Power on the alternating current side
P_{dc}	[W]	Power on the direct current side
P_{max}	[W]	Maximum power
P_{STC}	[W]	Power at STC
T_a	[°C]	Air temperature (or ambient temperature)
T_m	[°C]	Solar module temperature
T_{STC}	[°C]	Temperature at STC (25°C)
S	[W]	Irradiance level on the solar modules
S_{STC}	[W]	Irradiance level at STC (1000 W/m ²)
V_{ac}	[V]	Voltage at alternating current side
V_{dc}	[V]	Voltage at direct current side
V_{mpp}	[V]	Voltage at MPP
V_w	[m/s]	Wind speed

AC	[-]	Alternating Current
CET	[-]	Central European Time
DC	[-]	Direct Current
DWD	[-]	Deutschen Wetter Dienst
FH	[-]	Fixed Horizontal Combination (from <i>Festangestellt-Horiz.</i>)
FT	[-]	Fixed Tilted Combination (from <i>Festangestellt-Tilted</i>)
IRR	[-]	Internal Rate of Return
MPP	[-]	Maximum Power Point
NH	[-]	2-Axis Horizontal Combination (from <i>Nachgeführt-Horiz.</i>)
NOCT	[-]	Nominal Operating Cell Temperature
NPV	[-]	Net Present Value
NT	[-]	2-Axis Tilted Combination (from <i>Nachgeführt-Tiltet</i>)
PLC	[-]	Programmable Logic Control
PV	[-]	Photovoltaic
SRY	[-]	Standard Reference Year (or <i>TRJ</i> for <i>Test Referenz Jahr</i> in German)
STC	[-]	Standard Testing Conditions (1000 W/m ² , AM 1.5, 25°C)
TUM	[-]	Technical University of Munich
WBGU	[-]	Wissenschaftlicher Beirat der Bundesregierung Globale Umweltveränderungen

ABSTRACT

Photovoltaic generated energy is becoming more and more important at present, with an exponential growth in the installed capacity around the world. In addition to the standard fixed systems, solar tracking systems have been developed to increase the collected energy, maintaining the installed capacity, and are being used with a growing tendency. The contribution of these tracking systems has not been clear due to a great variety of academic results and the diverging industry.

After renovating two solar power plants located at the Technical University of Munich in Bavaria, measurements took place using a fixed solar power plant and a 2-axis tracked system with a VIAX-mechanism in order to analyze the energy gain using solar trackers. Computer simulation models were also developed for several tracking systems. The experimental data was used to validate the computer simulations. Later the simulation models were used to extend the analysis to longer periods of time, to other locations and to other tracking systems. In addition, some important simulation phenomena were studied.

The results show that from the energetic point of view all the tracking systems evaluated are recommendable. While in Munich the energy gain, using a double-axis tracking system, was around 27%, in northern Scandinavia the energy gain can rise up to 50%. The tracking systems could be modeled correctly and the distortions were explained, delivering important results for the research.

A short economic evaluation is presented in addition to a performance estimate of tracking systems in two locations in Chile.

Key Words: Solar tracking, Munich, simulations, PV system, computer modeling

RESUMEN

La energía proveniente de plantas solares fotovoltaicas ha aumentado su importancia en el último tiempo, mostrando un crecimiento exponencial de la capacidad instalada en el mundo. Aparte de los tradicionales sistemas fotovoltaicos estáticos, se han desarrollado sistemas de seguimiento solar con el objetivo de incrementar la energía recolectada manteniendo constante la potencia máxima instalada en la planta. El aporte energético como consecuencia del uso de estos sistemas de seguimiento no está claro, como se puede observar en la gran variedad de resultados académicos existentes, como también en lo que ofrece la industria solar.

Habiendo renovado dos plantas solares existentes en la Universidad Técnica de Munich en Baviera, se continuó con la medición de datos utilizando una planta solar estática y una con un sistema de seguimiento en 2 ejes con mecanismo VIAX, con la intención de analizar el aporte energético debido al sistema de seguimiento. A la vez se desarrollaron modelos computacionales para diversos sistemas de seguimiento. Los resultados experimentales se utilizaron para validar las simulaciones computacionales. Posteriormente se utilizaron los modelos en simulación para extender los resultados a periodos de tiempo más extensos, a otras regiones y a otros sistemas de seguimiento. Adicionalmente se estudiaron fenómenos asociados a las simulaciones computacionales.

Los resultados muestran que desde un punto de vista energético todos los sistemas de seguimiento estudiados son recomendables. Mientras que en Munich el aporte utilizando un seguidor en 2 ejes es en torno al 27%, en el norte de Escandinavia puede alcanzar un 50%. Los sistemas de seguimiento pudieron ser modelados correctamente y las distorsiones fueron examinadas, entregando resultados importantes para la investigación.

Finalmente se presenta una breve evaluación económica, además de estimar el rendimiento de los sistemas de seguimiento en dos lugares en Chile.

1 INTRODUCTION

The energy issue has been always an important topic in the development of human kind. Domination of fire, using the wind for sailing or mechanical work, water mills, thermo electrical power plants and nuclear energy are a few essential topics in the history which represent the evolution of the human being over a large period of time.

Nowadays in the 21st century, the world is facing new challenges. Energy has become a priority, not only to meet the energy demands of industrial countries, but also to meet the energy demands of the increasing world population. Fossil fuels, with an overwhelming contribution to the world's energy supply, are expected to have limited reserves, threatening the future of the world's development at the present rate. Fossil fuels are also involved in atmosphere's pollution and associated to global warming.

To overcome these problems, before it ends in a crisis, man has focused on the development of new energy sources, which will represent the next step in human history. Among them, there is no doubt that the sun's energy, directly or indirectly, will play a main role in the future.

In these days, photovoltaic systems directly collecting the sun's energy are increasingly being used and represent a growing trail of the solar industry and of the research in the scientific community. The improvement of the energy gain, via solar tracking systems, is one of the studied topics in this area and has not been out of discussion due to a variety of statements made about its efficiency.

With the intention to contribute to this discussion, solar tracking mechanisms will be studied in this master thesis.

Following some investigation lines of the Technical University of Munich, the research activity will center on experimental results using solar power plants and computer simulations.

1.1 Motivation

The global solar industry has developed a variety of solar tracking systems for photovoltaic power plants, offering different energy gains compared to solar power plants without tracking systems. The industry's mentioned values, when promoting their products, are mostly in the range between 20% and 40% gain. Some manufacturers even offer over 40% energy gain by using their solar trackers. How truthful these statements are for the southern part of Germany is not clear.

The Mechanical Engineering Faculty of the Technical University of Munich has a few solar power plants which could be used to research this, after solving some existing operational problems. Among there is a prototype of a new solar tracking system developed at the faculty itself, the VIAX. Also, a new standard solar tracking system is intended to be operational in the upcoming months. Despite existing installations and mainly due to some operational problems, there has been no serious research activity using these power plants. This research would be useful to compare the real energy gain in Munich, using solar tracking systems, with the statements presented by the industry which apparently has not been done in the past.

On the other hand, the computer simulations done in the past at the Faculty of Mechanical Engineering have shown some important distortions compared to expected results which are attributed to a simulation effect that has not been mentioned by other authors working with simulations of solar tracking systems.

One objective of this work is to carry out a measurement of the solar energy collected by the solar power plants in Munich and to compare the results to the ones obtained using simulation programs, in order to verify the statements done by the solar industry. This will allow to extend the evaluation mechanism to other locations where solar tracking systems could be of interest.

1.2 Investigation Outline

As previously stated, the main topic of this thesis will be to analyze solar tracking systems. The process includes measuring data with the solar power plants located at the Technical University of Munich and also evaluating the tracking systems with computer simulation programs. This process will also allow us to check the statements presented by the industry in relation to their solar trackers for the Munich area. It also might end in a decision tool that could be useful for future evaluations of solar tracking mechanisms in other locations.

1.1.1 Hypothesis

Analyzing the factors that influence the performance of a photovoltaic power plant such as the tracking system used (if any), its location and the meteorological conditions would allow quantifying its incidence on the performance of the power plant and be useful in creating a tool to take decisions in determining the best choice for each location.

1.1.2 Research Outline

To analyze the different solar tracking mechanisms, the research process of this thesis will be divided into following sections:

- Overview of the present state: After a brief introduction to solar energy, the existing tracking mechanisms will be reviewed with a summary of some scientific studies and the solar industry. The solar power plants at the Technical University of Munich and previous simulation, resulting with some disturbing effects, will also be presented, together with some additional information of interest like the climate at Munich.
- Methodology: Here the improvements made to the power plants and sensors for the measuring process will be explained. Also the data measurement process itself and the computer simulations used will be explained.

- Results and Analysis: The experimental and simulation results will be presented and analyzed. This will allow a comparison of the results, in order to validate the simulations with real data. An eventual validation of the data would allow extending the method to other tracking mechanisms and locations. The simulation distortions will also be commented.

1.1.3 Research Contribution

The main contributions of this thesis are the following:

- It will present experimental results for photovoltaic power plants located in Munich and compare real power plants with and without tracking systems.
- The simulations will be worked out thoroughly than before in order to get better results and to facilitate further development in this area. In relation to this, the simulation distortions will also be commented on, in order to correct past simulation results that could have been affected in a significant way and that should be considered in future simulation processes.
- Some criteria to assist the decision making process when considering the installation of solar tracking systems.

2 CURRENT STATE

The present chapter will mainly illustrate the state of the art in solar tracking systems, beginning with the global solar power and continuing with an overview of the existing mechanisms and their performance. It will also describe the present investigation conditions at the Technical University of Munich, with its power plants and some related computer simulations done in the past.

2.1 *Solar Energy*

The global warming debate, along with the high oil prices reached in the year 2008, has touched on the discussion related with how to meet the growing demand in power around the world. Thus, renewable energy sources have become more important and more economic resources are being used to finance research activities. Some countries have even offered significant incentives to increase the power generation capacity using renewable energy sources.

2.1.1 **Power Sources**

The main power sources used today and their importance in the world's primary energy supply can be seen at Figure 2-1. Fossil fuels are the dominating sources at present and they are expected to continue for the next 25 years. The predicted limited resources of fossil fuels in the world along with a growing demand for power and the high levels of environmental pollution in the world are forcing the politicians and scientists to focus on renewable energy sources. The idea is to decrease the use of fossil fuels such as oil, coal and gas in the future and to increase the use of renewable energy sources like hydropower, biomass, wind, solar power and geothermal. Nuclear power, not being considered as a

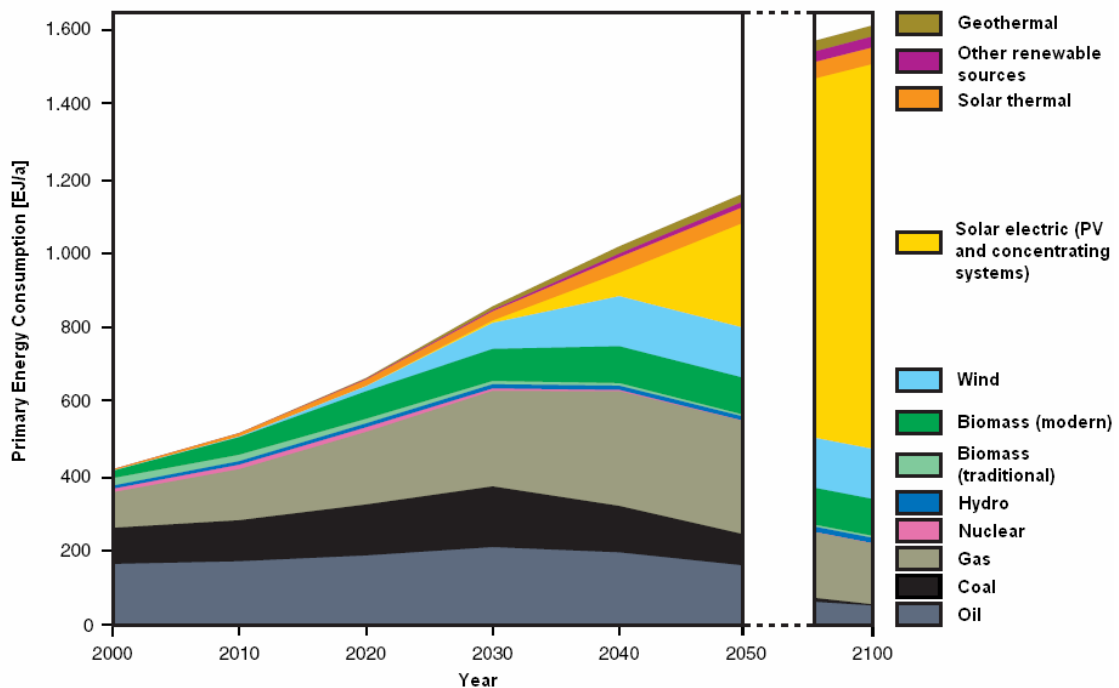


Figure 2-1: Evolution of world total primary energy supply (WBGU, 2003).

fossil fuel but also not as a renewable energy source, has an unclear future, since there exist a number of opinions concerning its development.

Focusing now on renewable energy sources, hope is placed in the long run into solar energy, more precisely in collecting solar radiation, which is the energy source with the largest development potential, considering the huge amount of solar energy available (information and predictions according to the German Advisory Council on Global Change, WBGU, 2003).

Other international organizations related with the study of the global energy development like the International Energy Agency and the Energy Information Administration (official energy statistics from the U.S. Government) disagree with some statements of the WBGU in matters such as the development of the nuclear energy participation in the future, predicting for 2030 still an important participation of this source of energy. These organizations also agree that the growth of renewable energy sources will be lower than the predictions of the WBGU and do not get involved with predictions beyond 2030.

2.1.2 Solar Energy at the Present Time

“Solar energy”, as previously stated, refers to the radiation energy of the sun that can be converted into power with special devices. Figure 2-2 shows the irradiance levels around the world, since the available amount of solar energy differs dramatically. The devices can be classified according to the technology used or how the energy is applied, for example, to generate electricity or for solar thermal heating. The solar thermal energy is

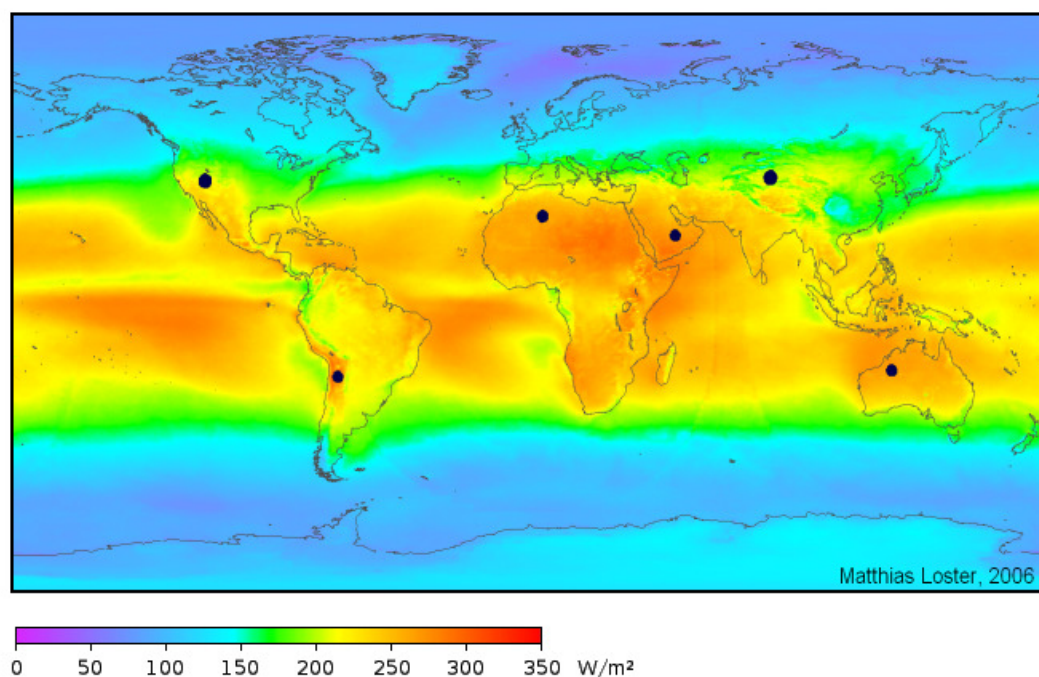


Figure 2-2: Local solar irradiance averaged over three years from 1991 to 1994 (24 hours a day), taking into account the cloud coverage available from weather satellites (Loster, 2006).

mostly used to heat up water or air ,using solar thermal panels for domestic hot water or space heating. Under the electricity generating group, the concentrating plants and the photovoltaic (PV) panels are the most known. While the first are used on larger fields in the form of power plants to generate power connected to the grid, the second are not

necessary used in larger power plants but also in smaller systems for domestic use, either as grid-tied or off-grid PV systems. An approximation of the installed capacity of global PV systems can be seen in Figure 2-3. The tendency shows that grid-connected systems are becoming much more important than off-grid systems, while the growing tendency has increased significantly. The estimated grid-connected solar PV installed capacity in the year 2008 worldwide was 12,950 MW. Germany, the country with the largest installed capacity, had 5,400 MW (REN21, 2009). According to the BMU (2008) from the 73.400 PJ of primary energy supplied to Europe, only 6.5% came from renewable energy sources. Only a 0.7% of this renewable supply came from solar power in general.

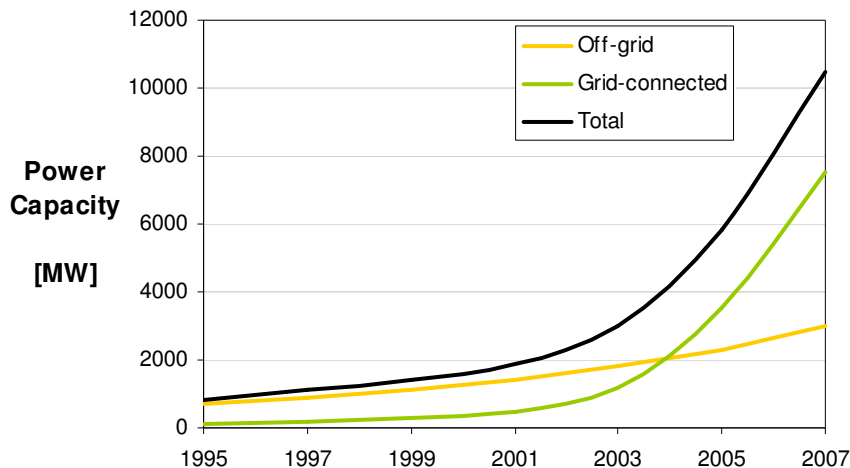


Figure 2-3: Installed power capacity of Solar PV in the world (REN21, 2009).

Solar power plants, either connected or not to the grid, have a similar component configuration. Let's focus here only on the grid connected ones. The power plants consist mainly of solar modules, the inverter, the data logger, some sensors, a grid supply meter, the mounting parts and other components that could be used. Basically, the solar modules collect the solar radiation and generate DC current which is transformed into AC current by the inverter and then delivered to the grid. For the solar modules, there are many cell types whose efficiency vary significantly, such as single-crystalline silicon ($\eta = 14\%$ to 18%), polycrystalline ($\eta = 13\%$ to 15.5%), thin films ($\eta = 10\%$ to 12%) and amorphous silicon ($\eta = 6\%$ to 8%). Data according to WBGU (2003) and Kaltschmitt et al. (2006). There are a series of possibilities for connecting the solar modules to the inverter (in series,

in parallel or in combination) and which additional parts should be used, mostly for measurement purposes. However, these connecting options are mostly related with the inverters' characteristics or on how many solar modules are being used. To increase the collected amount of energy, considering a determined amount of solar panels, one of the options is to enhance the panels orientation. This can be achieved by installing fixed systems at an optimal orientation angle or by using tracking systems which follow the sun.

2.1.3 Concepts on solar radiation

Before talking about the solar tracking systems, we will review some basic concepts concerning solar radiation and mention some important values to better understand the results of this work.

The sun, at an estimated temperature of 5800 K, emits high amounts of energy in the form of radiation, which reaches the planets of the solar system. The earth is also reached by the sun's radiation at intensity of 1367 W/m^2 according to the World Radiation Center (Duffie & Beckmann, 2006). This value, known as the Solar Constant G_{sc} , represents the energy per unit time received from the sun on a unit area of surface perpendicular to the direction of the sun radiation outside the atmosphere. This value however is not constant and changes during the year and over the years. The solar radiation is distributed over a wavelength range, including the visible wavelength range from $0.37 \text{ }\mu\text{m}$ up to $0.78 \text{ }\mu\text{m}$. The common wavelength used for the sun's extraterrestrial radiation goes from $0.25 \text{ }\mu\text{m}$ to $3 \text{ }\mu\text{m}$, considered as the short wave radiation. The radiation with a wavelength larger than $3 \text{ }\mu\text{m}$ is considered as long wave radiation. The short wave radiation can be divided into three groups: The ultraviolet radiation ($0.28 - 0.38 \text{ }\mu\text{m}$) with a 7% of the total short wave radiation's energy, the visible wavelength with a 47% of the energy and the infrared radiation ($0.78 - 3.00 \text{ }\mu\text{m}$) with a 46% of the energy (Pichard, 1999). Due to the components in the atmosphere, only a part of the extraterrestrial sun's radiation reaches the earth's surface. Once the radiation penetrates the atmosphere, a part of the radiation is absorbed by ozone in the ultraviolet range, by water vapor and carbon dioxide in the infrared range. The entering radiation is also scattered in the atmosphere by

air molecules, water vapor and small particles. Thus, the solar radiation that reaches the earth's surface is less than the Solar Constant.

Some important concepts about incident radiation on a surface are also mentioned here. Direct radiation (also called beam radiation) is the solar radiation of the sun that has not been scattered (causes shadow). The diffuse radiation is the sun radiation that has been scattered (complete radiation on cloudy days). Reflected radiation is the incident radiation (beam and diffuse) that has been reflected by the earth and reaches the surface. The sum of beams, diffuse and reflected radiation is considered as the global radiation on a surface.

2.2 Solar Tracking Systems

Solar tracking systems are used to improve the amount of power produced by a solar plant. There are different mechanisms used around the world, with different performance studies related to them. Also the solar industry has done its own assessments on this issue, which do not always coincide with the scientific results.

2.2.1 Solar Tracking Mechanisms

If considering collecting sun energy, the simplest way would be to do it as the surface of the earth does, on a horizontal surface (in the normal case). However, if the surface (here the solar modules) is oriented towards the sun path, the collected amount of energy can be greatly increased. There are several ways to do this. Some of them are:

1. Fixed modules installed at an tilted angle (β)
2. Seasonal adjustment of the tilt angle β (few adjustments per year)
3. Azimuth tracking: Modules mounted inclined on a single tracking vertical axis (at constant tilt angle β). See A in Figure 2-4
4. Polar tracking: Modules mounted on an inclined tracking axis oriented North-South (axis with a tilted angle β). See B in Figure 2-4
5. Double axis tracking (C in Figure 2-4)

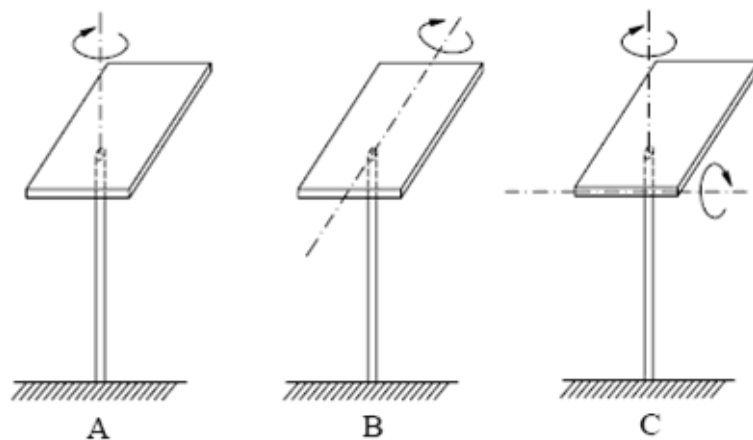


Figure 2-4: Some tracking mechanisms (by Canova et al., 2007).

At the present, most of the solar power plants are installed at fixed positions at an optimum tilt angle. The angle depends mainly on the location of the plant. Thus, this will be considered from now on as the base case for the comparisons of the performance between different tracking systems. Values referred to the energy yield on horizontal surfaces are then mostly just reference values.

Let's see some concepts related to surface orientation angles and the sun's position, for an easy understanding of the following topics. The orientation of the surface, representing the solar modules, will be described in this work with two parameters. First we have the elevation angle of the surface from the ground β , which will be referred to as the tilted angle when talking about a constant value. The second parameter is the orientation of an inclined surface in matters of cardinal direction. This parameter, the azimuth orientation of a surface denoted by γ , is for example equal to 0° when facing north and 270° when facing west. A similar convention is used for the sun. The position of the sun is determined by two parameters, α as the elevation angle of the sun and ψ as the solar azimuth angle. While α indicates the elevation of the sun from the horizon (at noon α would be maximum for the day), ψ indicates the position of the sun referred to the cardinal system as mentioned before. In the northern hemisphere, $\psi = 180^\circ$ at noon while in the southern hemisphere at the same time $\psi = 0^\circ$. It is also important to make the observation that α and ψ do not have the same values at the same time of the day over the year. This relates to the position of the sun and the earth throughout the year, but won't be explained here in detail. Duffie & Beckman (2006) is a good source of information on this topic. However, two helpful observations are stated here. The sun reaches its highest elevation point at noon in the summer (June, 21st in the northern hemisphere) and its lowest elevation point at noon in the winter (December 21st in the northern hemisphere). For the southern hemisphere, the occurrence days are inverted. During summer, when the days are longer, the solar azimuth angle reaches a larger range of values than in the winter.

2.2.2 Performance Studies

A series of publications discussing the research of tracking systems have been published in the past and the topic is still being discussed year after year in conferences around the world. Good examples of this are the last three PVSEC meetings (European Photovoltaic Solar Energy Conference) with several presentations and papers about this issue. A brief review of some recent results is presented in this section.

Huld et al. (2008) presented at the 23rd PVSEC interesting results from a map-based method for estimating the yearly solar irradiation on PV modules mounted on sun trackers around Europe. Their results for Munich gave an increase in yearly solar irradiation using the azimuth tracking system of 24%, compared to a fixed system at optimum angle. Using polar tracking there was no significant difference to the azimuth tracking system. For a 2-axis tracking system the gain was around 2% compared to a single axis tracking, about 26% compared to a fixed system. For the southern part of Spain the values are 32% using an azimuth tracker and 35% using a two-axis tracker. For the west coast of France the values are 28% and 31%. The highest gains are reached in northern Scandinavia with 50% and 52%. Here the performance of an azimuth tracker is clearly better than the performance of a polar tracker. See a comparison on Figure 2-5.

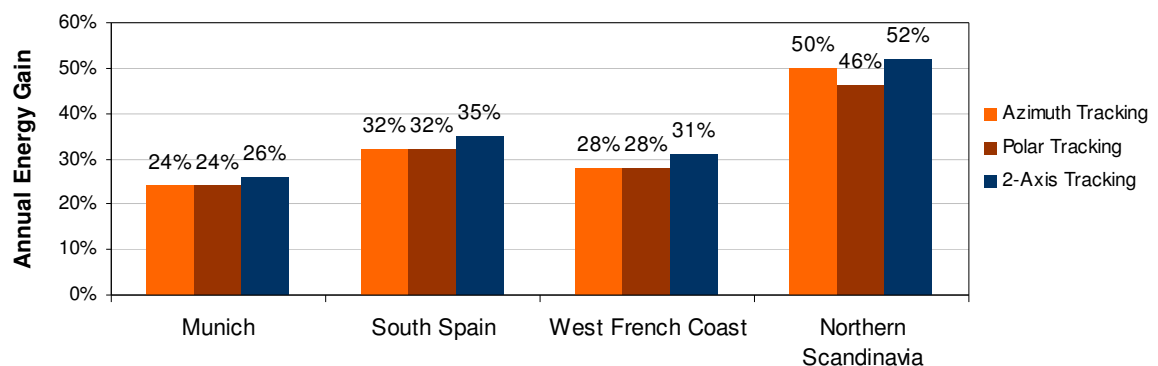


Figure 2-5: Energy gain using tracking systems (Huld et al., 2008).

Hoffmann et al. (2008) refers to previous results concerning this topic obtained by the author at the Technical University of Munich in cooperation with the Technical

University of Darmstadt. The results for Munich obtained using simulations implemented in INSEL and MATLAB are the following: Gain of 21% on annual irradiance comparing an azimuth tracker to a fixed system. Gain of 22% using a 2-axis tracker. The values corresponding now to the gain in AC-energy are 22% and 24% respectively. The gain using a polar tracker was slightly higher compared to an azimuth tracker and lower than a 2-axis tracker. Anyways, it can be considered as non- significant.

Canova et al. published an interesting paper in 2007 on irradiance gain using tracking systems. Two models are used for the irradiance simulation (Moon-Spencer and the Aste model) and the results for a location near Turin in Northern Italy (45.1°N , 7.7°E) change significantly according to the model used. With the Moon-Spencer model the annual gain of a 2-axis tracker, compared with a fixed system, is 44%. With the Aste model the gain is 32%. Also some experimental data for a single axis tracking system is also published for Saluzzo, Italy (44.65°N , 7.48°E). However only some AC-power output information for three different days are shown and commented on, but no comparison is made to fixed systems. Therefore, no energy gain values are mentioned. The experimental data has also no relation with the simulations.

Sorichetti and Perpiñan (2007) studied, with a computer program, the irradiation levels and the energy gain using tracking systems on seven locations in Europe, South America and Africa. The values obtained match the results obtained by Huld et al. (2008). The conclusions of the work however, relying importantly on the latitude of the locations, show that this dependence on latitude is not enough. The results from Huld et al. make this clear. Also these authors mention in their work some experimental results of an installed power plant in Toledo, Spain with the intention to validate their computed results. The experimental results are not precise enough to achieve this.

Narvarte & Lorenzo (2007), along with discussing in their work the effects of shadows and ground cover ration relations, also mention some values of our interest since they included simulation results of energy yields (including inverters) for two particular locations and a mean value of 15 locations in Europe. The results without shadow effects, differ significantly from other works and can be seen on Figure 2-6. The gain values are relatively high in comparison with other studies.

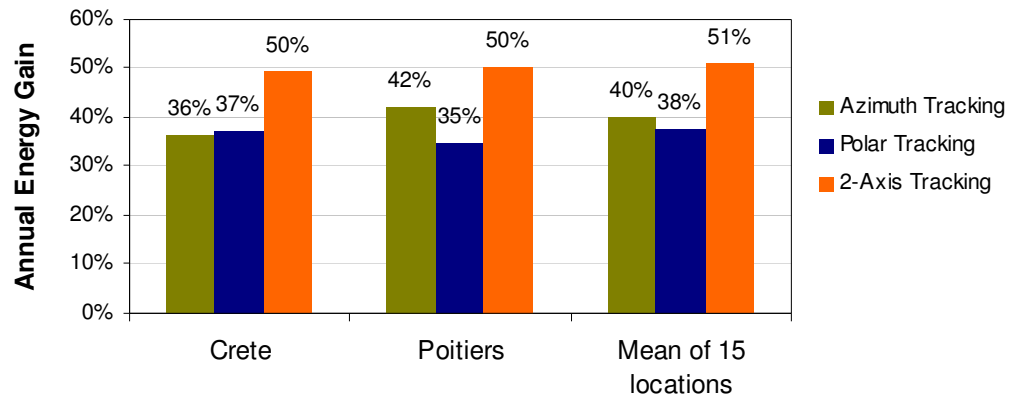


Figure 2-6: Energy gain using tracking systems (Narvarte & Lorenzo, 2007).

One more publication from Mohring et al. (2006) is commented on here, due to its methods and results. Simulation results using as input hourly radiation values and validation with installed power plants are presented. The simulation and experimental results give for Widdershall in southern Germany (48.53°N, 9.72°E) a gain of 22.5% to 23%, using a polar tracker tilted at 30° compared to a fixed surface at 40° elevation. For 2-axis tracking the gain is 27% (simulated and measured). Extending the simulation results, an azimuth tracker would gain 23%. For a location in southern Europe (Monte Aquilone, Italy) the gains are: polar and azimuth tracking 30%, 2-axis tracking 34%.

As seen here, many studies have given an interesting variety of results. Mostly simulation programs without precise input data, like the desired meteorological hourly values, are used to predict the energy gain of the tracking systems. A few estimations coincide with others, while some seem to be pretty far from reality. Also a huge variety of conclusions can be found starting from the simulation results obtained. One of the most commonly mentioned is the gain dependence on the latitude. Most of the simulation results also have not been validated, thus the simulation results can't be easily trusted. This is even more important when considering the variety of simulation methods and computer programs used.

2.2.3 Brief Review of the Solar Industry

In the previous years, solar energy has developed rapidly in Europe, mostly due to subsidies of the German and the Spanish governments towards solar generated power.

Table 2-1: Energy gain estimations of the solar industry (kWh/kWp). Information by author.

Company	Energy gain by using tracker	Location with guaranteed gain	Tracked axis	Company location
PVStrom	24%	Spain	1	Germany
Conectavol	25%		1	Spain
Solea	25%		1	Germany
Sonnentraelen	25%		1	Germany
DEGERenergie	30%		1	Germany
Soemtron	30%	Europe	1	Germany
SunCarrier	30%		1	Germany
Sunpower	30%		1	Worldwide
Traxle	30%	Europe	1	Czech Republic
Lorentz	40%		1	Germany
Traxle Mirror	40%		1	Czech Republic
Quantum Solar	28%	Burgos, Spain	2	Spain
Soltec	31%	Bavaria, Germany	2	Spain
Quantum Solar	34%	Murcia, Spain	2	Spain
Helios	35%	Spain	2	Spain
Meca Solar	35%		2	Spain
Pevafersa	35%		2	Spain
Sonnen_System	35%	Alheim, Germ. (51°N, 9°E)	2	Germany
Conergy	40%	Worldwide	2	Germany
MP-TEC	40%	Spain	2	Germany
Pesos	40%	Europe	2	Germany
Solar.trak	40%		2	Germany
DEGERenergie	45%		2	Germany
Sinosol Technologies	45%		2	Germany
Sonnen_System	45%		2	Germany

Thus these are the countries that have developed most of the new tracking systems in Europe. On Table 2-1 it is possible to observe the offer of almost all of the companies that presented tracking systems in the fair InterSolar 2008. This show takes place annually and is the largest fair related to solar energy of this type in Europe. It brings together the most important solar companies of the world. We could then assume that these companies are a good representation of the solar industry in general. It is possible to see that the offered tracking systems, with one axis tracking, have in general a smaller gain compared to the two-axis tracking systems, which would have been expected. But it is interesting to see how different the maximum gain values are, from 24% gain using one-axis trackers “up to” 40% gain. The same happens with the 2-axis tracking system, from 28% up to 45% gain. Considering the two-axis trackers, the author expected that the Spanish companies would offer higher gains compared to the German ones, since the installed power plants in Spain should gain more energy than the ones installed in Germany, due to the irradiance levels in both countries. But as we can see, the Spanish plants also have done projects in Germany and vice versa. Now, why German companies offer such high energy gains, is a mystery for the author. It could lie on the fact that these gains are possible to be reached in northern Europe and Germany is the country, at the time, closest to these regions with a “mature” solar industry. Anyways, more than speculating on those reasons, we should notice that the values differ significantly, which brings us to the question if these values are correct. This is one of the various motivations of this work.

2.3 Photovoltaic Plants at the Technical University of Munich

The Technical University of Munich has its Faculty of Mechanical Engineering near the town of Garching, located 15 km north of downtown Munich. There are a few solar plants installed at the faculty, some of them used only to generate power and two intended to be used also for research, which will be presented here.

2.3.1 The Fixed Solar Plant MW-5

The MW-5 solar plant owes its name to the building where it is placed, the Maschinenwesen 5, located at $48^{\circ}15'55''\text{N}$ and $11^{\circ}40'07''\text{E}$. At its roof, we find the facilities shown by Figure 2-7 and Figure 2-8.



Figure 2-7 and Figure 2-8: West and East wing of the MW-5 solar power plant.

The Plant consists of two inverters SMC 5000A from SMA, each with a nominal power of 5000 W. Inverter 1 has four strings of 7 modules each, while Inverter 2 has three strings of 9 modules each (see Figure 2-9). The solar panels used are STM 210 FWS from SunTechnics with monocrystalline cells and a P_{\max} at Standard Testing Conditions of 210 W. Thus we have a maximum DC Power of 5880 W and 5670 W for Inverter 1 and

Inverter 2 respectively, with a total maximum DC Power of 11550 W for the power plant. The power plant was installed at the end of 2006. The solar modules are fixed mounted, pointing south and are inclined at 25° from the horizontal.

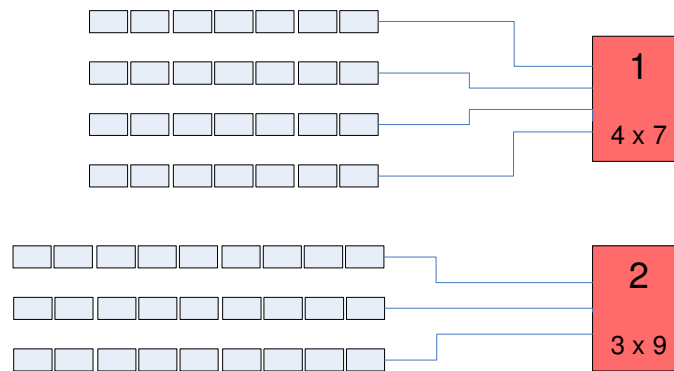


Figure 2-9: Scheme of the MW-5 power plant.

Since the power plant started operating, it has had problems with its data recording system. At the beginning, the installed Sunny WebBox from SMA recorded only information related to the inverters, but did not store any information of the incident solar radiation or the module temperature, despite having a SensorBox from SMA connected to



Figure 2-10: Sunny SensorBox at the MW-5 power plant.

fulfill this purpose. The SensorBox has a solar cell type sensor to measure the solar radiation (see Figure 2-10) and an external PT100 temperature sensor connected to it, to measure the module temperature. Some time later, the WebBox did not store any more information, thus making it impossible to use the power plant for research purposes at the present conditions. A functional WebBox is usually connected to the internet and allows to obtain remote data over a site from SMA, such as recorded information stored over a longer period of time. Over the internet, it is also possible to get instant values.

More information related to the solar modules can be found on Appendix A.

2.3.2 The 2-Axis tracked Plant VIAX

The VIAX solar power plant is a prototype of a new design developed at the Technical University of Munich a few years ago. The main characteristic of this design is its solar tracking mechanism, the VIAX (VIRtual AXis), which allows the plant to follow the sun as a 2-axis tracker would do, but using only one engine. In other words, it reduces the two conventional degrees of freedom to one. The mechanism was designed by Dr. Dieter Seifert (patented in 1983) and implemented later by a team of students in the year 2004, as they built the VIAX power plant. The main advantages of this design compared to a conventional 2-axis tracker are two. First of all, it reduces the design costs of the plant by having only one engine. The second advantage is that by having only one engine, it reduces the amount of energy needed to move the tracker, thus making the system more efficient.

In the following lines, a brief description of the VIAX tracking mechanisms will be presented. Figure 2-11 shows a schematic drawing of the tracking system. The solar panel to be tracked is represented in the middle of the drawing receiving the solar radiation. It is connected to the bar AB in perpendicular position. Point B of the system is connected also to point C, which is to be adjusted according to the season of the year. Point C moves on a parallel to the earth axis. Extending this parallel, it would connect also to point A. Points B and C are a ball-and-socket joint. Bearing A has only one degree of freedom. It turns around an axis perpendicular to the drawing. When the horizontal main axis of the system turns, the joint on point A causes point B to move, which follows a circular path around the

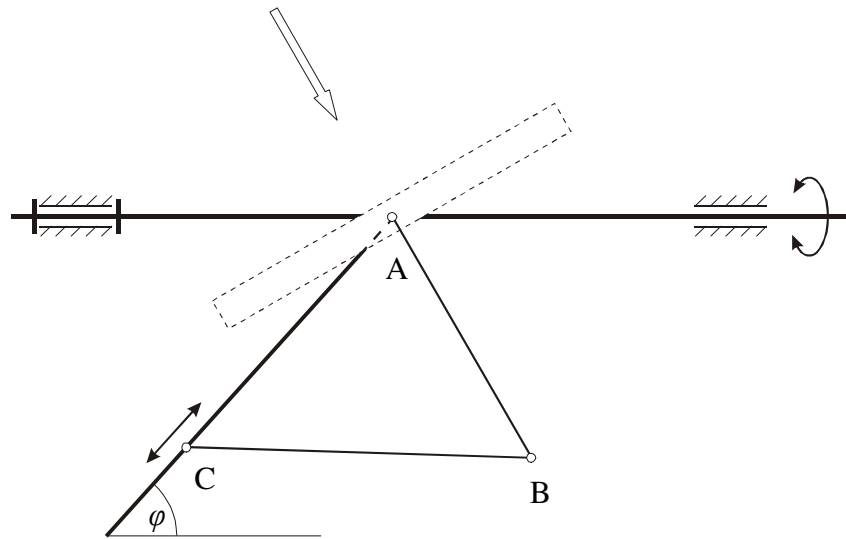


Figure 2-11: Schema of the VIAX tracking mechanism (Bauer et al., 2005).

AC axis. As a result, the axis BA follows the sun path. Point C allows adjusting the mechanism to compensate the declination changes of the sun throughout the year. As we have seen here, only one angle (turn position of the main axis), equivalent to one degree of freedom, is necessary to track the sun, since the other position angles adjust according to the position of the first one. More information to the VIAX tracking mechanism can be found at Bauer et al. (2005), Pelzl (1988), Keller (1989) and Seifert (1983).



Figure 2-12 and Figure 2-13: VIAX power plant.

The plant showed in Figure 2-12 and Figure 2-13 is placed near a parking lot of the Campus at $48^{\circ}15'47.5''\text{N}$ and $11^{\circ}39'53''\text{E}$, at a straight distance of 375 m from the MW-5 plant. It consists of one inverter SB 2100TL of SMA with a nominal power of 1900 W and 8 solar modules from Solon, Solon P210/6+, with polycrystalline cells and a P_{\max} at STC of 210 W. The maximum DC power of the plant is 1680 W. The plant is looking south and the tilted angle of the modules (considering the middle position) is changed manually four times a year. The tracking system is controlled by a programmable logic control (PLC) and follows the sun according to a stored sun path register.

The original design of the VIAX, allowed it to move up to the end positions looking completely east at sunrise and completely west at sunset. At the time the plant was built, the original design was implemented. Some time later it was modified, limiting the movements towards its ends. Since the mechanism could not follow the sun path completely anymore, during the morning and evening hours a measurement error appeared, due to the shadow generated by the same tracking mechanism (Figure 2-14). This malfunction considering the daily profile of generated power can be seen at Figure 2-15. It reduces significantly the daily yield.



Figure 2-14: Example of how the upper bars of the tracking mechanism generate shadow on the solar panels.

Limiting the movement of the system towards its ends would conduce to a small divergence between the VIAX and a conventional 2-axis tracker without considering the shadow effect. Due to the shadow, this limitation has a greater incidence on the measurements. Under these conditions it is not possible to get reliable data for scientific analysis.

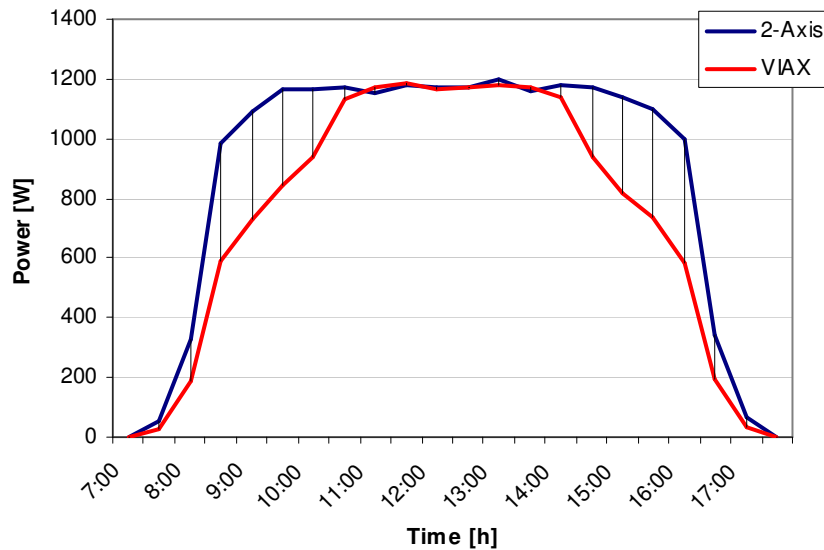


Figure 2-15: Comparison of the diminished power generated by the VIAX and a conventional 2-axis power plant without the shadow problem.

The measured data at the VIAX is recorded with a Sunny Boy Control of SMA. Besides the information related to the inverter, some other meteorological variables, such as air temperature, solar module temperature, horizontal radiation, total tilted radiation and diffuse radiation at tilted surface are measured. Wind direction and intensity is also recorded.

2.3.3 The Meteorological Center of the LMU at Garching

The campus of Garching has also a meteorological Center which belongs to the Ludwig Maximilian University, located at 48°15'53''N and 11°40'20''E.

This center allows the recording of a many data series, which are useful to compare them with the data measured at the solar power plants. Under such data series we find: Air temperature and wind speed series at different elevations, air pressure and horizontal radiation. The radiation is measured with pyranometers (Figure 2-16). There is no additional information about the specific measurement instruments available.



Figure 2-16: Pyranometer.

2.4 Present State of Computer Simulations

Some previous work done at the Technical University of Munich, related to computer simulations of solar tracking systems, have revealed some important facts at the simulation results, which should be reviewed here in order to consider it for further work.

2.4.1 The Standard Reference Year

One of the main resources of climate data used in Germany for research is the Standard Reference Year (SRY), also known in German as *Test Rereferenz Jahr (TRJ)*,

which corresponds to a database containing a group of meteorological variables for each region. Every few years, considering measured values of the last 20 years and statistical models, the German agency Deutschen Wetter Dienst (DWD) releases new databases for research. The last two databases available for Munich correspond to the years 1995 and 2007. The databases contain information like global and diffuse radiation on horizontal surfaces, air temperature and pressure, and wind speed for each hour of a standard year.

2.4.2 Computer Simulation Problems

Recent simulation experiences for Munich (Bernal, 2007) using two different software programs, INSEL and TRNSYS, have shown important divergences to measured values. Figure 2-17 represents measured values for a 2-axis tracking system. The measured global tilted radiation G_t increases faster after sunrise than the global horizontal radiation G_h . In general terms, while G_h tends to represent a sinus curve, G_t tends more to a square shape. Figure 2-18 instead, represents the simulated curve for the tilted radiation with 2-axis tracking. It shows a different shape for G_t with an unexpected peak after sunrise and a faster decrease at the evening hours, while maintaining the sinus shape for G_h .

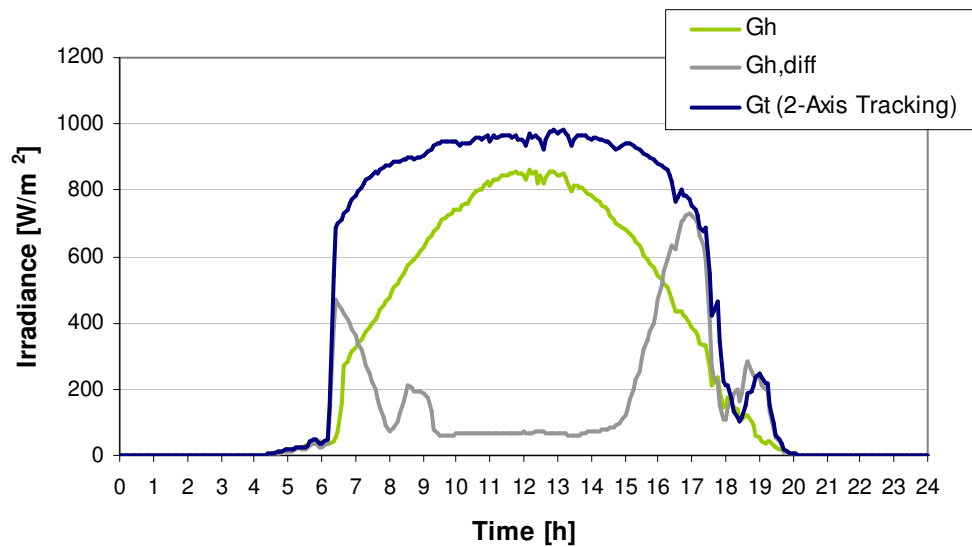


Figure 2-17: Global horizontal, diffused horizontal and global tilted with 2-axis tracking radiation for the 27th of May 2005 from measured values (Bernal, 2007, p.48).

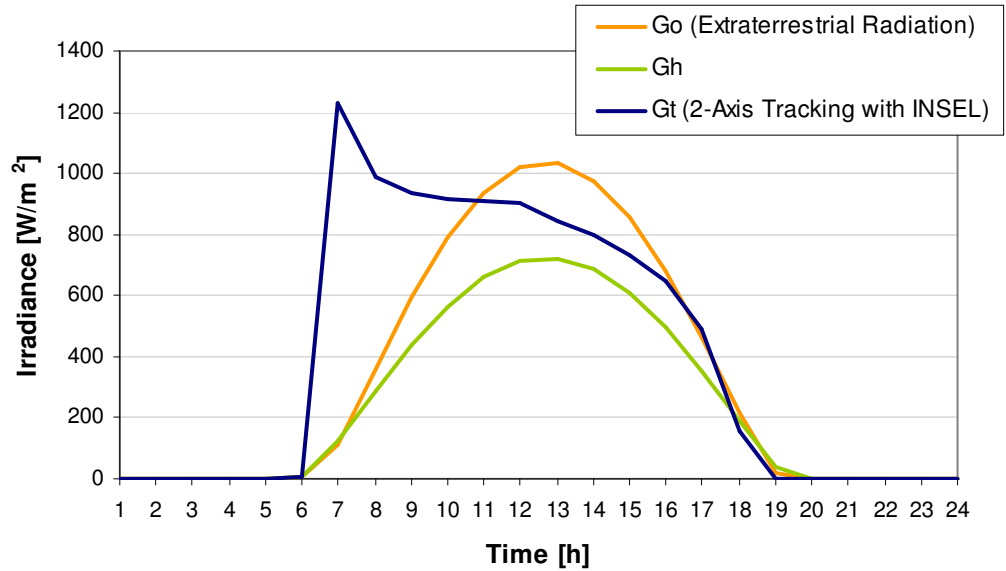


Figure 2-18: Extraterrestrial, global horizontal and simulated global tilted with 2-axis tracking radiation for the 1st of September using the SRY (Bernal, 2007, p.50).

At this point it is important to mention some criteria used for these simulations. First, to calculate the radiation on a tilted surface from the given horizontal radiation, the Liu & Jordan Model was used by default. This model assumes that the diffuse radiation is isotropic, distributed over the whole sky dome (Doppelintegral, 2006). The global radiation on a tilted surface is calculated by

$$G_t = G_{t,beam} + G_{t,diff} + G_{t,ref} \quad (2.1)$$

which in terms of the horizontal radiation is

$$G_t = G_{h,beam} \cdot \frac{\cos(\theta)}{\cos(\theta_z)} + \frac{1}{2} \cdot G_{h,diff} \cdot (1 + \cos(\beta)) + \frac{1}{2} \cdot \rho \cdot G_h \cdot (1 - \cos(\beta)) \quad (2.2)$$

Second, to simulate the two axis tracking mode shown at Figure 2-19, a fictitious day was used. The data for this day was generated using

$$G_{h,beam} [W / m^2] = 100 \cdot \sin(h) \quad (2.2)$$

$$G_{h,diff} [W / m^2] = 50 \cdot \sin(h) \quad (2.3)$$

where $h \in [0^\circ, 180^\circ]$.

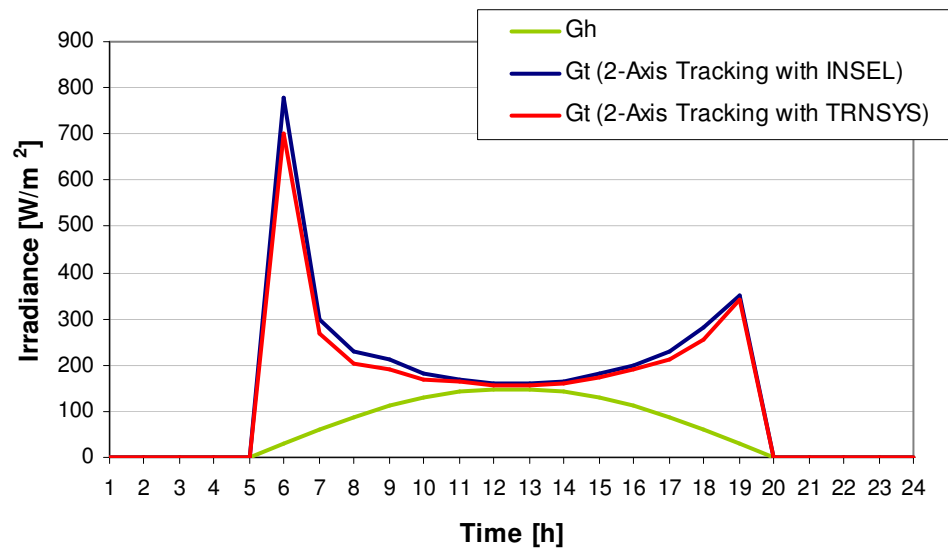


Figure 2-19: Two axis tracking mode simulated with INSEL and TRNSYS using as input data a fictitious day (Bernal, 2007, p.53).

In the case represented by Figure 2-19, it is possible to notice an unexpected peak immediately after the sunrise and one peak just before sunset, which harms the use of these results for any serious analysis. This two peak effect, reaching such high values compared with the horizontal radiation, appears only using the fictitious days as input for the simulation. This effect has been named as the “Batman-Effect” (Hoffmann et al., 2008). Other results from Bernal (2007) using the data from the SRY, show that the peaks are not as high and tend to appear mostly on the first sun hours, with smaller peaks, if any, in the evening hours.

Some adjustments were made by Bernal (2007), trying to reduce these peaks. One of them consisted in changing the longitude of the simulated power plant by almost 4° to the east, placing the plant at the same latitude of Munich, but at 15°E . This tends to reduce the morning peak but increases the evening one. Although as expected, a symmetrical behavior is reached, it gives results that are not suitable for a rigorous analysis. The only mention done to describe the appearance of these peaks is related to the coefficient at the first term on the right hand side of Equation 2.2. The peaks observed at sunrise relates to the fact that the cosine of the incidence angle of the beam radiation adopts high values, whereas the cosine of the zenith angles is rather low.

The developers of the simulation program INSEL (Doppelintegral, 2006) have recognized this problem and warned of it, when explaining the functions of the software. However they haven't solved the problem.

2.5 *The Climate at Munich*

Munich, at an altitude of 520 m, lies on the elevated plains of upper Bavaria, some 50 km north of the northern edge of the Alps. It has a modified continental type of climate, strongly influenced by the proximity of the Alps. In general, summers are fairly warm and very wet, prone to thunderstorms, while winters are rather cold with light snowfalls. Two special weather situations, due to the Alps, can change the normal weather conditions. The *Föhn*, are winds from the SW to SE, that loose their moisture upon crossing the Alps, bringing warm, dry weather during the season. A Strong *Föhn* can bring exceptionally clear viewing conditions. However, strong *Föhn* conditions only affect Munich few days per year and it is a less significant factor in the local climate, than popularly believed. Winds blowing from NW to NE lead to a damming-up of the airflow against the northern Alps, and is known as *Alpenstau*. This can produce prolonged precipitations, accompanied by low temperatures. *Föhn* is most common in autumn and winter, and rare in mid-summer, while *Alpenstau* is most common in spring and summer.

Important for this work are the amount of clear days and its distribution during the year. In a qualitative description, during autumn every once in a while a clear sky day occurs, with decreasing intensity from September until December. The winter, from December until March, has even less days without clouds. On the other hand, spring has a few outstanding weeks during April and May, with very clear skies and excellent conditions for the measurement of the solar radiation. The summer is not the best time of year for the measurement of solar data, since days often have a high density of clouds in the skies with common rain periods and fast changing weather conditions.

Some quantitative information of rainfall and temperatures can be seen at the climate chart of Figure 2-20.

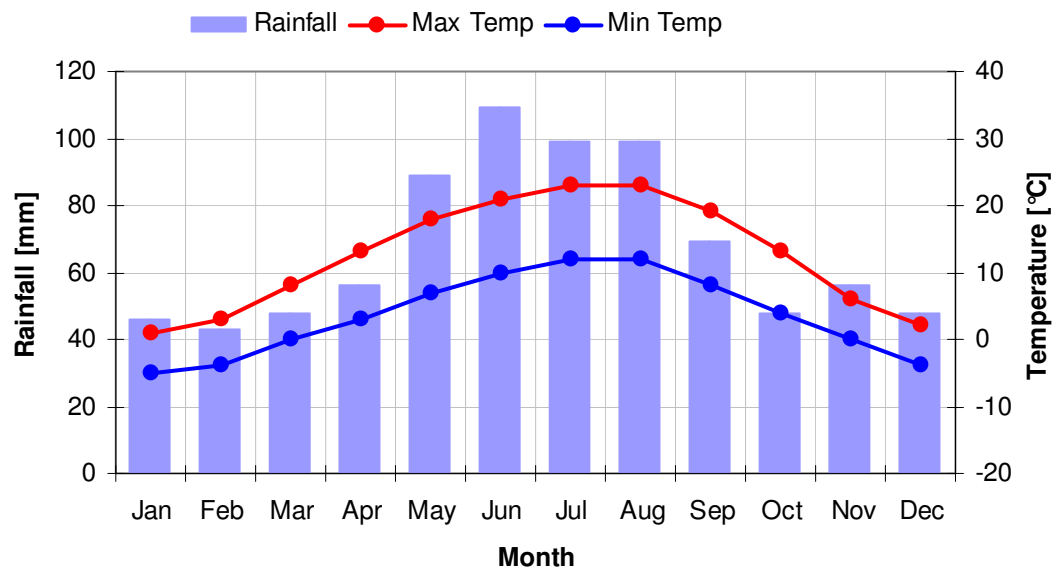


Figure 2-20: Climate chart for Munich.

Summary

As we saw in this chapter, the sun power has high development potential in the following years. The solar tracking systems have high utilization potential which can vary significantly with the used mechanism. There are important cost differences between these mechanisms. The Technical University of Munich has at least two power plants that could be used for serious research after some repairs that have to be done. The simulations carried out up to here related to tracking systems in Munich (the ones analyzed in this chapter) can be considerably improved in order to get better results.

3 METHODOLOGY

The content of this chapter intends to describe the work done by the author in order to obtain proper results to be used for an accurate analysis. At first, the measurement instruments were inspected and calibrated. Later, the existing power plants were repaired and upgraded. With both solar power plants working properly, they were calibrated together and used to measure data over an extended period of time. Simultaneously the existing solar power plants were modeled with computer simulation software. In addition other mechanical tracking systems were evaluated using computer simulations. After getting the experimental data from the power plants, the computer simulations could be validated and the work with the simulations would continue for further analysis.

Additional information related to the experimental assembly can be found on Appendix E.

3.1 Calibration of Sensors

Before the measurement of data could take place, the radiation sensors and the temperature sensors used at the power plants had to be calibrated. The three radiation sensors of the VIAX power plant, along with four pyranometers, were mounted on a structure on the roof of the MW-5 building, designed to hold the radiation sensors at the same position of the radiation sensor of the MW-5 power plant. The radiation sensors were calibrated together during two periods with a variety of weather conditions: from 3rd until 10th of June and from 18th until 24th of September 2008. The second calibration was necessary to corroborate the first calibration and to include the radiation sensor of the MW-5 that was not working in June. During the calibration of the radiation sensors, the module temperature sensors were calibrated as well, using a digital thermometer that had been calibrated with a mercury-in-glass thermometer. While the pyranometers were very

accurate, according to the manufacturers' indication, the radiation sensors using PV-cells were not accurate and the configuration of the sensors at the data logger of the VIAX plant had to be adjusted (this configuration has been maintained until the end of this work without changes). The radiation sensor of the MW-5 and the temperature sensors could not be adjusted at the power plants, thus the measurement data had to be corrected afterwards. The main results of the calibration are shown on Table 3-1, in the form of the calibration factor that has to be applied to the original measurement data. For further measurements, the calibration should be carried out again, since the working years affect the radiation sensors significantly. Pyranometers also have to be calibrated every once in a while.

Table 3-1: Calibration results of the radiation and temperature sensors.

Sensor	Calibration Factor
Pyranometer 1 (Nr. 955711)	1.000
Pyranometer 2 (Nr. 924241)	0.997
Pyranometer 3 (Nr. 830194)	1.014
Pyranometer 4 (Nr. 7468)	Faulty
PV-Detector (Nr. 1211)	1.133
PV-Detector (Nr. 1016)	1.075
PV-Detector (Nr. 1018)	1.056
PV-Detector SensorBox MW-5	1.140
T-Sensor VIAX-module	0.734
T-Sensor VIAX-air	0.867
T-Sensor MW-5-module	1.100

Additional information about the sensors presented at Table 3-1 can be found on Appendix C.

3.2 Improvements made to the Power Plants

As mentioned in the previous chapter, some malfunctions were detected on both solar power plants, which did not allow the use of the plants for research, despite being connected to the grid and producing power. Some work done, in order to correct these problems, is presented in the following sections.

3.2.1 The MW-5 Plant

The problem of the MW-5 power plant was that it did not store any information on its data logger, the WebBox. The complete solar power plant was checked, including all the hardware connected and the software. The hardware includes: Solar modules, Inverters, data logger, solar and temperature sensors, internal bus RS485, RS485 power injector device, and internet connection. The software includes the internal software of the WebBox and the internet site of SMA, the Sunny Portal. The main detected problem after many hours of inspection by technicians of SMA was found to be at the connection of the internal bus RS485 which presented some problems. This was reconnected, allowing the WebBox to get data from the inverters and the sensors. In addition, the data logger was configured to record all important variables. The internet portal collecting the information from the WebBox was also set up improving its appearance and the format of the information displayed. The MW-5 power plant reached normal operating conditions on September 17th, 2008.

3.2.2 The VIAX Plant

To be able to use the VIAX power plant for scientific purposes, emulating a 2-axis tracker, the shadow problem had to be solved to eliminate the decrease in power related to this malfunction. To achieve this, the tracking mechanism of the VIAX was not modified, even if this was causing the shadow. Moreover the plant shown in Figure 2-4 and Figure 2-5 kept his construction configuration. Instead, the connection configuration of the solar

panels was changed. At its time of construction, the 8 existing solar panels were connected in series, having a I_{mpp} at the inverter of 6.9 A and a V_{mpp} of 243.6 V. The idea now was to separate both sides of the power plant, connecting the east side and the west side to separate inverters. By doing this, the east side inverter would deliver reliable data from sunrise until noon, while the west side inverter would deliver reliable data from noon until sunset, periods in which each side is not affected by the shadow effect. The shadow effect however would remain, keeping the amount of real generated energy under the expected level. At the beginning, the solar project company proposed two SB 700 inverters from SMA. This would have had the following configuration, due to the solar generators connected in series of four modules: I_{mpp} of 6.9 A and V_{mpp} of 121.8 V. Since none of the voltage input ranges of the inverter shown at Table 3-2 was satisfied with this configuration, the inverters had to be changed.

Table 3-2: Voltage input range of the SB 700 inverters.

Voltage Input Range	Nominal Power Output
19 ... 250 V DC	700 W
96 ... 200 V DC	600 W
73 ... 150 V DC	460 W

The final connection configuration used two SB 1100LV inverters from SMA. Two conditions have to be met for these two inverters. The maximum input voltage can be 60 V (DC), while the maximum input current can be as high as 62 A (DC). Connecting each string in parallel now, we get an I_{mpp} of 27.6 A and V_{mpp} of 30.45 V, thus meeting the necessary conditions for a proper operation of the power plant.

In addition to the replacement of the inverters, the complete electrical panel had to be redone, as shown on Figure 3-1. The new inverters were installed; the consumption meters (one for the generated energy and one for the self consumption) and the thermostat were kept; a switch for the DC current was added; and the circuit, most of it contained in an electrical box, was redesigned. Some other minor changes were made to the electrical panel as well. The wires connecting solar modules and inverters had to be replaced too.



Figure 3-1: New electrical panel for the VIAX power plant.

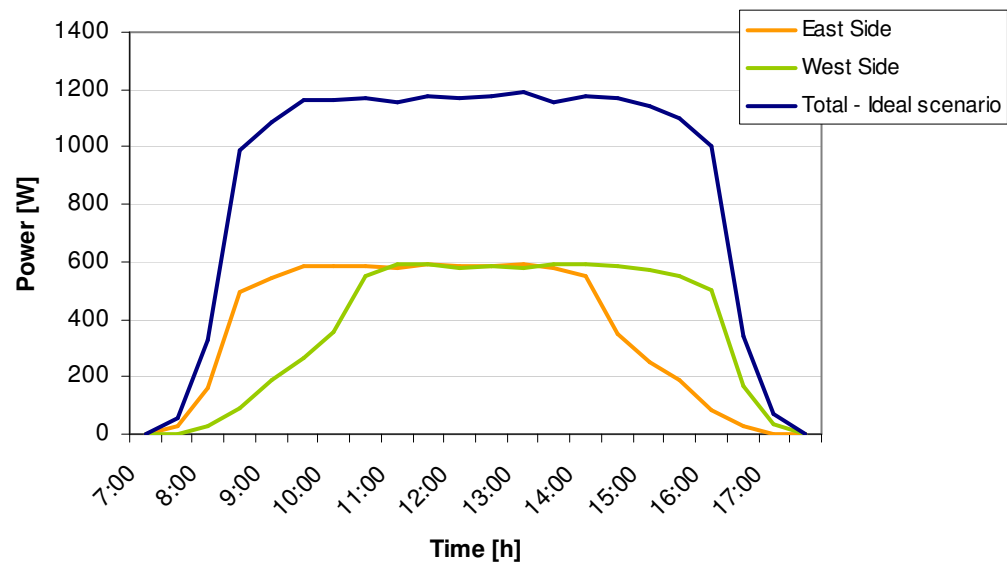


Figure 3-2: Power generated by each side of the VIAX and the ideal scenario without the shadow effect, calculated with the 2-inverter system.

Figure 3-2 shows the expected power generated by each side of the VIAX power plant as well as the total optimum power generated by a VIAX power plant without the shadow problem. This ideal VIAX power is calculated using the data of the east side during the first half of the day and data of the west side during the second half of the day. Since both sides have equal devices installed, we assume that the power generated by the east side in the morning represents half of the ideal power. Same method is used for the evening. The VIAX power plant came into normal operation conditions on August 29th, 2008. It was ready for research, including all sensors, on September 26th, 2008.

3.3 Data Measurement

3.3.1 Calibration of the Power Plants

After calibrating the radiation sensors of the power plants together and both plants into proper operations, the plants had to be calibrated with normal operating conditions. This was carried out in two phases, from the 27th of September until the 8th of October and from October 9th until the 20th of the same month. The second phase was the most important, since both power plants had almost equal elevation (VIAX at 27°) and azimuth angles on his solar modules. The VIAX power plant was set still at middle position. During this last period of time, the weather conditions alternated permanently going through cloudy and complete sunny days. The 16th of October was chosen as a representative cloudy day and the 18th of October as a representative complete sunny day for the calibrations.

3.3.2 Measurement Period and Weather Conditions

Once both power plants were calibrated together, the measurements could take place, beginning on October 20th, 2008. In a regular year, the month of October may present different weather conditions associated to autumn. November is usually considered

as the end of autumn and the beginning of winter, with the first snow falls and the first cold days with temperatures below 0°C. In the year 2008, this was not an exception, but it happened just at the end of the month. December is considered as a part of winter, with low temperatures, usually around 0°C and increasing snow falls. Temperatures may vary from days with -10°C up to days with 10°C, but most of them present temperatures between -5°C and 5°C. The measurements finalized on the first week of December 2008 due to the low temperatures, which prevented to obtain the data from the data logger of VIAX power plant anymore.

Based on the weather conditions for the measured period, which lasted 47 days, between October 20th and December 3rd 2008, we obtain the information shown on Table 3-3. During this period, three days presented good sun conditions over the complete day: November 5th, November 27th and December 3rd. Most of the days of the period can be classified as mostly cloudy days (13) or complete cloudy days (20). Under the complete cloudy days, six of them presented showers or snow falls. The remaining eleven days had some extended periods of sun. Four of these days changed from a complete cloudy day in the morning to a complete sunny day in the afternoon or vice versa, generating some interesting data for analysis in addition to the sunny days.

Table 3-3: Weather Condition of the days during the measurement period
from October 20th until December 3rd 2008.

Weather Condition	Number of days
Sunny Days	3
Mostly cloudy or complete cloudy days	33
Days with sunny periods	11

3.3.3 The MW-5 Plant

After the MW-5 power plant was set into work on September 17th, 2008, it started recording measured data properly. The variables recorded relate to the sensors and to the

inverters. The radiation sensor and the module temperature sensor give information 24 hours a day, while the inverters just provide data during its full operation period, which extends from sunrise until sunset. This is regulated with the power generation of the solar modules. As long as the power generated is greater than the self consumption of the inverters (20 W), the inverters keep working. The inverters deliver information on its operational status, input voltage and current, output voltage and current, power generation, total energy generated and some other variables that are not relevant for this work. An average value of each variable is recorded every five minutes.

The MW-5 power plant has measured radiation, module temperature and power generated since September 18th, 2008. There are still some days at which the power plant does not record any data or there is no data available on the internet portal. However, there is no information about the malfunction causing this or how to solve this occasional problem.

3.3.4 The VIAX Plant

Beginning September 27th, the VIAX power plant was fully operational, including its radiation sensors, which were taken away for calibration. Similar to the MW-5 plant, the VIAX records information related to the inverters and the sensors. Its three radiation sensors (global horizontal, global tilted and diffuse tilted), its two temperature sensors (ambient and module) and the wind direction and intensity sensors record information on the data logger 24 hours a day. The inverters provide information related to their power generation on the direct current and on the alternating current side during the daylight time, as the MW-5 plant does. The information is recorded every five minutes, storing average values of each variable.

The VIAX plant stores only data of the last 5 days of operation due to its limited data storage capacity. This data cannot be accessed via Internet as it must be transferred directly to a computer connected to the data logger. The procedure takes almost an hour to download 5 days stored data from the data logger. Since the weather conditions do not always make this operation feasible, there is no continuous register of the measured data of

the VIAX. However the important days during the measurement period were measured and the data was saved.

Some error in the programming of the PLC causes the solar tracker to move wrongly sometimes once a day. This problem occurs in the afternoon, mostly during one hour, from 3pm to 4pm for example. During this time, the tracker moves away from the sun path, interrupting the normal power generation and the measurement of the tilted radiation sensors.

3.4 Computer Simulations

In order to get results from computer simulations and analyze them, it is advisable to introduce the simulation program to be used and explain how the solar power plants are modeled with this software. Additional simulated models are explained in the following sections as well.

3.4.1 The INSEL Simulation Program

INSEL stands for INtegrated Simulation Environment Language. According to Doppelintegral (2006), it provides an integral environment and a graphical programming language for simulation applications. The basic idea of INSEL is to connect blocks to block diagrams that express a solution for a simulation task.

Instead of using only the classical programming format, with statements based on algorithmic programming languages like C or Fortran, INSEL facilitates the work by offering a graphical interface to the user, as most of the simulation software does today. For advanced simulation, the classical statement programming format is still available, allowing the user to personalize its software to its requirements. The graphical interface presents different graphical symbols (blocks) which can be interconnected by an easy

mouse operation to build up larger structures. The blocks can represent mathematical functions, real components like photovoltaic modules or inverters.

The main component of INSEL is the `inselEngine`, which is a full compiler that can interpret and execute applications written in INSEL language or graphical preprocessors like HP VEE. The graphical results are displayed by means of a public-domain software called Gnuplot.

INSEL can be used to carry out simulations of energy systems like solar thermal components, solar electricity components, wind turbines or water pumps.

The blocks used with INSEL can be classified in seven groups, depending on the task executed by each block, for example if the blocks are simply constants, some mathematical functions, timing blocks, loop blocks or decision points.

3.4.2 Simulation Models of the Existing Power Plants

Both Power plants, the MW-5 and the VIAX had to be modeled in order to compare the simulation results with the measured data and therefore validate the results of the simulations. The approach used to model the power plants can be separated into two different cases, depending on the input data used:

1. On the one hand, the horizontal radiation, the air temperature and the wind speed were used as input data for the simulation.
2. On the other hand, the total tilted radiation on the solar module and the module temperature were used as input data for the simulation.

Combining the two model options with the two tracking systems, we obtain four options shown on Table 3-4. Each one of these combinations will be explained in more detail in the following sections.

To get additional detailed information of the simulations related to block parameters see Appendix D.

Table 3-4: Four simulation combinations, using two different approaches with two power plants each.

		Tracking Mode	
		Fixed (MW-5)	2-Axes (VIAX)
Input Data Used	Horizontal Radiation (1)	FH	NH
	Tilted Radiation (2)	FT	NT

Using the horizontal radiation as input data, the general case can be represented in a simplified way by the flow chart of the modeled plant with INSEL at Figure 3-3. COUNTER runs the simulation with 288 iterations, each representing a 5 minute period. The DATA INPUT reads some meteorological data from a file, such as the global radiation on a horizontal surface G_h , the diffuse radiation on a horizontal surface $G_{h,diff}$, the Albedo value (ground reflectance ρ), the air temperature T_a and wind speed V_w . For each record representing a five minutes period, the time is also available. DATE indicates the year, month and day of the simulation. TRACKING MODE calculates the orientation of the power plant in function of the time and date, expressing the orientation as function of the azimuth orientation γ and the tilted angle β of the surface. HORIZONTAL TO TILTED RADIATION converts the input radiation on a horizontal surface to the radiation on a tilted surface, calculating the global radiation G_t , the direct or beam radiation $G_{t,beam}$, the diffuse radiation $G_{t,diff}$ and the reflected radiation $G_{t,ref}$ on a tilted surface, which corresponds to the tracked surface. PV-GENERATOR represents the solar panel and calculates the DC-voltage V_{dc} , the DC-current I_{dc} and the module temperature T_m . INVERTER calculates the AC-power P_{ac} . DATA OUTPUT writes the simulated results on a file. Table 3-5 shows which INSEL blocks are represented by the flow chart. TRACKING MODE and HORIZONTAL TO TILTED RADIATION have parameters related to the location of the power plants that have to be set before simulating.

The diffuse radiation on a horizontal surface $G_{h,diff}$, not being a measured value has to be calculated in order to use it as input data. This is carried out with a separate INSEL model comparing different calculation models explained later in this section and also considering standard irradiance values for $G_{h,diff}$ at the period of the year being studied. Also, a different INSEL tool to calculate the diffuse radiation was used to verify the accuracy of the results.

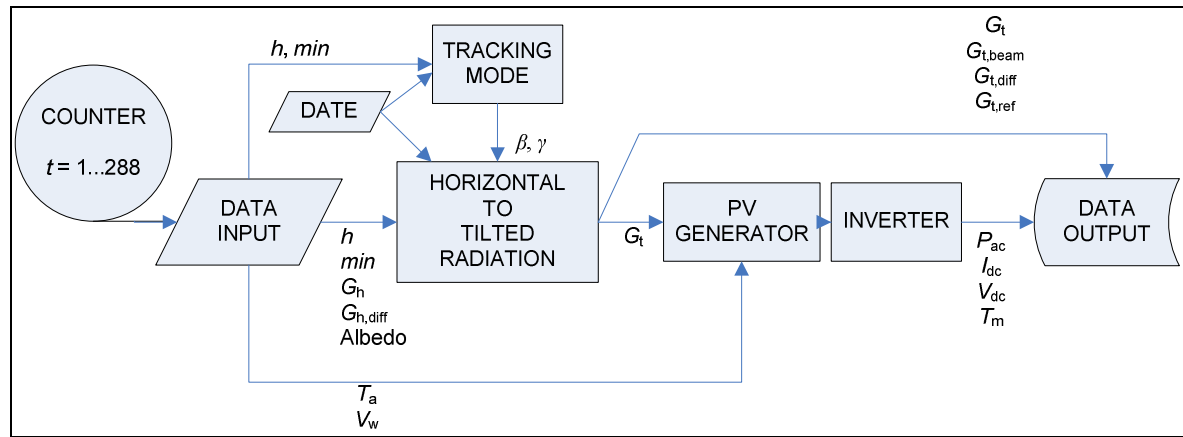


Figure 3-3: Flow Chart of the general case using the horizontal radiation, ambient temperature and wind speed as input data.

Table 3-5: INSEL blocks represented by the flow chart on Figure 3-3.

Flow Chart	INSEL block
COUNTER	do
DATA INPUT	readd
DATE	constant
TRACKING MODE	sunae, constant, math operations
HORIZONTAL TO TILTED RADIATION	gh2gt
PV-GENERATOR	pvi, mpp
INVERTER	ivp
DATA OUTPUT	write

The INSEL block *sunae* indicates the position of the sun and is used in these models if applicable to calculate the orientation of the tracking systems. To calculate the position of the sun, the *sunae* block offers three different approximations: Spencer, Holland & Mayer (set by default) and Michalsky. According to Doppelintegral (2006), Spencer is the fastest model in calculation time, but not very accurate. The Michalsky model is rather accurate (more than the other models), but slows the simulation down. The model of Holland & Mayer, chosen for this work, is a good compromise between calculation time and accuracy. The deviation of the Holland & Mayer model against the model of Michalsky is negligible and thus the best choice for the required accuracy of the work.

Another block used in the model, the *gh2gt* (global horizontal to global tilted), converts the radiation as described by its name. This block also offers a few models to make the calculation. The models are:

- Liu & Jordan
- Temps & Coulson
- Bugler, Hay and Kambezidis
- Klucher
- Hay
- Willmott
- Skartveit
- Olseth
- Gueymard
- Perez et al.
- Reindl et al.

The Liu & Jordan model from 1963, also known as the isotropic diffuse model and the default model on INSEL, assumes the total radiation on a tilted surface to be the sum of the beam radiation, the diffuse radiation and the ground reflected radiation. For the diffuse radiation, it considers this component to be completely isotropic. This has been the model

used in past simulations at the Technical University of Munich for 2-Axis tracking systems (Bernal, 2007). Equations 2.1 and 2.2 describe this model.

Duffie & Beckman (2006) refers to the Perez et al. model (1990) to be the most complex to use and the least conservative, although it is strongly recommended for tilted surfaces with γ far from 180° in the northern hemisphere or 0° in the southern hemisphere. Since this work relates more to azimuth angles close to 180° and less with angles far from 180° , the additional accuracy provided by the Perez et al. model should not be that relevant and will not be evaluated at this time. The main reason for this decision relies on the fact, that at morning and evening hours the measurement of the data is not easy to carry out and tends to show inaccuracies which make these measured hours less interesting. However, the effort considering the accuracy will be put on the hours close to midday, which does not require the application of the Perez et al. model.

Most of the other models offered by INSEL tend to be very similar since they have been developed considering the previous work done by the other investigators. Actually, some of them are better known as one model that integrates them, known as the HDKR-Model (Hay-Davis-Klucher-Reindl-Model) of 1990. These models seem to be less accurate than the Perez et al. model, but are good improvements of the Liu & Jordan model, based on the assumption, that the diffuse radiation is not just isotropic and thus again a good compromise between accuracy and complexity for this work.

Considering the last comments made on the offered models to calculate the different radiation components on a tilted surface using the radiation on a horizontal surface as input, the models used to simulate the power plants will be mainly the ones associated to the HDKR-Model and the Liu & Jordan Model.

In relation to the *pvi* block, which is used as a model of the PV module, it can be separated into two parts (Doppelintegral, 2006): an electrical model (the “two diode model”) and a thermal model based on energy balance. It is important to explain how the module temperature is calculated using the input data mentioned above. The block offers three possibilities:

- Assuming that the module temperature is equal to the air temperature

$$T_m = T_a$$

- Calculating it as a function of the voltage, the global tilted radiation on the module, the air temperature and the wind speed using. An extra timing variable is also required.

$$T_m = f(V, G_t, T_a, V_w, t)$$

- Calculating it using as reference the NOCT temperature (acronym for Nominal Operating Cell Temperature).

$$T_m = f(\text{NOCT}) = f(G_t, G_{\text{NOCT}}, T_a, T_{\text{NOCT}})$$

The first option does not really calculate any cell temperature and only interprets the input temperature of the *pvi* block as the module temperature. It is not a real option when only the air temperature is known, but it can be used for simulations where the module temperature is an available variable of the input data set. The second option is based on an energy balance which considers the energy absorbed by the module due to solar radiation, the energy losses due to convection and radiation, and the electrical power output of the generator. The most important item of this option is that it considers the wind speed, important for the forced convection. The third option calculates T_m using the NOCT temperature of the PV module. The nominal operating cell temperature is defined as the temperature of a PV module operated in its maximum power point under 800 W/m^2 of irradiance at an ambient temperature of 20°C and a wind speed of 1 m/s . If the NOCT temperature is known, the module temperature can be calculated at INSEL using the third option, which relies on the following equation:

$$T_m - T_a = (T_{\text{NOCT}} - T_a) \cdot \frac{G}{G_{\text{NOCT}}} \quad (3.1)$$

It is important to notice that the wind speed is not included in Equation 3.1 and therefore not considered in this model. This model is recommended to be used when the wind speed is not relevant or does not differ much from 1 m/s , value used for testing. For the simulations of this work using the air temperature as the input data to calculate the module temperature, the chosen model will depend mostly on the magnitude of the values of the wind speed. The first model will not be considered in this case.

The alternative case presented in this section, to simulate the solar power plants, was considering the measured global radiation directly on the solar panels, that means using the measured G_t and not converting G_h to G_t anymore. Along with using directly G_t , the temperature used was also the one registered at the solar panels. That means T_m . Again the general case of this option is presented in a simplified structure by Figure 3-4. Table 3-5 also shows which INSEL blocks are represented by the flow chart. The description of the chart resembles to the description of the first chart, thus it will not be written down again. From the INSEL blocks discussed above, the only relevant is the *pvi* block. It is important to state here, that the first model for calculating the module temperature is the chosen one, since the module temperature is a variable available at the data input.

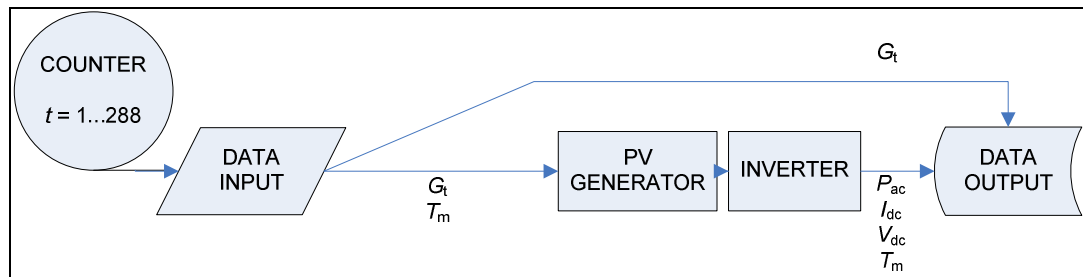


Figure 3-4: Flow Chart of the general case using the global tilted radiation and the module temperature.

At last, before describing each model in detail, one important issue must be addressed here. PV-GENERATOR represents the solar module and INVERTER represents the real inverter of the solar power plant at these models. INSEL provides a large database of PV modules and inverters to be used at the simulations. If a solar module or an inverter is not found at this database, the block representing these parts can be created according to Doppelintegral (2006). Searching at the database of INSEL, only the solar panels installed at the MW-5 power plant could be found. The solar modules used at the VIAX power plant, as well as the inverters of both power plants, could not be found and therefore have

to be created using information contained in the data sheets of the solar modules and the inverters, to determine the parameters needed by INSEL which simulate these parts.

3.4.2.1 FH Model - Fixed Plant with Horizontal Radiation as Input Data

This model represents a fixed plant, without any tracking system, where the solar modules are inclined towards the middle point of the sun path, trying to simulate the MW-5 power plant. The horizontal radiation and the air temperature are used as the main input data, along with the wind speed. The orientation of the power plant is towards south with $\gamma = 180^\circ$ and tilted angle $\beta = 25^\circ$. The horizontal radiation used corresponds to the radiation measured at the meteorological center of the LMU and at the VIAX power plant. The air temperature and the wind speed are measured at the LMU center as well. Figure 3-5 illustrates this model.

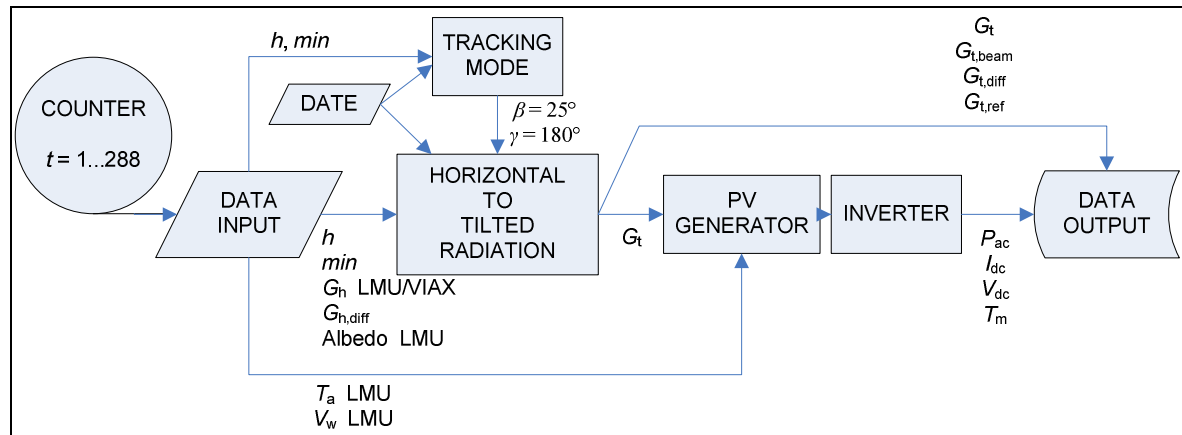


Figure 3-5: Scheme of the FH model.

3.4.2.2 FT Model - Fixed Plant with Tilted Radiation as Input Data

The FT model stands for a fixed solar power plant inclined towards the middle point of the sun path, as the FH model does. However, in this model, the position of the

sun and the orientation of the solar modules are not important, since the input data used corresponds to the measured data at the solar panels of the MW-5 power plant itself. The global tilted radiation is measured directly at the solar panels (see Figure 2-3) and embraces all incident radiation on the modules, such as beam radiation, diffuse radiation or reflected radiation. The air temperature is not considered here too, since the measured module temperature at the MW-5 plant is used as input variable. A simplified scheme of the model can be seen at Figure 3-6.

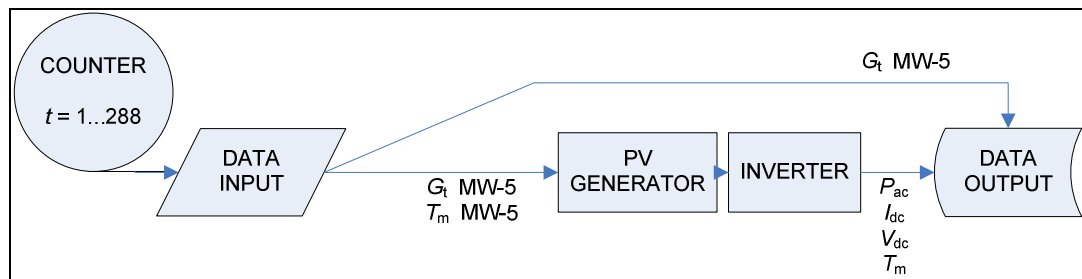


Figure 3-6: Scheme of the FT model.

3.4.2.3 NH Model - Two Axis Tracking with Horizontal Radiation as Input

Data

NH stands for “*Nachgeführt-Horizontal*” and means tracked-horizontal, thus being the model that corresponds to the VIAX power plant using horizontal radiation. In this model, the tracker follows the sun perfectly from sunrise until sunset. The horizontal radiation, the air temperature and the wind speed are used as input data, similar to the FH model. The radiation data comes from the LMU and the VIAX power plant; while the air temperature and the wind speed data comes from the VIAX, after crosschecking it with the data from the LMU center. Figure 3-7 shows the structure of the model.

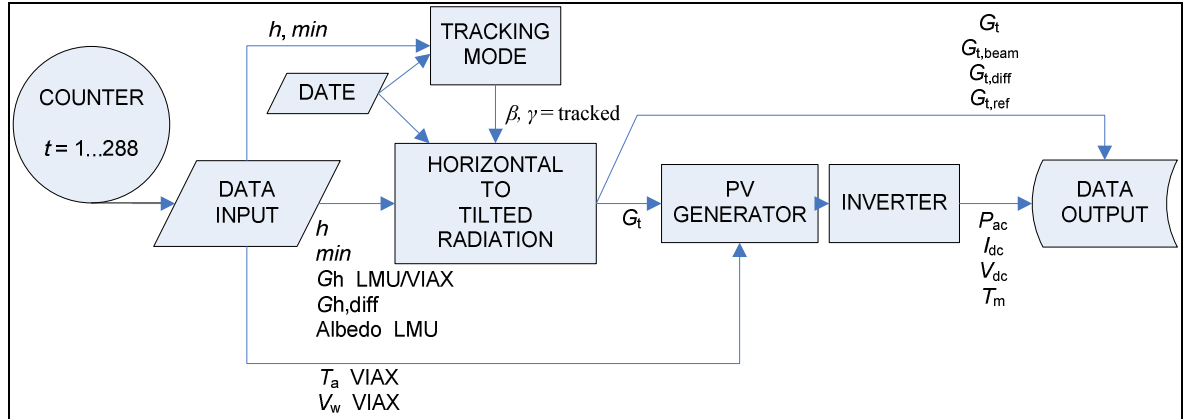


Figure 3-7: Scheme of the NH model.

3.4.2.4 NT Model - Two Axis Tracking with Tilted Radiation as Input Data

Finally the NT model is used to simulate a 2-axis tracker like the VIAX power plant, but using the global tilted radiation and the module temperature as data input. The global radiation on the solar modules of the VIAX is measured directly with the installed radiation sensors at the plant, as shown on Figure 3-8. The module temperature measured at the VIAX power plant is also used directly on this model, as it can be seen on Figure 3-9.



Figure 3-8: Radiation sensors at the VIAX power plant.

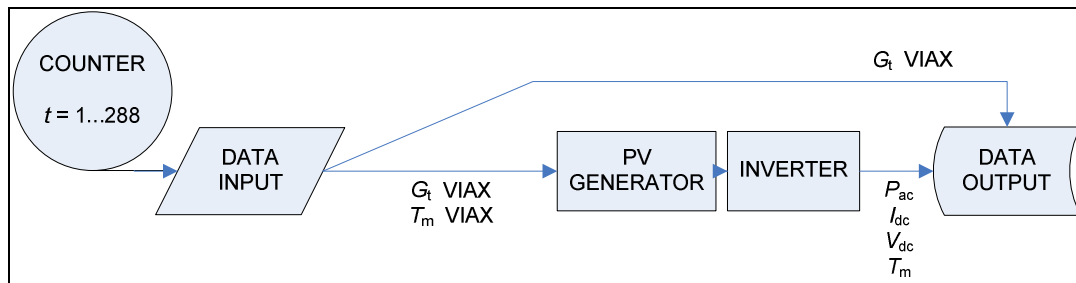


Figure 3-9: Scheme of the NT model.

3.4.3 Other Tracking Mechanisms

If the simulations of the tracking mechanisms, used at the Technical University of Munich, are validated with measured data, the software for simulation can be considered as a good estimating tool for the energy generated at solar power plants. The precision of the estimating tool will depend on the accuracy of the results obtained during the validation process. If the precision is good enough, the simulation models can be extended to generate new models representing other tracking mechanisms. This can then be used to compare several other different tracking mechanisms, more than just the ones represented by the power plants of the TUM. The idea is to evaluate all systems over a longer period of time, a year for example, and decide which one is the more appropriate.

In order to simulate the system over months, a year or just hours, the weather information contained in a weather data base of the location has to be used. For Munich, the SRY will be used. In general, as it is the case with the SRY too, the data is provided on an hourly basis, allowing to run the simulations over a desired period. In Figure 3-10, which shows a scheme of the simulation model, CLOCK represents the *clock* block of INSEL and is used to determine the period to be simulated, indicating which hours are being simulated to other process points like DATA INPUT, TRACKING MODE and HORIZONTAL TO TILTED RADIATION. This information can be delivered as the hour of the year ($h \in [1-8760]$) to DATA INPUT for example, or as time and date to the other tasks of the simulation process. The other processes of the model work the same way as

described in the previous sections. The simulation method used compares to the first model used to simulate the real power plants that means using the global horizontal radiation, the air temperature and the wind speed as input data.

The main solar power plant systems simulated are:

- No tracking, fixed solar modules during the whole year at the optimum tilted angle
- Seasonal tracking, with two or four steps a year with fixed modules at a constant tilted angle during each season of the year
- Azimuth tracking
- Double axis tracking

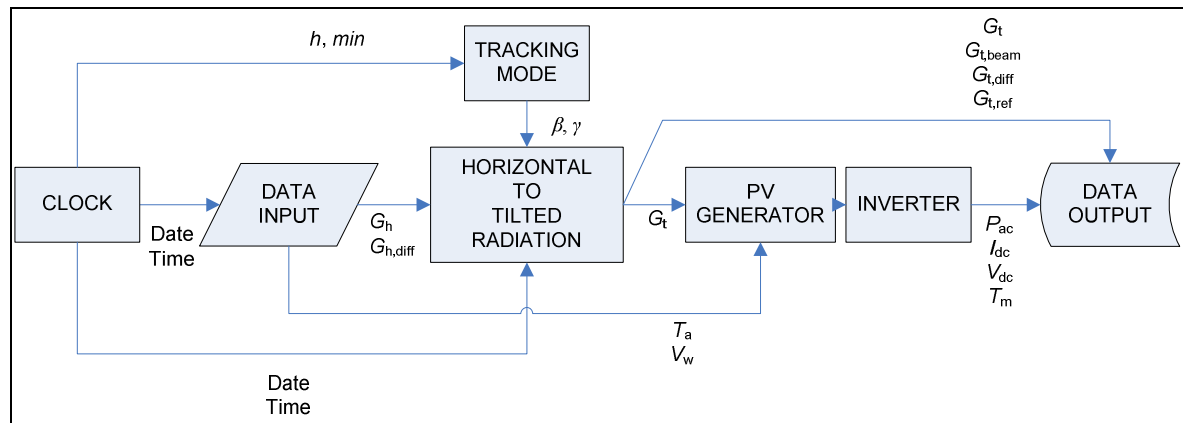


Figure 3-10: Scheme of the simulation model for all tracking mechanisms using the SRY as input data.

Summary

As seen in this chapter, at first, the radiation and temperature sensors of the power plants had to be calibrated, which will have to be done again the next time that measurements are carried out. Despite that the power plants were repaired and improved, and are currently working and recording data, some additional improvements could be done, for example, changing the radiation sensors and installing pyranometers. Also, the tracking control of the VIAX power plant has to be checked. An extensive measurement work carried out in order to get enough data for analysis was also commented. The simulation models were explained in detail, considering two different approaches for simulating the measured days. Further simulation work to extend the utility of the models was also mentioned.

4 RESULTS AND ANALYSIS

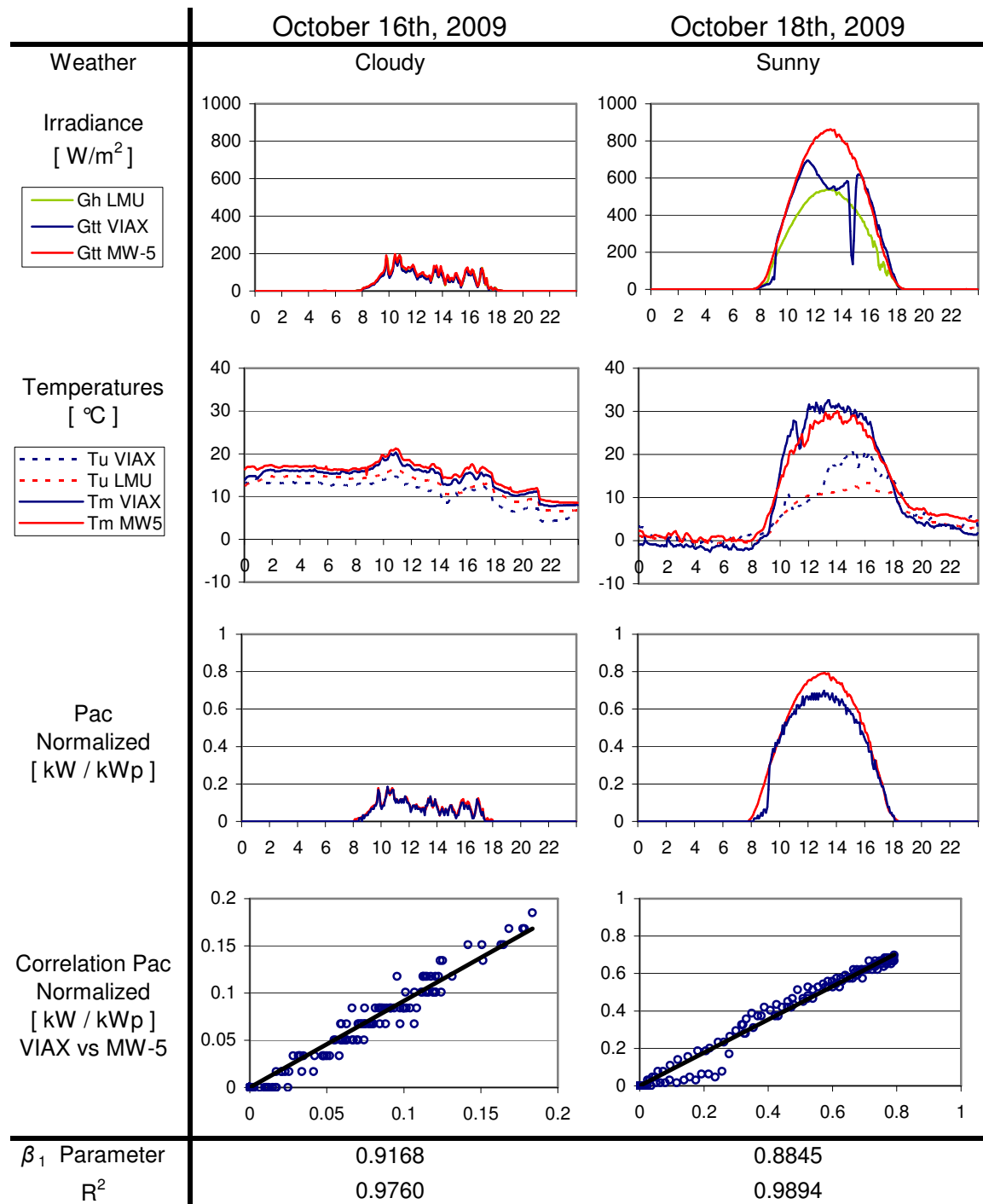
The present chapter will expose the results obtained during the measurement period with the solar power plants in Munich as explained in the last chapter and the results of the simulations with the computer software. It will also analyze both approaches and compare them, trying to obtain a relation between real data and simulated data. Further some essential problems of the computer simulations, like the Batman-Effect will be discussed. The existing results will be used to extend the computer simulations to other solar tracking mechanisms and evaluate them together. At last, some practical applications of the previous results are used for Chilean locations and a brief economic evaluation is exposed.

To facilitate the interpretation of the results in this chapter, a color convention will be applied. Results according to the MW-5 power plant will be presented in red color from now on, while the results related to the VIAX will be presented in blue. This is for means of the tilted radiation on the solar modules, the power generation or the temperatures. The global horizontal radiation will be shown in green. Orange will be assigned to the simulated values. This convention will be kept during the complete chapter unless otherwise told.

4.1 Measured Data with the power plants at Munich

Before the measurement of the meteorological data could take place, as proposed, both power plants, the MW-5 and the VIAX had to be calibrated together, as mentioned in Section 3.3.1. Two days were chosen as representative days for cloudy and sunny weather conditions during the calibration period. The results of the calibration process are shown in Table 4-1. October 16th, 2008, presents a typical cloudy day in autumn, with low irradiance levels, module temperatures that are not much influenced by the solar radiation and small power generation for both power plants (normalized and expressed as kW/kWp).

Table 4-1: Calibration information on a cloudy and a sunny day for the MW-5 and the VIAX power plants, and the parameters of the linear regression.



October 18th, 2008 on the other hand, has been chosen as a typical complete sunny day in autumn (happens not to often), with a nice shape of the measured irradiance for the day, solar module temperatures that are obviously higher than the air temperatures due to the incidence of the sun and an expected shape for the power generation curve. The radiation graph showing the irradiance levels for the sunny day has an uneven curve for the global tilted radiation on the VIAX power plant. This can be explained due to the fact that as shown on Figure 3-8, the metal plate designed to create shape on the solar sensor measuring diffuse radiation levels, has shaped the tilted radiation sensor. Remember that the VIAX has been set still, at an elevation angle of 27° and oriented towards the south, thus not at the right position for the radiation sensors, considering that the sun reaches an elevation of 32.24° that day. At least the first and the last hours of the daylight time illustrate the coincidence of the radiation measurement on both power plants. Taking a look now at the power generation graph of the same day, it can be observed that the VIAX power plant reaches clearly a lower normalized radiation than the MW-5. For the cloudy day this also happens, but can not be recognized easily in this graph. To quantify this decline, the values of the normalized power were compared and a linear regression of the form

$$Y_i = \beta_0 + \beta_1 \cdot X_i + \varepsilon_i \quad (4.1)$$

was used to estimate the relationship between both power plants. At night, when the power generation of the MW-5 equals zero ($X_i = 0$), the power generation of the VIAX equals zero as well ($Y_i = 0$) and thus $\beta_0 = 0$. In consequence only one parameter, β_1 , has to be estimated. The values for the estimated β_1 parameters are shown in Table 4-1. For the cloudy day, the value of β_1 equals 0.9168 with $R^2 = 0.9760$, while for the sunny day, the value of β_1 equals 0.8845 with $R^2 = 0.9894$. Since the values of the coefficient of determination are close to 1, the linear regressions are assumed to be representative for the cases. These calculated values for the parameters of the linear fit will be used when adjusting measured data to compare both power plants. The difference between the values for cloudy and sunny days will be taken into consideration.

Previous to the review of the measured data, some operational aspects of the solar power plants have to be discussed. The improvements made to the MW-5 power plant have allowed, in general, to obtain reliable data concerning its operation. In the case of the VIAX power plant, the upgraded power plant also allowed to get consistent data from its data logger, considering mostly the changes in its operation due to the new inverters installed, separating the data measurement on both sides. For October 18th, 2008, the comparison of the power generation of both sides can be seen in Figure 4-1. It is easy to see how the east side of the power plant gets smooth data during the morning, while the west side does the same in the evening. During the first hour of the day, a small decrease in the values of the east side appears in the graph due to shadow caused by a few trees. For a measured day with normal tracking operation of the VIAX, the Figure 3-2 represents very well the situation as it was expected to be, confirming the success of the applied measures. Having the chance to separate the data measurement on both sides, the ideal power generation of the VIAX can be calculated and used for further analysis.

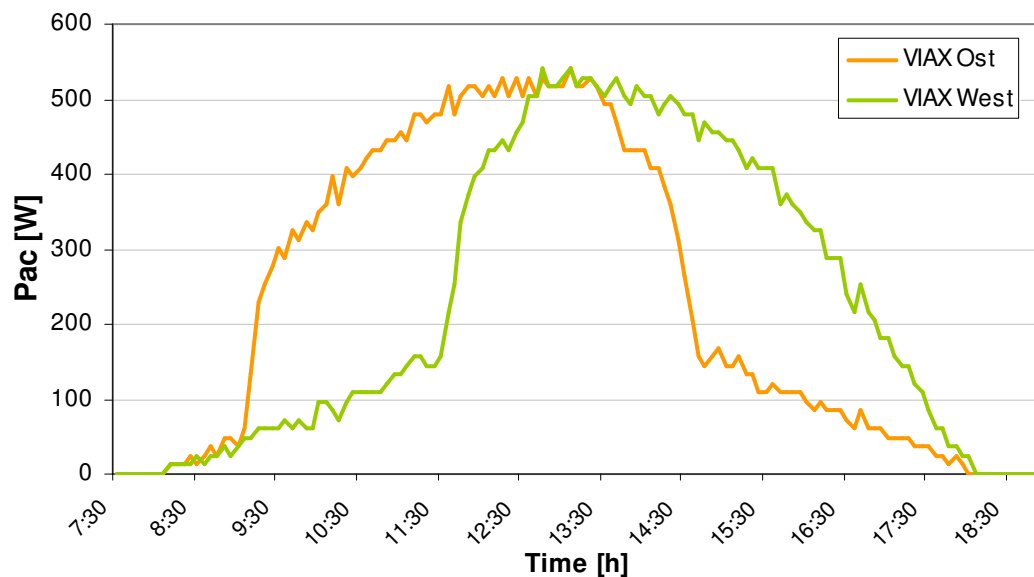


Figure 4-1: Power generated by each side of the VIAX during a sunny day (October 18th, 2008) with no tracking operation, using the 2-inverter configuration.

As mentioned in Chapter 3, the measurement period extended over 47 days, with 3 complete sunny days, 33 cloudy days and 11 days with changing weather conditions. Some chosen representative days for each weather condition can be seen in Table 4-2. From the 3 complete sunny days in this period, only one day (November 5th, 2008) provides reliable data for analysis, since the tracking system of the VIAX failed during the other two days, which had extraordinary weather conditions for analysis, with clear skies. Under the

Table 4-2: Measurement results of representative days for the measurement period (October 20th to December 3rd 2008) commented with the selected days.

Date	Weather Condition	Data Recording		Comment	Selected
		MW-5	VIAX		
24-Oct-2008	Cloudy	✓	✓	Regular	
25-Oct-2008	Cloudy-Sunny	✓	✓	Cloudy in the morning, sunny in the afternoon. Appropriate data for analysis.	✓
01-Nov-2008	Cloudy-Sunny	✗	✓	Cloudy in the morning, sunny in the afternoon. Appropriate data. MW-5 failed.	
03-Nov-2008	Changing	✓	✓	Fast changing weather, not appropriate for simulation.	
05-Nov-2008	Sunny	✓	✓	Almost complete sunny day. Ideal data for analysis.	✓
06-Nov-2008	Cloudy	✓	✓	Heavy clouds. Appropriate.	✓
26-Nov-2008	Cloudy	✓	✓	Regular	
27-Nov-2008	Sunny	✓	✗	Complete sunny day. Ideal data for analysis. VIAX tracking system failed during a few hours	
03-Dec-2008	Sunny	✓	✗	Complete sunny day. Ideal data for analysis. VIAX tracking system failed during a few hours	

cloudy days, even if a few days were available for analysis, only one day (November 6th, 2008) was chosen to represent the weather conditions of days with small irradiance levels and almost no beam radiation. Days with fast changing weather conditions are not appropriate for analysis, since the simulation results are not reliable in such cases, due to the irregular evaluation of the data by the simulation software. Other interesting days for measuring are discussed here, which had cloudy conditions in the morning and sunny weather conditions in the afternoon, with a relatively smooth transition from one condition to the other. Unfortunately during one of these days, the MW-5 power plant did not record any data, so just one of these days (October 25th, 2008) will be available. Summarizing, we have following days for analysis:

- November 5th, 2008. **Sunny** day with almost complete clear sky.
- November 6th, 2008. Complete **cloudy** day with low irradiance.
- October 25th, 2008. **Cloudy** in the morning, **sunny** in the afternoon.

The measurement results for these days will be presented in this previous order in the following pages, showing for each day its irradiance levels for:

- Global horizontal radiation (LMU and VIAX)
- Reflected horizontal radiation (LMU)
- Global tilted radiation (Fixed MW-5 and 2-axis tracked VIAX)
- Tilted diffuse radiation (2-axis tracked VIAX)

also its temperatures:

- Air temperature (LMU and VIAX plant)
- Module temperature (MW-5 and VIAX)

its power generation, the efficiency of the power plants in relation to its maximum generation capacity and some comparisons.

The **5th of November** was one of the last complete sunny days during the year 2008 in Munich and surroundings, almost without clouds. This weather condition can be the result of a *Föhn* day, with higher temperatures than the average for that time of the year and a clear sky. As we see on Figure 4-2 and Figure 4-3, these conditions are met on this

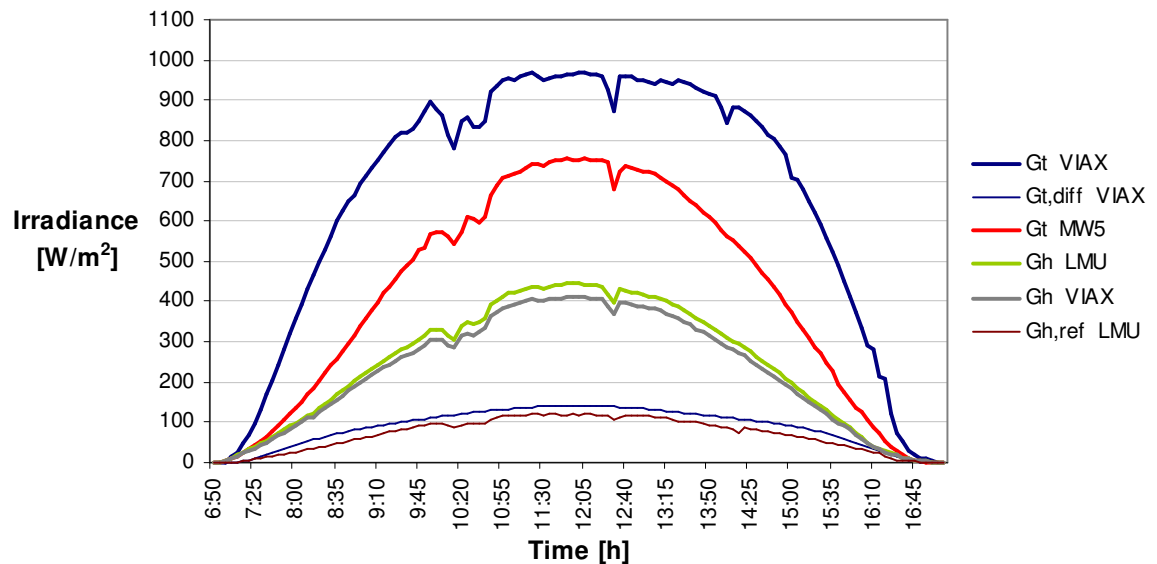


Figure 4-2: Irradiance levels measured at November 5th, 2008 in Garching at Munich.

day. Figure 4-2 shows the shape of the horizontal radiation is as it would expected to be for a sunny day (close to a sinus curve), with some impurities that reveal the presence of some clouds during the day. These impurities avoid it being a perfect day, but they help us to read the graph. It can also be observed, that the tilted radiation sensor of the MW-5 measured a higher irradiance due to its inclination towards south ($\beta = 25^\circ$) and that the irradiance measured by the sensor of the VIAX is even higher due to its tracking system. All these observations would have been expected. Some important information for this day is that the sun reaches an elevation over the horizon of 26.18° at noon, sunrise time is 7.10 a.m. and sunset is at 4.44 p.m., with a day length of 9h 34min. It is important to notice, that the horizontal radiation measured at the VIAX power plant does not match the measurement at the LMU meteorological center. The horizontal radiation measured at LMU is 7.91% higher than the measurement at the VIAX. There are two important arguments to state that the LMU data is the right one. First, the LMU measurement center uses pyranometers to measure the sun and not radiation sensors made of solar cells, thus being more accurate, since pyranometers are instruments for radiation measurement and not just photovoltaic detectors, which can have important errors according to Duffie &

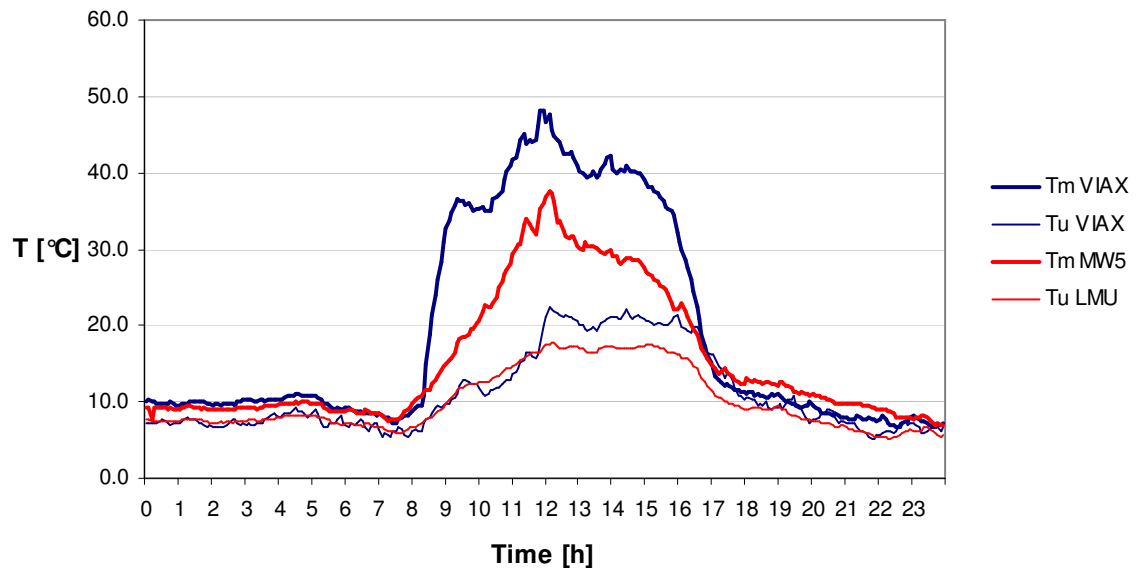


Figure 4-3: Temperatures measured at November 5th, 2008 in Garching at Munich.

Beckman (2006). One important item is that the pyranometers are not easily affected by the reflection of the sun beam, as it happens with a common radiation sensor. This measurement error may not be clear enough now, but we will come back to it later in this section. The second argument to state that LMU measurements are right, is that comparing the measured data with another student, doing other experiments at the roof of the MW-7, measured irradiance levels (also measured with pyranometers) which resemble quite well the measurements of the LMU.

Figure 4-3 shows the development of the temperatures on that day. It is interesting to see how the module temperatures reach a peak in both power plants at 12:10 p.m. The reason for this seems to be the effect of the wind around this time of the day. The wind speed can be seen on Figure 4-4, with its lowest point during the middle of the day at exactly 12:10 p.m. This variation in the wind speed of about 2 m/s affects the module temperature in 5 up to 10 degrees Celsius. However these changes in the module temperature do not seem to influence the power generation of the power plants as can be seen in Figure 4-5. There are no such peaks in this graph that could be attributed to the

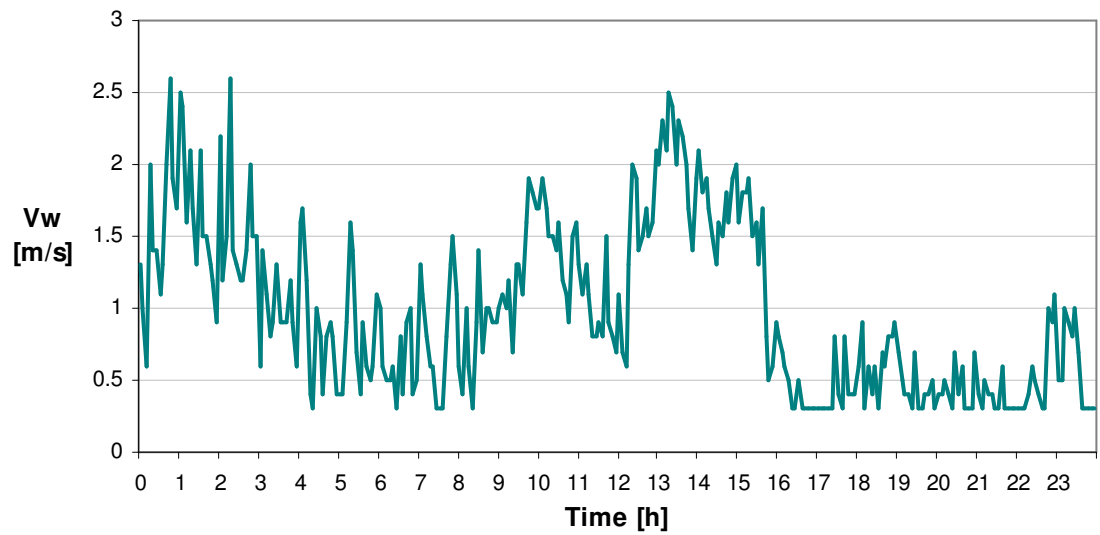


Figure 4-4: Wind speed measured at November 5th, 2008 in Garching at Munich.

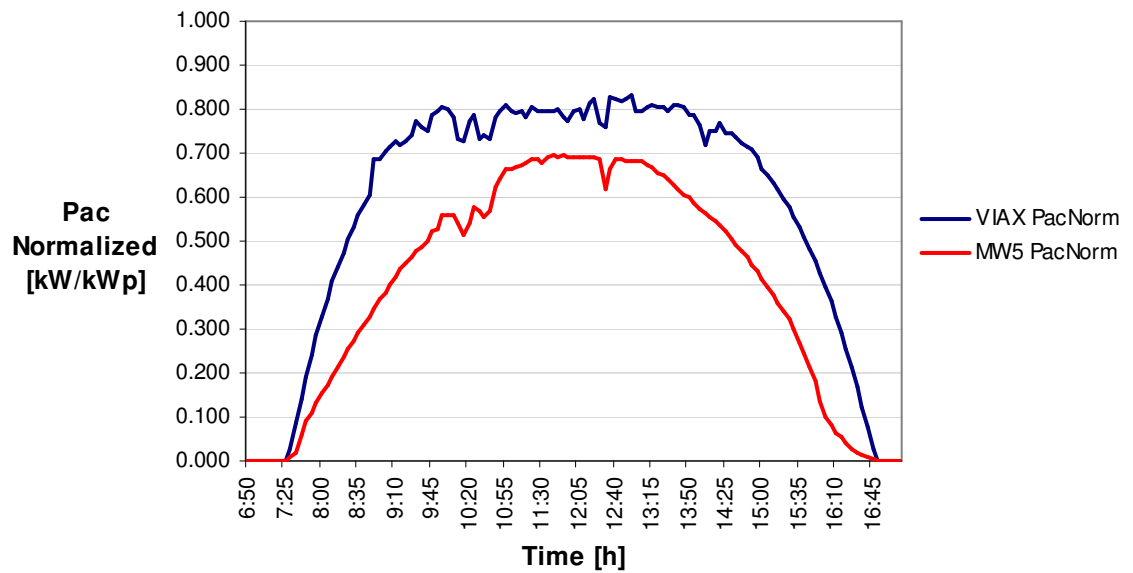


Figure 4-5: Power generation measured at November 5th, 2008 in Garching at Munich.

changes in the wind speed, and therefore in the module temperature. The effect of the clouds affecting the radiation, instead, can be distinguished much easier on the power generation, as it does for example between 10:05 and 10:50 a.m. and around 12:30 p.m. for the MW-5. Some other considerations have to be made at this point relating the power generation of the power plants. As it can be also seen on Figure 4-5, the MW-5 power plant generates at its maximum for the day about 70% of its peak generating potential (kWp) at Standard Testing Conditions. At STC, modules are tested at 25°C and 1000 W/m². While the MW-5 works in the range between 30°C and 40°C having therefore a variation between 5°C and 15°C to STC, the VIAX works at temperatures between 40°C and 50°C having between 15°C and 25°C of difference to STC. The difference in the module temperatures seems to be due to the difference of the irradiance on the modules. If, respecting the logic of the temperature effect, the VIAX, having a higher temperature divergence should also have a lower working efficiency. This does not happen. More important seems to be the effect of the radiation differences. While the MW-5 gets only 75% of the STC irradiance, the VIAX gets almost 95%. Since the VIAX has a higher irradiance level and also a higher relative power generation (kW/kWp), it is clear that the changes in radiation levels are much more crucial than the temperature variations. However, the temperature seems to play some role anyway, since the 20% difference comparing radiation decreases to only about 10% comparing power generation.

To get a closer look of what was mentioned in the last paragraph, let's take a look at the following approach. The idea is to remove the effects due to irradiance levels and temperature, normalizing the power values and therefore being able to better compare the efficiency of the power plants before going into the inverters. To do this, we will normalize with the Standard Testing Conditions of the solar modules, parameters that are known for each solar module type and use them in the following equation:

$$F = \frac{P_{dc} \cdot \frac{S_{STC}}{S} \cdot [1 - k_p \cdot (T - T_{STC})]}{P_{STC}} \quad (4.2)$$

where,

P_{dc}	=	Power generation of the plant at the DC side
P_{STC}	=	Power of the solar power plant at STC
S	=	Irradiance level on the solar modules (G_t)
S_{STC}	=	Irradiance level at STC (1000 W/m^2)
T	=	Temperature of the solar Modules (T_m)
T_{STC}	=	Temperature at STC (25°C)
k_p	=	Temperature coefficient of power

Since $k_p = -0.44 \text{ \%}/\text{K}$ for the solar modules used at the MW-5 and at the VIAX (information obtained from the data sheets of the solar panels), all values for the Equation 4.2 are known. F should be then considered as a calculated factor that will show the efficiency of the power plants, once the effects of the temperature and the solar radiation have been set aside. The results for F for November 5th, 2009 are shown at Figure 4-6. Early and late hours should not be considered as truthful information at this diagram due to some measuring problems, generating some marked inaccuracies.

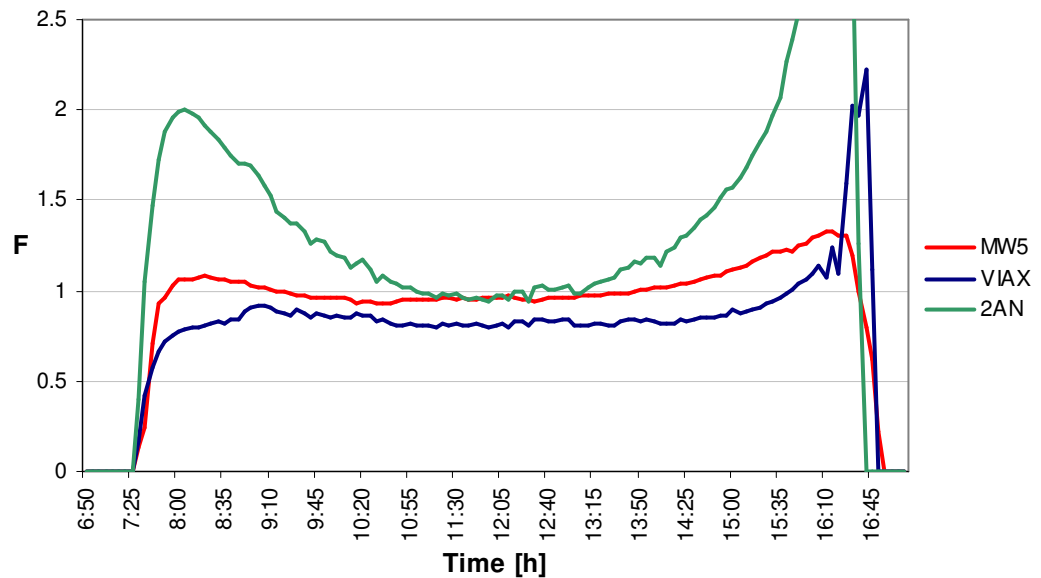


Figure 4-6: Comparison factor (F) for both power plants measured at November 5th, 2008 in Garching at Munich.

As it can be seen at Figure 4-6, the values of F for the MW-5 are close to 1.00, this means that the power plant works with a high efficiency, or generating the power that would be expected for the parameters given by the manufacturer. The VIAX instead, shows values for F around 0.80. There is no clear reason for this behavior. Now mixing values from the MW-5 and the VIAX, the curve 2AN of the Figure 4-6 can be drawn. This curve normalizes the power of the VIAX with the irradiance and the module temperature of the MW-5, in order to see the gain due to the tracking system. It is easy to observe how the shape of the line curves up before and after noon, compared with the MW-5 curve, showing the gain in comparison to a static system. Using tendency lines at these curves to compare values of these two systems, the gain of the tracked system over the static system lies between 42% and 53%. Notice also that the red line also curves up slightly before and after noon, which can be explained by the fact that the radiation sensors of the MW-5 are being affected by reflection at the time when the sun does not shine directly on the sensor and this effect is stronger in early and late hours. This means that the measured irradiance is lower than the real one, causing F to increase in Equation 4.2. Some could argue and say that the reflection also affects the solar modules, which would mean that P_{dc} is lower than it really is and would make F decrease in Equation 4.2, compensating the effect of reflection on the sensor. This might be true in some way. However the reflection on the radiation sensors is much higher than the radiation on the solar modules, due to the glass surface of the parts. While the solar modules have a slightly rough glass on its surface, the solar sensors have a flat glass, which tends to be more prone to reflection.

Comparing now the real gain between the static tilted (MW-5) and the tracked (VIAX) systems, we get the results shown on Table 4-3.

Table 4-3: Measurement results for November 5th, 2008.

	Irradiation kWh/m ²	Energy kWh/kWp
MW-5	4.29	4.18
VIAX	6.73	5.99
Gain	56.75%	43.31%

There is a difference of over 13% between the gains in irradiation and energy. The inverters work with an efficiency difference of about 2% to 5% comparing both plants, thus a remaining 8% to 11% difference can be attributed to other factors, for example the module temperature. The reflection should affect the measurement of the irradiance and would not play a role in the difference. An approximate 3% to 4% difference as it will be seen later could be caused by the running time of the power plants. Thus a remaining 4% to 8% could be attributed to the effects of the module temperature and measurement inaccuracies. Considering a 10°C difference between the module temperatures, this would mean a 4.4% loss ($k_p = -0.44 \text{ \%}/\text{K}$). The numbers seem to match. Recalling what was said before, according to the differences calculated with F for P_{dc} , the range from 42% to 53% also fits quite well between the 43.31% of the energy difference and the 56.75% of the irradiation variation.

November 6th, 2008, was a typical cloudy day in autumn like most of the days in that season of the year. Low irradiance levels and moderate temperatures are characteristic conditions for such days. Looking at Figure 4-7 and 4-8 this can be confirmed.

Figure 4-7 shows the irradiance levels for the day, which were very low, compared to the 5th of November. The global horizontal radiation moves between 10% and 40% (at the peaks) of a sunny day. For the tilted radiation on the power plants the decrease is even stronger, with a range from 5% to 30% for the MW-5 and 4% to 14% for the VIAX. The irradiance for the day is only about a 10% of sunny day, as will be seen later. There is no visible gain for the tracked system compared to static system. Moreover, the MW-5 shows higher irradiance levels than the VIAX, the inverse situation of a sunny day.

It is important to mention here, that the diffuse radiation measured by the VIAX lies around 60% of the global tilted radiation. This measured data however, will not be considered, in view of the fact that on a complete cloudy day all the radiation from the sun is scattered by the water in the atmosphere, according to the Mie scattering (Mie, 1908). Since, at this work, all the radiation affected by scattering is considered to be diffuse radiation, the values for the diffuse radiation will be set equal to the ones measured as global radiation. In addition, the global horizontal radiation measured by the VIAX is not shown on the graph, since it differs only by 1% from the measurements of the LMU center.

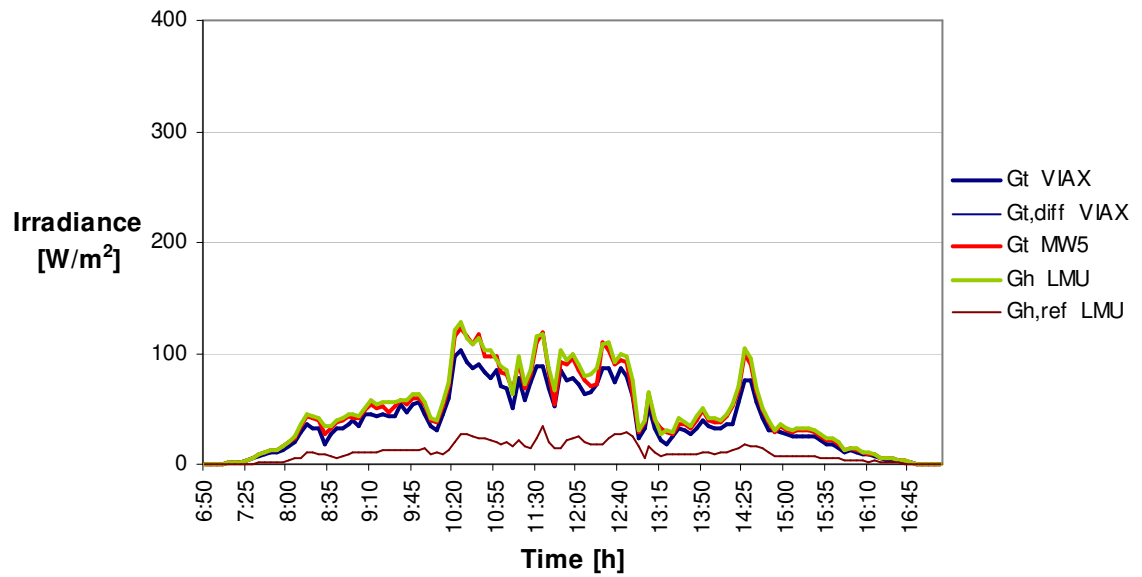


Figure 4-7: Irradiance levels measured at November 6th, 2008 in Garching at Munich.

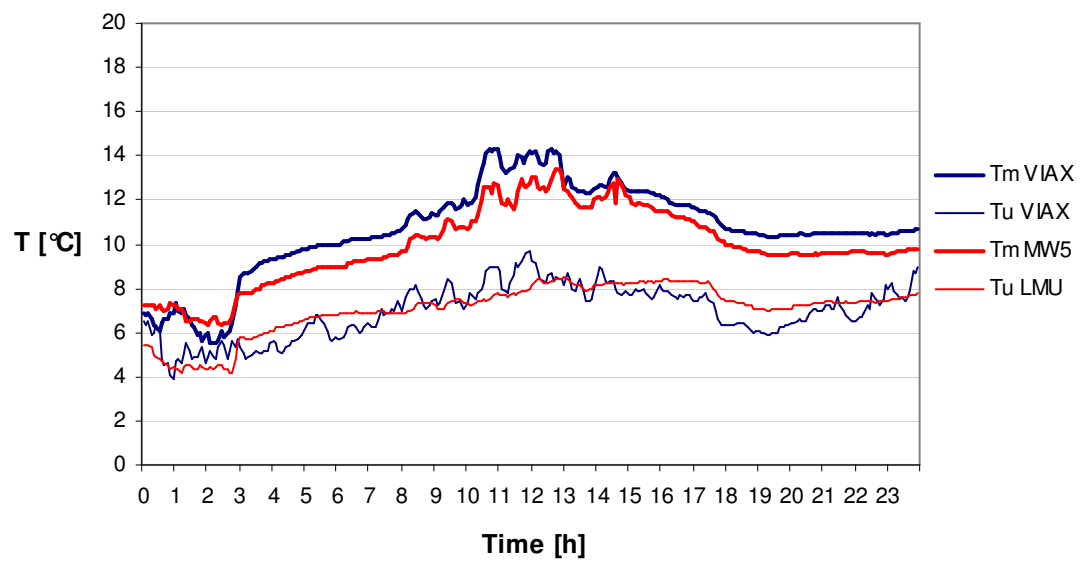


Figure 4-8: Temperatures measured at November 6th, 2008 in Garching at Munich.

The temperatures for the day are shown on Figure 4-8. The air temperature increases only from 4°C to almost 10°C. These are moderate changes, considering the previous day. The module temperatures are between 2°C and 4°C higher during the daylight time and are also moderate values. Some peaks in the module temperature can be easily attributed to the changes in radiation.

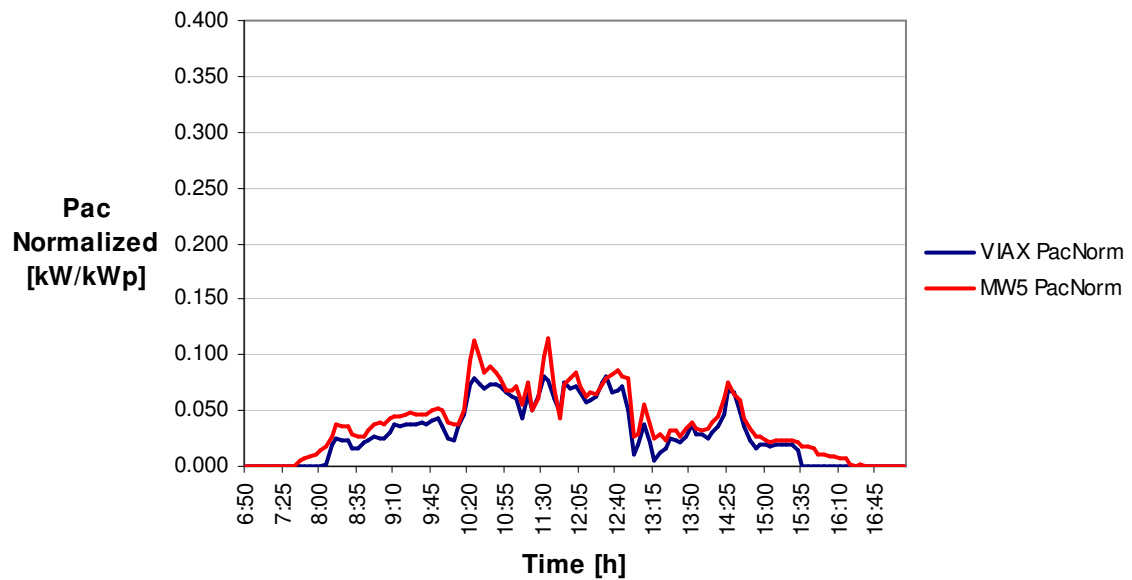


Figure 4-9: Power generation measured at November 6th, 2008 in Garching at Munich.

The power generation can be seen at Figure 4-9. The shape of the curve resembles visibly the shape of the irradiance curve. The power generation levels are also very low varying from 1% to 12% of the peak generation capacity. Again, like in the irradiation levels, there is no significant gain in energy comparing the VIAX with the MW-5. What is more, it seems to be a decrease in the generated power for the VIAX. To compare now both power plants, let's take a look at the numbers shown in Table 4-4. If these results are correct, that means that on cloudy days, a tracked system loses energy compared to a static system, the amount of energy gained in one sunny day like the 5th of November would be lost in 21 days like the 6th of November.

Table 4-4: Measurement results for November 6th, 2008.

	Irradiation kWh/m ²	Energy kWh/kWp
MW-5	0.472	0.396
VIAX	0.398	0.310
Gain	-15.70%	-21.68%

The last day analyzed here will be **October 25th, 2008**. This day had some special weather conditions, which will help to better understand the first studied days in this chapter. It started with sun in the early morning, turned cloudy for a few hours and then turned sunny again just before noon for the rest of the day. Figure 4-10 and Figure 4-11 show this situation, where the weather conditions of November 5th and 6th are combined in one day. The effects described before considering irradiance and temperature repeat here as well.

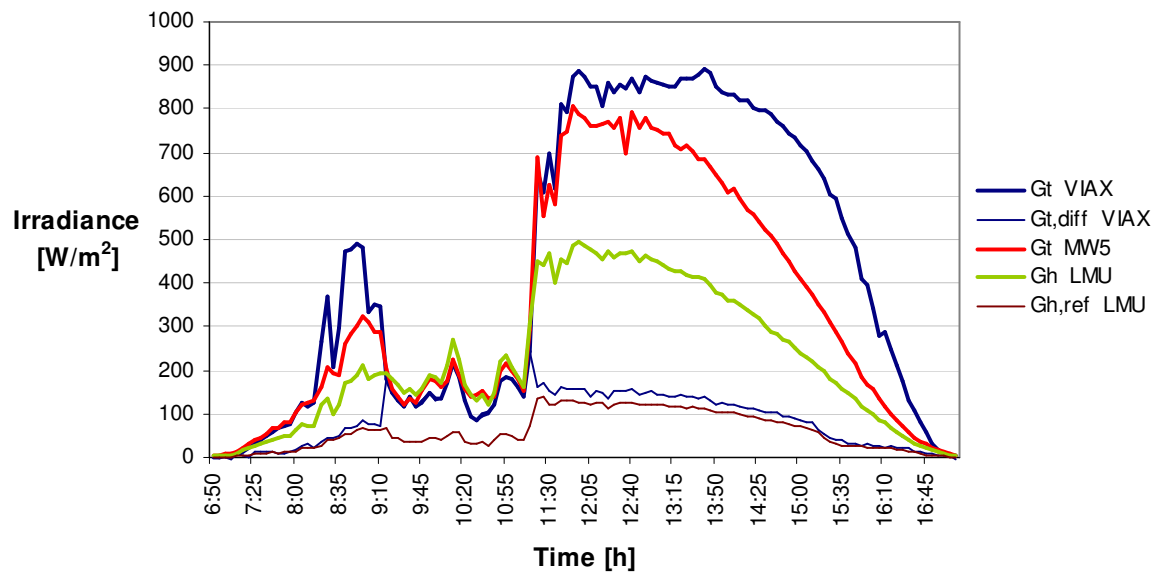


Figure 4-10: Irradiance levels measured at October 25th, 2008 in Garching at Munich.

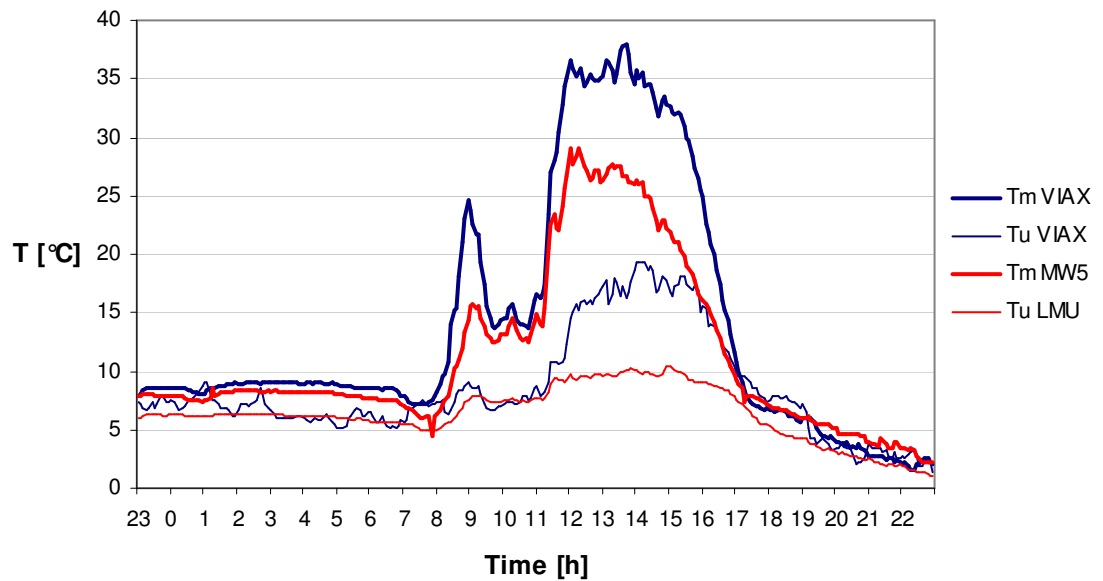


Figure 4-11: Temperatures measured at October 25th, 2008 in Garching at Munich.

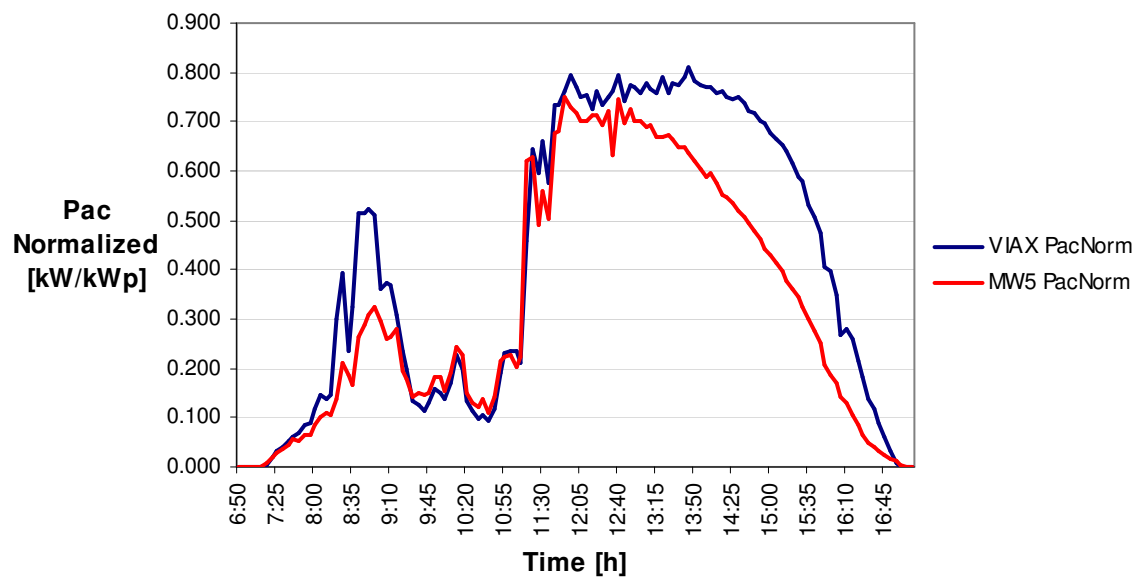


Figure 4-12: Power generation measured at October 25th, 2008 in Garching at Munich.

One remark has to be made here about the data of October 25th. The irradiance levels were higher during the sunny time of the day than the irradiance levels of November 5th, considering the global horizontal radiation. This explains also why the tilted radiation on the MW-5 for this day was higher than for November 5th. The tilted radiation on the VIAX however did not increase as expected. For this day we had a regular maximum around 850 W/m² with peaks up to 900 W/m², values that were lower than the maximum measured at November 5th of 960 W/m². We passed from a 28% of irradiance gain of the VIAX over the MW5 to only a 12%. The same remarks apply to the power generation levels, with values lower than expected considering the precedent established on November 5th. Here the gain in power generation of 17% reduced to only 8%. This decrease may lie at least in part on the fact that the sun reached an elevation of 29.76° over the horizon, 3.58° higher than on November 5th. Thus the angle of incidence of the radiation changed, reducing the benefit of the solar tracking system over the static one. Let us compare now more precise results of irradiation and energy for this day, shown on Table 4-5.

Table 4-5: Measurement results for October 25th, 2008.

	Irradiation kWh/m ²	Energy kWh/kWp
MW-5	3.50	3.40
VIAX	4.47	4.29
Gain	27.93%	26.05%

Let us go back now to a topic mentioned before in this chapter related with differences concerning the radiation measurement at the VIAX plant and at the LMU center. More specific, it deals with the difference in the measurement using photovoltaic detectors as radiation sensors or pyranometers. Table 4-6 shows the measurement losses on the global horizontal radiation for some days during the measurement period. As we can see, as time passes and the sun reaches lower elevation angles at noon, the incidence angle

Table 4-6: Irradiance measurement losses with photovoltaic detectors compared to pyranometers.

	Irradiance Decrease	Sun Elevation at Noon
October 18 th , 2008	4.59%	32.24°
October 25 th , 2008	5.54%	29.76°
November 5 th , 2008	7.33%	26.18°
November 27 th , 2008	12.62%	20.74°

of beam radiation increases at our horizontal sensors. This seems to affect in a different way the measurement accuracy of the photovoltaic detector and the pyranometer. Pyranometers are instruments built to measure solar radiation, and it can be assumed that the values given by these instruments are more accurate in comparison to other irradiance sensors. This is also stated by Duffie & Beckman (2006). It can be thus concluded, that reflection plays an important role on the measurement accuracy of the photovoltaic detectors. This could be avoided using pyranometers.

4.2 *Simulated Data for the plants at Munich*

To facilitate the evaluation of the simulated results, they will be presented in this section briefly, in order to see some shapes, but will be analyzed in more detail in the next section when compared with the measured data. Results can be seen in Figure 4-13, Figure 4-14, Figure 4-15 and Table 4-7. The rest of the section deals with some considerations during the simulation procedure.

Some models used at the different blocks of INSEL have to be commented here. For the *gh2gt* block, the options were the Liu & Jordan Model and the models related to the HDKR-Model. The models associated to the HDKR-Model presented very similar results considering the global radiation. Also for the diffuse radiation the results were alike and showing almost the same tendency. Finally the Klucher Model from INSEL was chosen to represent this group. Analyzing the results obtained with the Liu & Jordan Model, there were two main problems. First, the global radiation calculated for the tilted surfaces differed strongly from the measured data, with results under the measured values. By comparing the irradiance at midday for November 5th, the error was 17.1%. Second, the diffuse radiation also differed from the measured values. Even more important, according to the Liu & Jordan Model, the diffuse radiation decreases on tilted surfaces oriented towards the sun when compared with a horizontal surface on a sunny day. These results do not match the measured values. Actually both arguments are related, and this is a consequence of the isotropic model for diffuse radiation. On the other hand, the results for the global and the diffuse radiation on tilted surfaces of the Klucher Model give similar values to the measured ones. It also models better the diffuse radiation, in the sense that the diffuse radiation increases when the surfaces are oriented towards the sun. Since the differences between both models are evident, only the Klucher model was used for the calculations.

Considering the *pvi* block now, the model used to calculate the temperature of the solar panels was the one that uses as reference the NOCT temperature. The main reason for this choice was that the wind speed was not high enough during the measurement period (autumn) to be considered as a significant parameter for the simulations, affecting the

calculation of the module temperature. The results for module temperature with and without the wind speed do not differ considerably.

Since the database of INSEL did not contain files for most of the parts used at the power plants, the blocks needed had to be created using information contained in the data sheets of the solar modules and the inverters. This method however, did not work correctly, since the INSEL process to create these blocks failed and determined wrong parameters. To work out this problem, only one kind of standard solar modules and inverters were used, for which INSEL had the required information in its database. The values for power output were normalized to its peak capacity and could be compared in future with simulation models using the real components of the power plants. The configuration of the simulated power plant used is two strings of 12 Solon P220/6+ (230 Wp) modules and an inverter SB 6000U of SMA.

Table 4-7: Measurement results for the simulated models.

		Irradiation kWh/m ²	Energy kWh/kWp	
Input Radiation		Horizontal	Horizontal	Tilted
MW-5 VIAX		FH		FT
		NH		NT
November 5th 2008	MW-5	4.28	4.07	4.20
	VIAX	6.75	6.20	6.36
	Gain	57.44%	52.36%	51.26%
November 6th 2008	MW-5	0.479	0.387	0.377
	VIAX	0.382	0.291	0.302
	Gain	-20.11%	-24.81%	-19.94%
October 25th 2008	MW-5	3.53	3.43	3.47
	VIAX	4.72	4.36	4.31
	Gain	33.58%	27.21%	24.05%

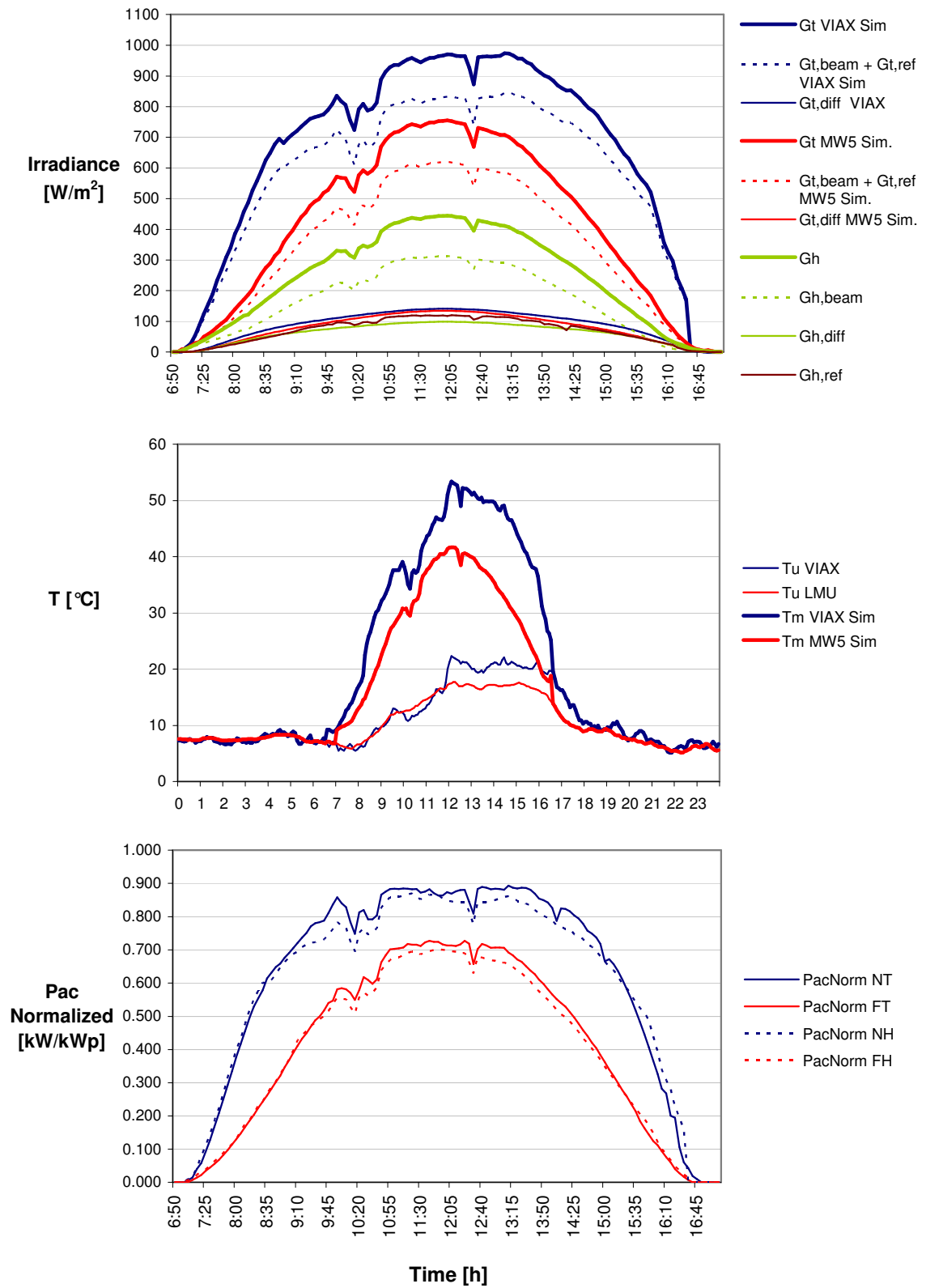


Figure 4-13: Simulation results for November 5th, 2008.

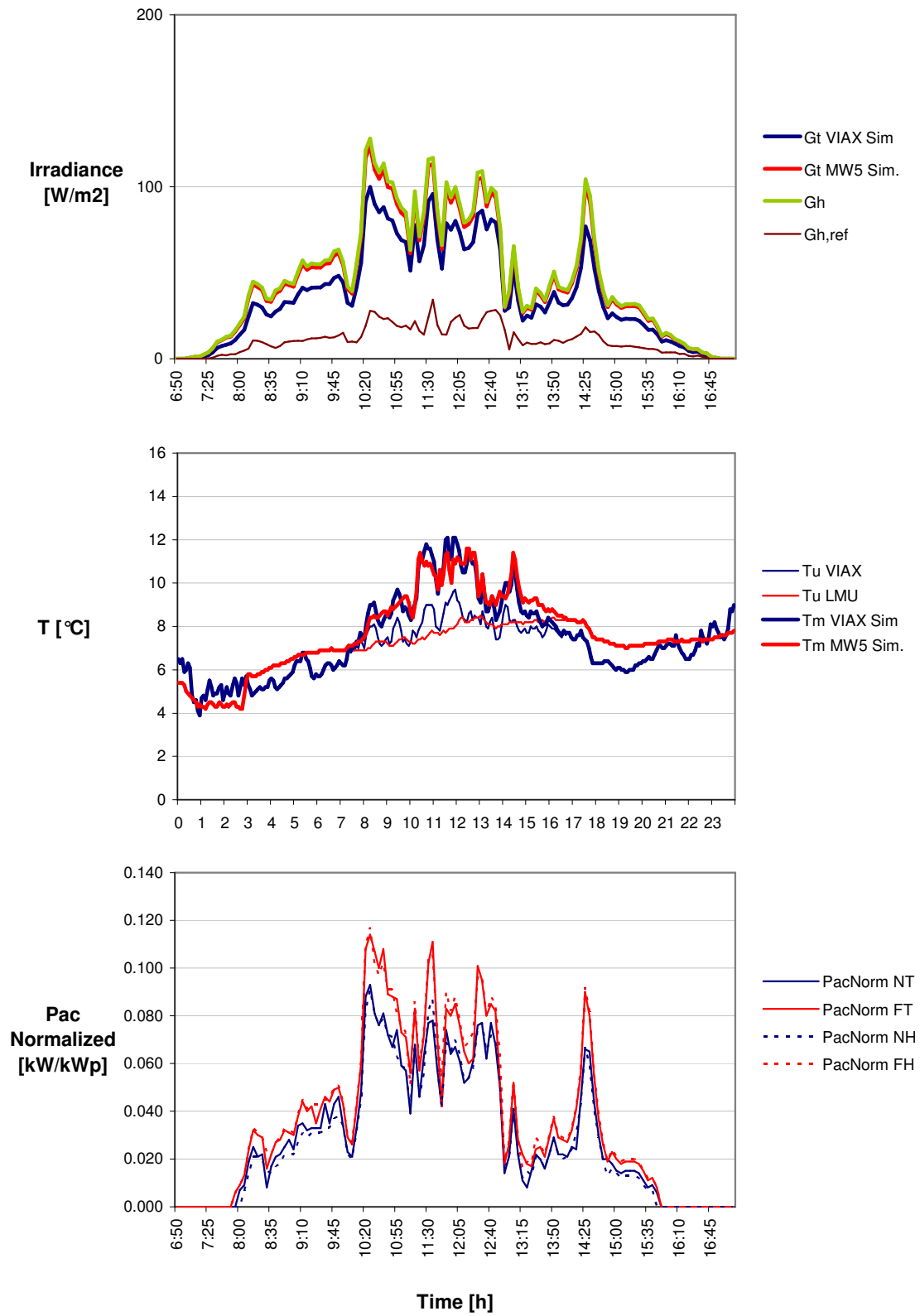


Figure 4-14: Simulation results for November 6th, 2008.

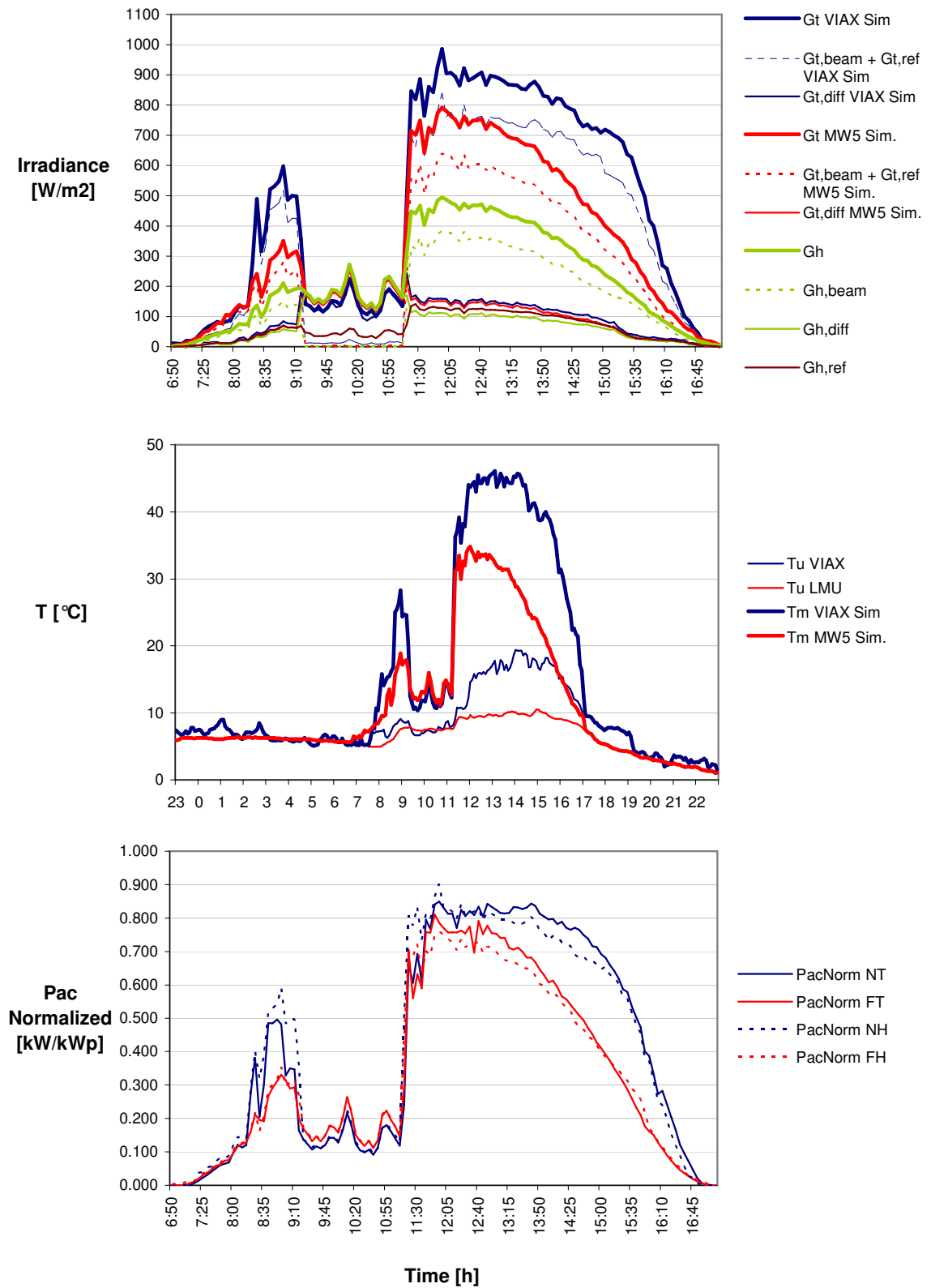


Figure 4-15: Simulation results for October 25th, 2008.

4.3 Comparison of Experimental and Simulated Data

The main purpose of this section is to compare the measured data of the solar power plants with the simulated results of INSEL. If the results are close enough, it could be assumed that the simulations with INSEL represent in a good manner the real data, thus allowing us to simulate other periods of the year and other tracking mechanisms.

Starting with our sunny day, the **5th of November 2008**, comparing solar radiation levels, we get the results shown in Figure 4-16. The simulated curves in yellow, in this case, correspond to a fixed tilted power plant (MW-5). Comparing the global radiation on the tilted surface (“ G_t MW-5” and “ G_t MW-5 Sim”), the curves seem to match in a good way. Also the simulated diffused radiation behaves as expected, being higher

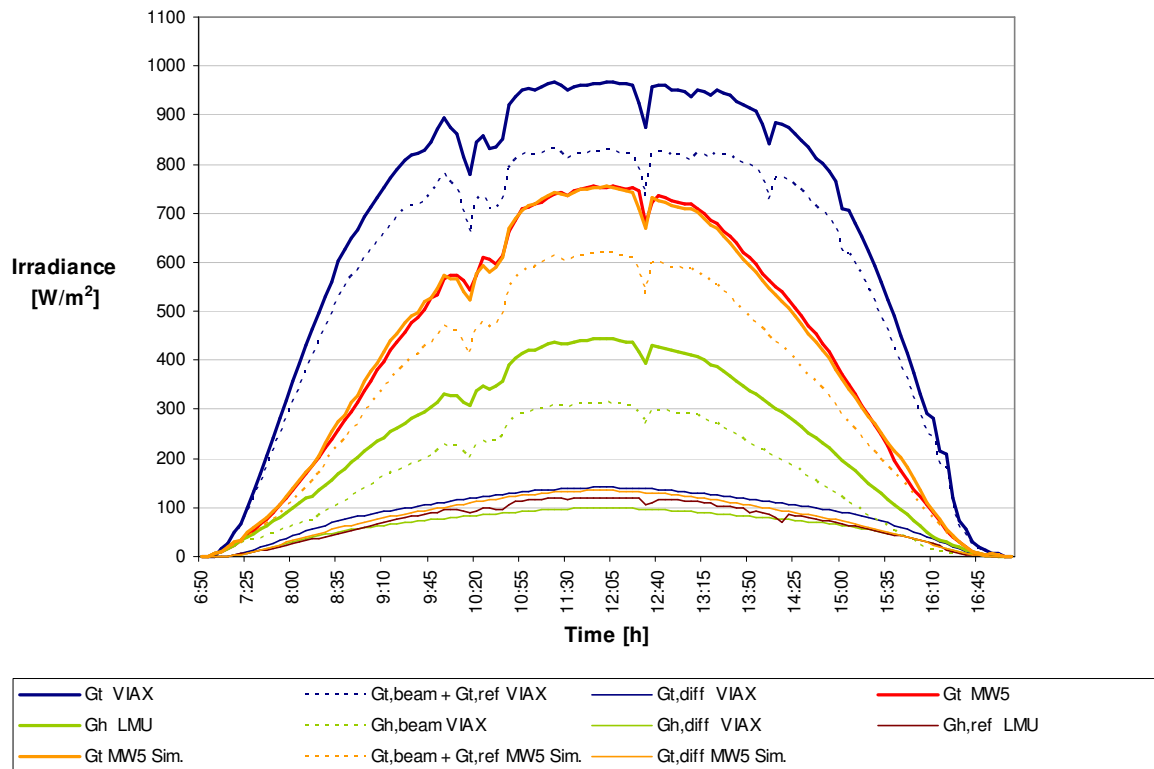


Figure 4-16: Comparison of irradiance levels for measured data and simulation results on a tilted fixed surface, November 5th, 2008 in Garching at Munich.

than the diffused radiation on the horizontal surface but lower than the diffused radiation on the VIAX plant. The error of the simulation results, compared to the experimental results considering irradiation, over the complete day is -0.16%.

Figure 4-17 shows the comparison of the simulated curve for the tracked power plant (VIAX) and the curve for the measured data. Also this time the curves (“ G_t VIAX” and “ G_t VIAX Sim.”) seem to match, but not as well as in the last case. The main differences can be observed at the global tilted radiation, as a consequence of the differences in the beam radiation. The diffuse radiation tends to be very similar and helps to validate the assumption made by using the Klucher Model for the simulations. Comparing the irradiation over the day, the errors tend to compensate, since the simulated irradiance is lower in the morning and higher in the evening. In numbers, the simulated irradiance over the day is 0.28% higher than the experimental irradiation.

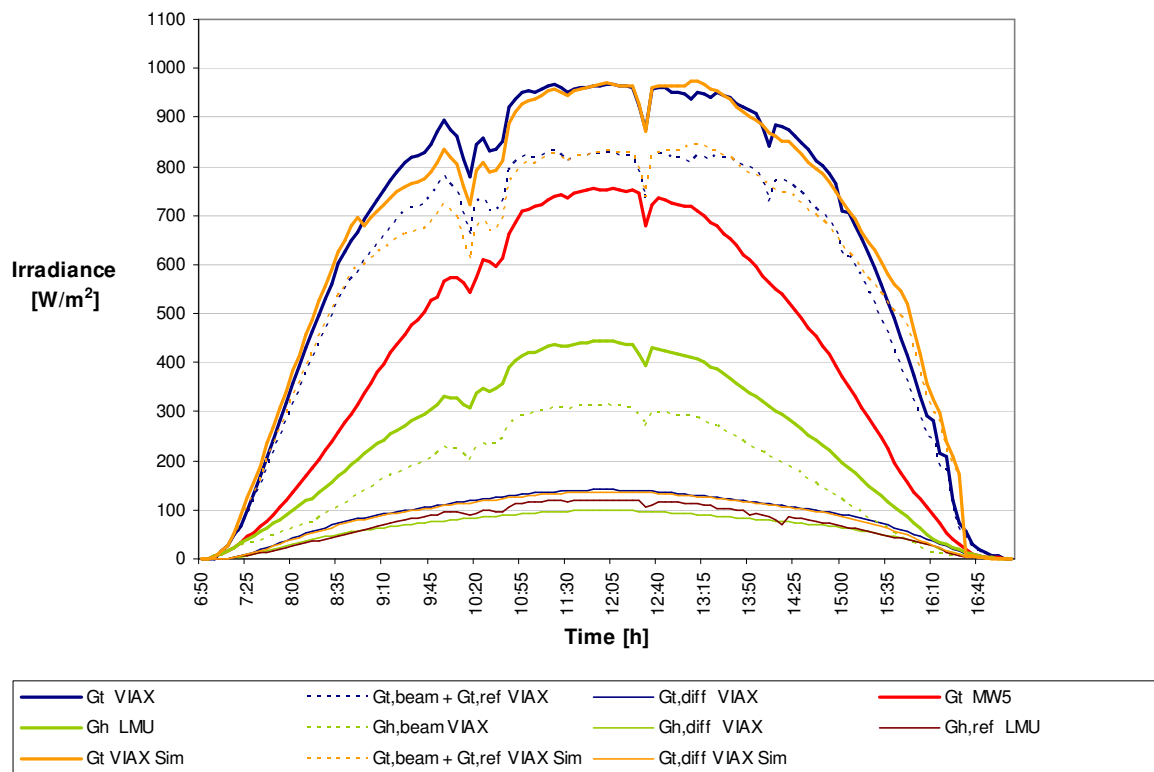


Figure 4-17: Comparison of irradiance levels for measured data and simulation results on a tracked surface, November 5th, 2008 in Garching at Munich.

Figure 4-18 shows the temperatures over the day. As can be seen, the simulated temperatures reach higher values than the real temperatures. These differences could be attributed in some way to the wind speed, as seen in section 1 of this chapter, but not completely. The precise reasons for these differences, with its exact effects on the module temperatures, escape from the purpose of this work and will not be treated here. The effects of the temperature differences however will be mentioned.

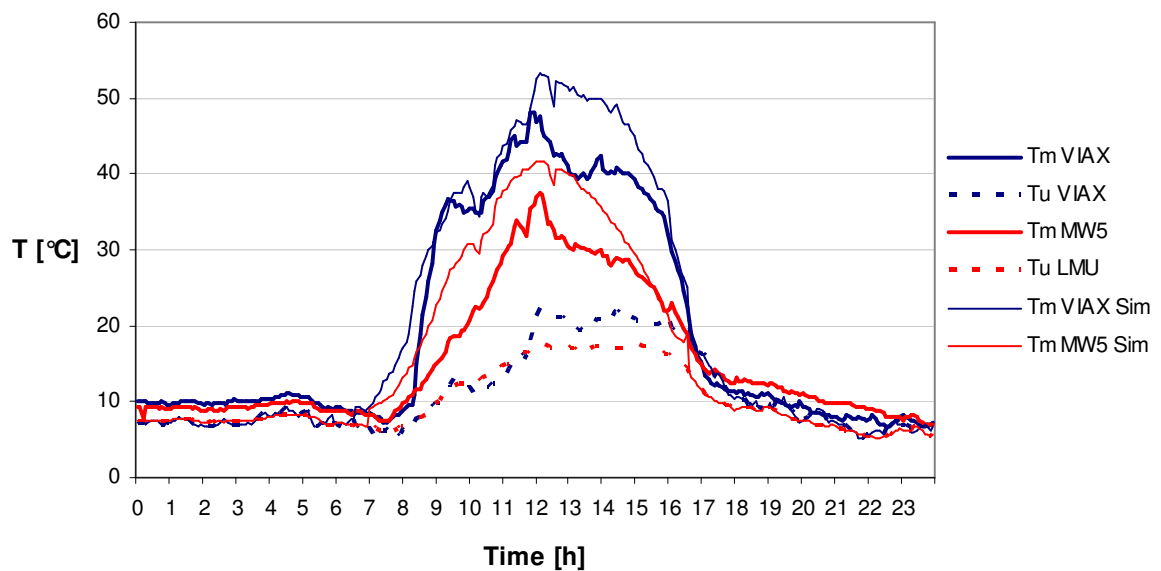


Figure 4-18: Temperatures of measured data and simulation results, November 5th, 2008 in Garching at Munich.

Finally the comparison of the power generation is showed on Figure 4-19. For the fixed power plant (MW-5) the simulated values fit very well, with some small divergences of course between both simulation models. Considering that the real radiation and the simulated radiation have almost the same irradiance levels as it was seen before, the difference between the two models (FH, using the horizontal radiation as input and FT, using the tilted radiation as input) could lie in the temperature differences mentioned before. For the FH-Model, the error at 11.30 a.m. for the power generation is 1.09% and the error for generated energy over the day is -2.65%. This last difference is caused by the

divergence seen in the afternoon. For the FT-Model, the errors are 4.92% for the power level at 11.30 a.m. and 0.56% for energy generation. For this last error, we see again the compensation between the error during the midday and the error in the evening hours.

The simulation results of the VIAX power plant, on the other hand, show higher differences to the measured values. Here the temperatures are not the only source of error between the two models (NH, using the horizontal radiation as input and NT, using the tilted radiation as input). As seen before, there are some differences between the measured radiation and the simulated radiation as well. Comparing now the models with the experimental results, the results are the following: For the NH-Model, the error on the power generation at 11.30 a.m. is 6.97% and 3.50% for the energy generation over the day. For the NT-Model, the error values are 9.48% for the power and 6.14% for the energy.

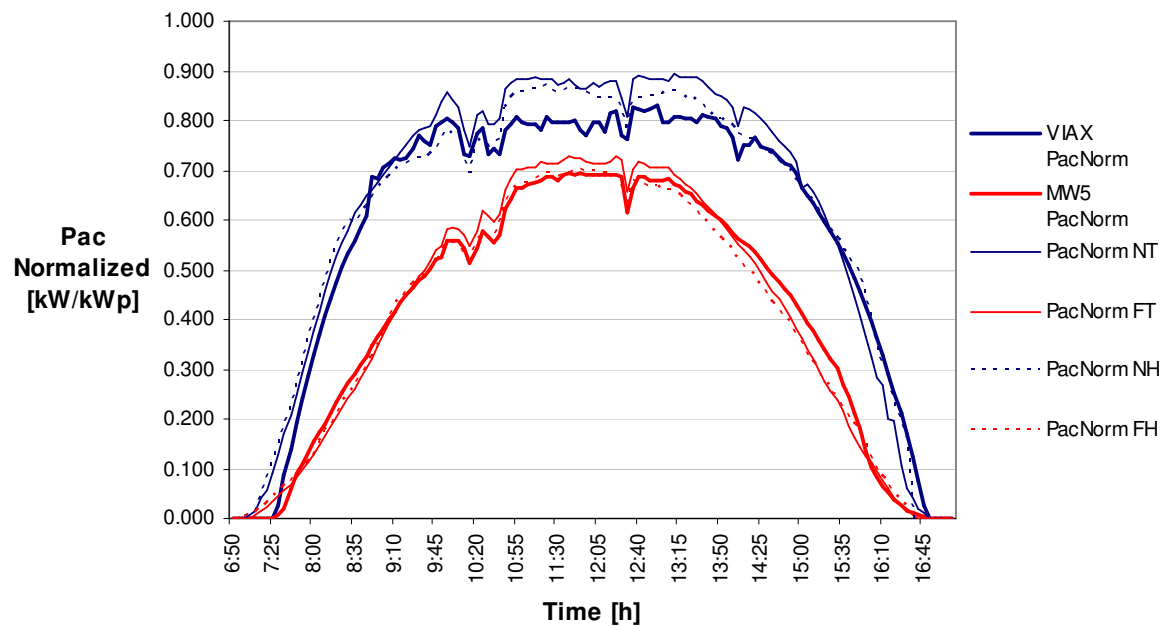


Figure 4-19: Comparison of power generation levels for measured data and simulation results on tilted and tracked surfaces, November 5th, 2008 in Garching at Munich.

The errors in simulating the MW-5 plant could be attributed to measurement accuracy or similar factors involved in scientific investigation and are thus acceptable. The errors in simulating the VIAX show instead, some external factors affecting the values as it was also seen on Figure 4-6 with the comparison factor F . The plant is not working at its expected efficiency. A possible reason causing this could be the antiquity of the solar modules. The plant was built during the northern summer of 2004 while the measurements took place in autumn 2008, having thus being working over 4 years. According to the specifications of the manufacturer of the solar panels, the guarantee lasts 25 years and assures the nominal power generation of the cells at 80%. If we consider the worst case scenario for the manufacturer, the solar cells would loose 20% of its efficiency in 25 years. If this happens, following a linear function over the time, the loss in 4 years would be 3.2%. This should be considered here and would help understand the results. However, this wear out of the solar cells could have been accelerated due to the tracking system, which increases the generation level of the solar panels and with it the loses in efficiency.

Continuing now with **November 6th, 2008**, the results are shown from Figure 4-20 up to Figure 23 and summarized in Table 4-8. Figure 4-20 shows the comparison between the simulated radiation on a tilted surface and the measured radiation. It can be observed, that the simulated radiation resembles quite well the measured radiation on a tilted surface and is also close to the global radiation on a horizontal surface. The same observation, respectively, can be done looking at Figure 4-21, this time for the simulated radiation on a tracked surface. It is close to the measured radiation on the tracked surfaces, with some small differences, which can, for example, be noticed in the morning hours between 8.30 a.m. and 10.00 a.m. One common observation that can be made for the radiation graphs is that the radiation measured at the VIAX plant tends to be more irregular than the curves of the MW-5 or the LMU, which are smoother. For the differences in the temperature diagram at Figure 4-22, there is no available justification for the shown divergences between 2°C and 4°C. Finally in Figure 4-23, it can be noticed that the simulated power values are quite lower than the real ones, giving as a result, some slightly lower values for the energy generation over the day as seen on Table 4-8.

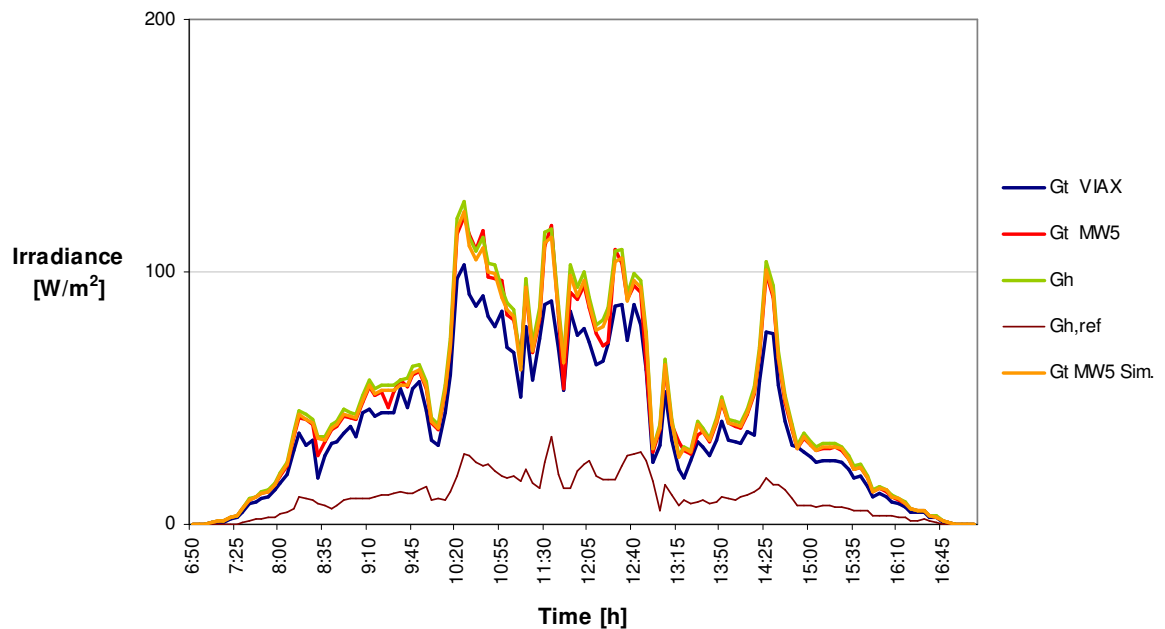


Figure 4-20: Comparison of irradiance levels for measured data and simulation results on a tilted surface, November 6th, 2008 in Garching at Munich.

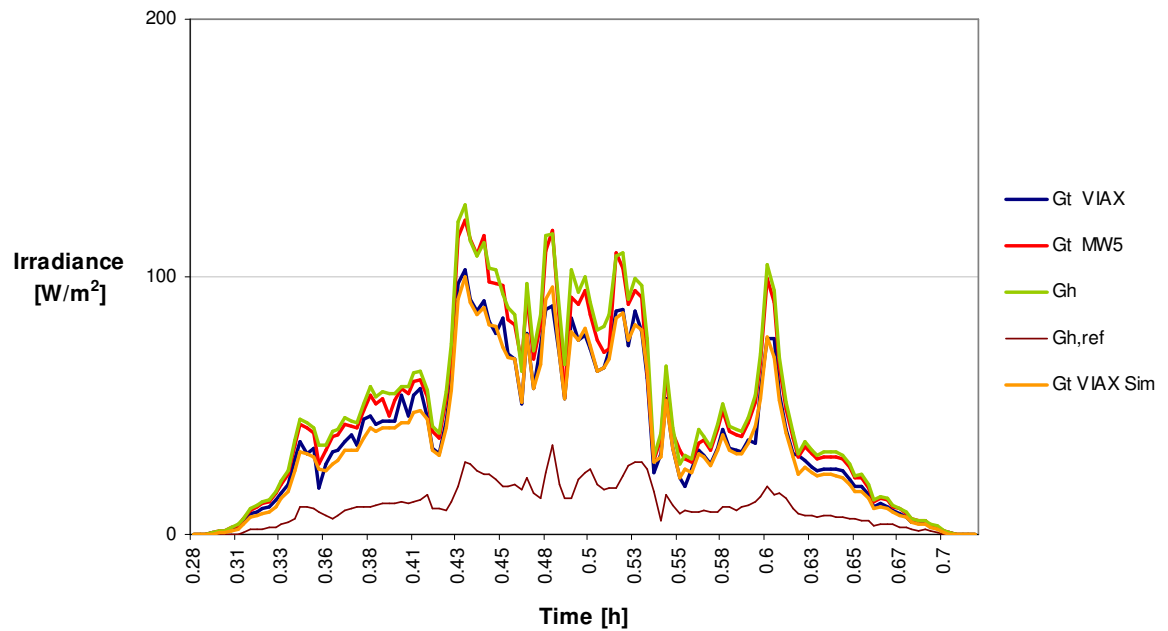


Figure 4-21: Comparison of irradiance levels for measured data and simulation results on a tracked surface, November 6th, 2008 in Garching at Munich.

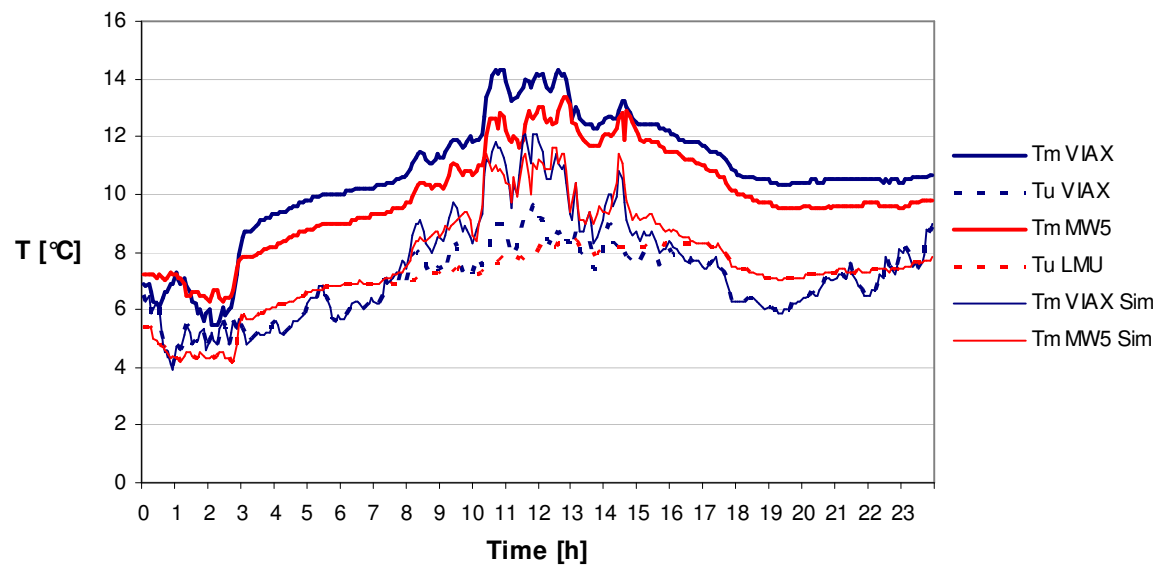


Figure 4-22: Temperatures of measured data and simulation results, November 6th, 2008 in Garching at Munich.

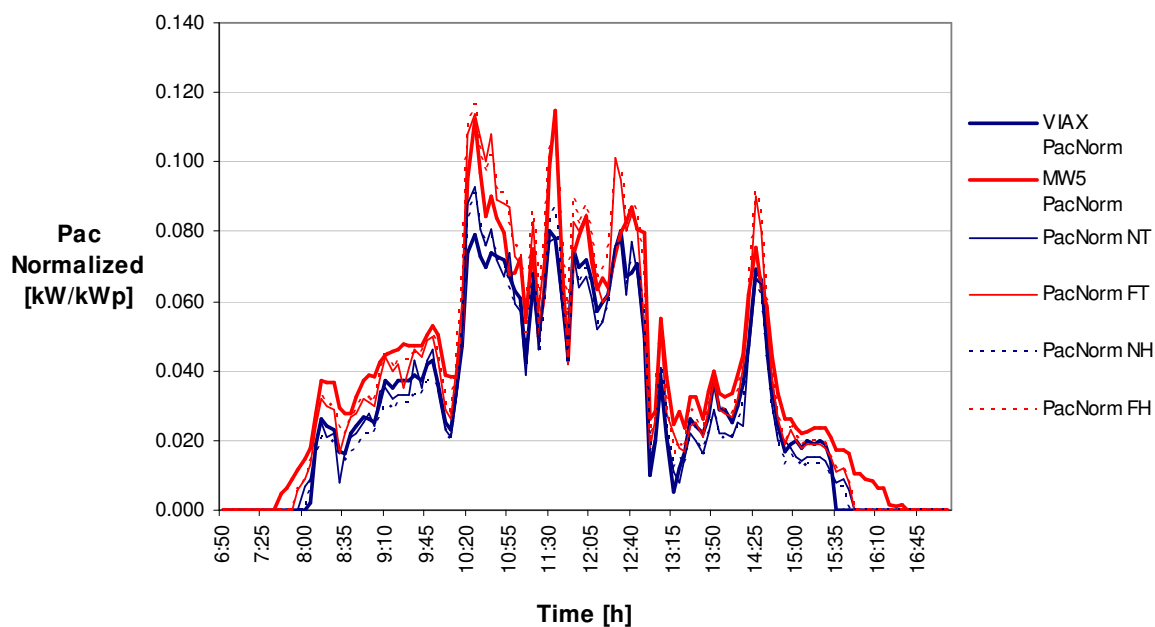


Figure 4-23: Comparison of power generation levels for measured data and simulation results on tilted and tracked surfaces, November 6th, 2008 in Garching at Munich.

Table 4-8: Error comparing the simulated results to the experimental results, November 6th, 2008.

	Irradiation kWh/m ²	Energy kWh/kWp	
Input Radiation	Horizontal	Horizontal	Tilted
MW-5		FH	FT
VIAX		NH	NT
Fixed Tilted / MW-5	1.50%	-2.21%	-4.82%
Tracked / VIAX	-3.82%	-6.13%	-2.71%

Lastly, the results for **October 25th, 2008** are presented. Figure 4-24 compares the measured radiation again with the simulated radiation on a fixed tilted surface representing the MW-5 plant. The shape of the curve is similar to the curve representing the measured radiation on the MW-5 plant. However, in the morning hours the simulated radiation is lower than the experimental one, which changes in the afternoon, thus compensating the error which is only 1.01% for the energy over the day. Figure 4-25 compares the simulated radiation on the tracked surface (VIAX). Here the error is greater and does not compensate in the same way. Figure 4-26 shows that the simulated temperatures over the daylight time are up to 10°C higher than the experimental ones, mainly on sunshine hours. Some of this difference could be due to the wind, although it is not really significant (between 1 m/s and 1.8 m/s over the day). Finally Figure 4-27 shows the power generation levels, which confirms the statements done for the other two days analyzed here. See values at Table 4-9.

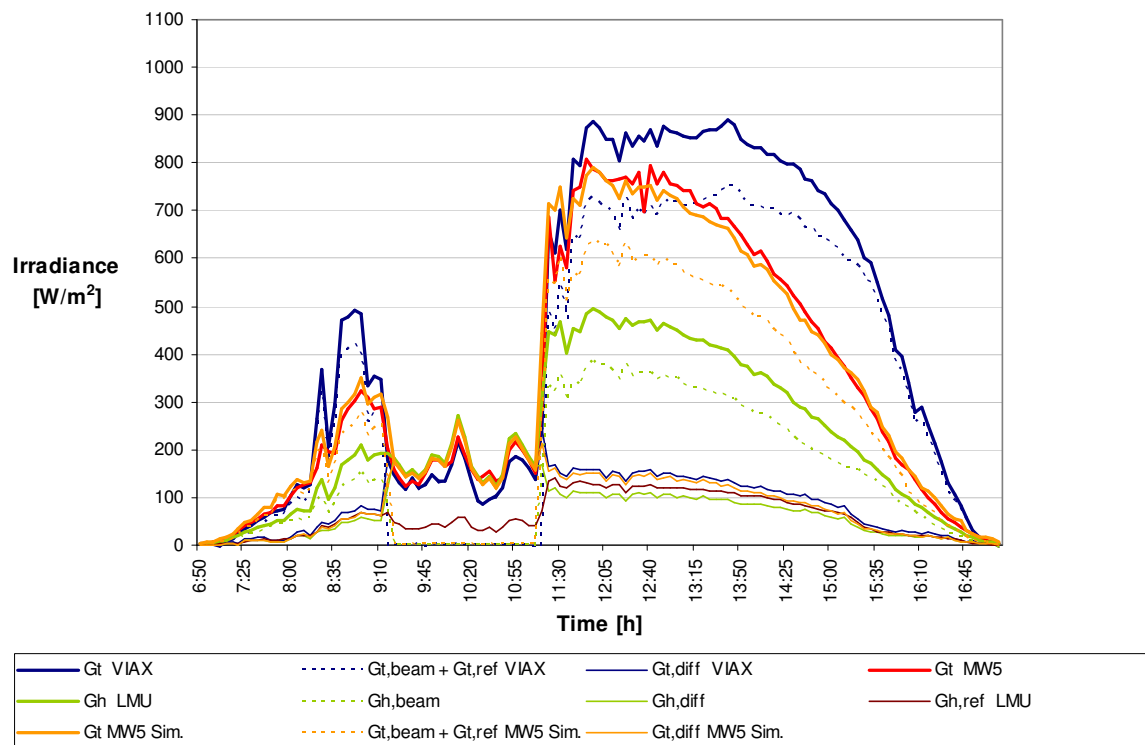


Figure 4-24: Comparison of irradiance levels for measured data and simulation results on a tilted surface, October 25th, 2008 in Garching at Munich.

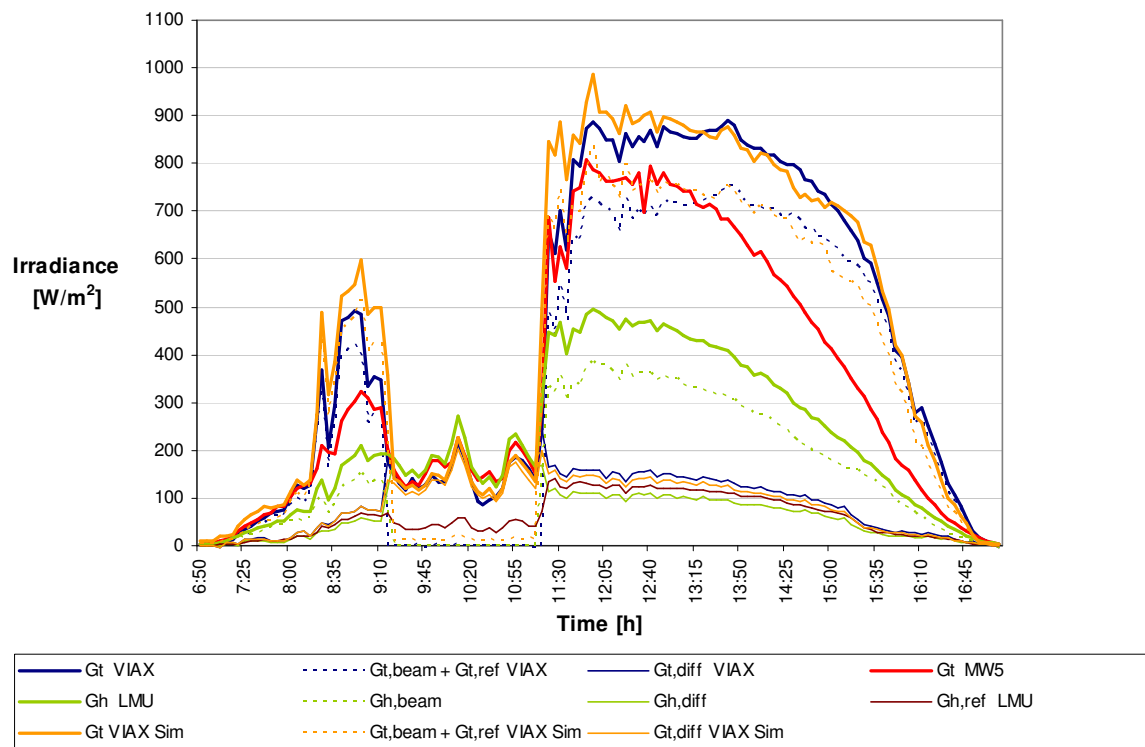


Figure 4-25: Comparison of irradiance levels for measured data and simulation results on a tracked surface, October 25th, 2008 in Garching at Munich.

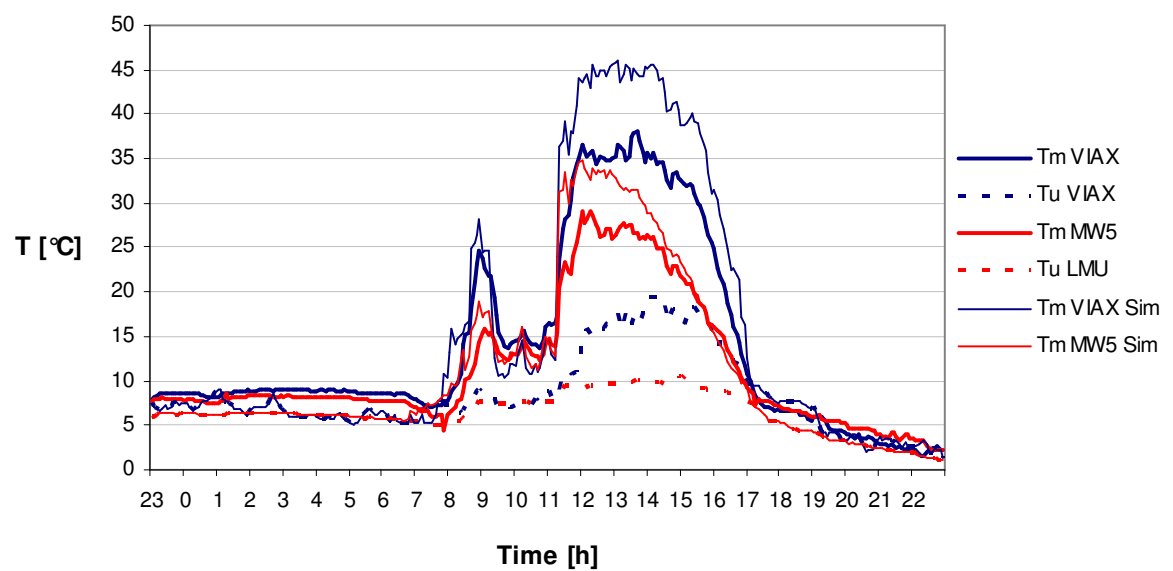


Figure 4-26: Temperatures of measured data and simulation results, October 25th.

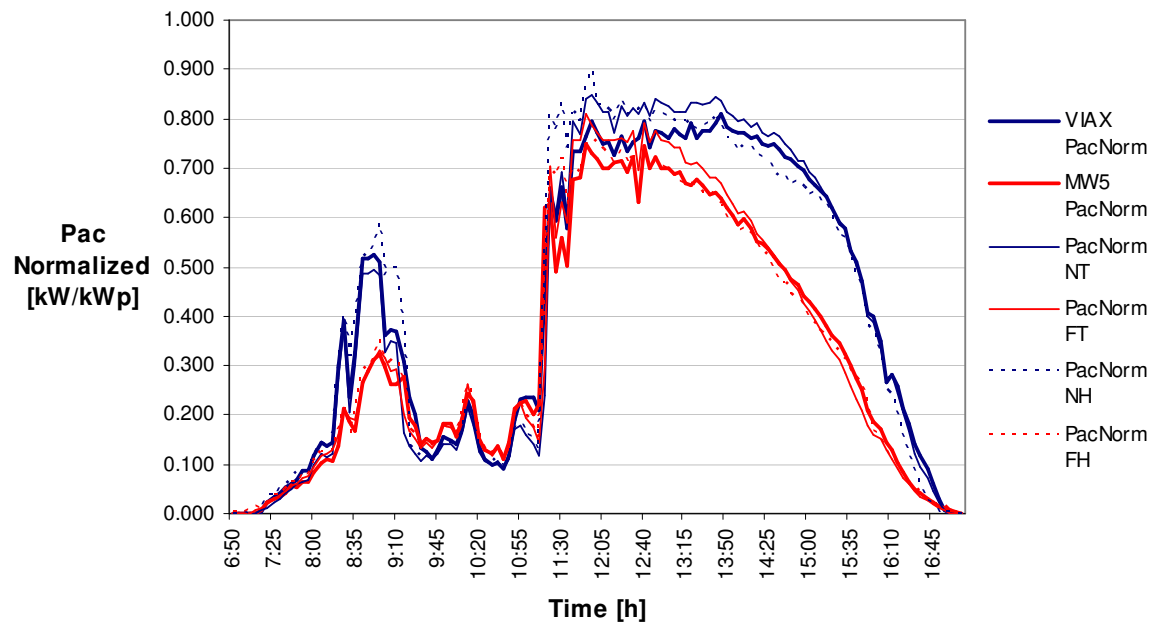


Figure 4-27: Comparison of power generation levels for measured data and simulation results on tilted and tracked surfaces, October 25th, 2008 in Garching at Munich.

Table 4-9: Error comparing the simulated results to the experimental results, October 25th, 2008.

	Irradiation kWh/m ²	Energy kWh/kWp	
Input Radiation	Horizontal	Horizontal	Tilted
MW-5		FH	FT
VIAX		NH	NT
Fixed Tilted / MW-5	1.01%	0.73%	2.10%
Tracked / VIAX	5.47%	1.65%	0.47%

Concluding this section, it can be said, in general, that even when the simulation values are not exactly the same as the experimental ones, the similarities are evident. Some small divergences for the irradiance levels can be observed, mainly at the simulated radiation for the tracked power plant (VIAX), with the rare behavior of being different in the morning and in the evening, thus compensating when comparing irradiation over the day. The simulation values for the MW-5 plant on the other hand, give quite accurate values. The temperatures as could be seen, have higher values at sunny periods with significant differences while being lower than the experimental values at cloudy hours, however with less significant differences. In the case of the power generation, it could be said also that the simulations predict in a good way the real behavior of the power plants, but only if considering the fact that the real power plants are not working as it would be expected due to the years they have been working.

Considering the last comments, it can be said that the simulations predict the performance tendency of the solar power plants in a very precise way and also give acceptable values which helps to quantify this tendencies. This allows us to extend the simulation to other experiments in the following sections.

4.4 More Solar Tracking Systems

Since the simulations with INSEL have been proved to be a good predictor of the behavior of real power plants, the simulations can be extended now to longer periods, a complete year for example, to compare the performance of fixed and tracked power plants. It also allows us to extend the simulations to other tracking mechanisms, in order to compare all the tracking possibilities.

Let us look at the beginning, as an example at the daily simulation of September 1st, a sunny day in the database of the Standard Reference Year 1995. This is probably the best day for simulation contained in the database for autumn and one of the only complete clear days of the year. It has to be considered, that the maximum elevation of the sun that day in Munich reaches 50.15°.

Figure 4-28 shows the daily profile of the irradiance on a fixed surface and on a tracked surface with two different tracking mechanisms. The global radiation is also separated into diffused and beam radiation. It is possible to see the irradiance levels and some interesting behaviors. For example, the fixed power plant reaches at noon a higher irradiance level ($G_t = 925 \text{ W/m}^2$) than the azimuth tracked one (914 W/m^2). This lies in the incidence angle of beam radiation. Since the optimum elevation angle of the surface at noon for this day would be 39.85° ($\theta = 0^\circ$), the elevation angle of the fixed plant ($\beta = 32^\circ$, optimum elevation angle for the year) is closer than the elevation angle of the azimuth tracked surface ($\beta = 53^\circ$, optimum elevation angle for the year). As we can see, this is not that important when compared with the 2-Axis tracked surface that has an elevation angle of 39.85° at noon and reaches an irradiance level not much higher than the other options (930 W/m^2).

Despite the higher irradiance level at noon reached by the fixed plant, it has a lower irradiation over the day. This is the interesting value to be analyzed here and thus we will focus on it from now on. Looking at the graphs, the lower irradiation on the fixed surface can be easily recognized, since it is represented by the area under the G_t curve. In view of the fact that the difference between the 2-Axis tracking and the azimuth tracking is not that evident, the global radiation of each system is illustrated on Figure 4-29.

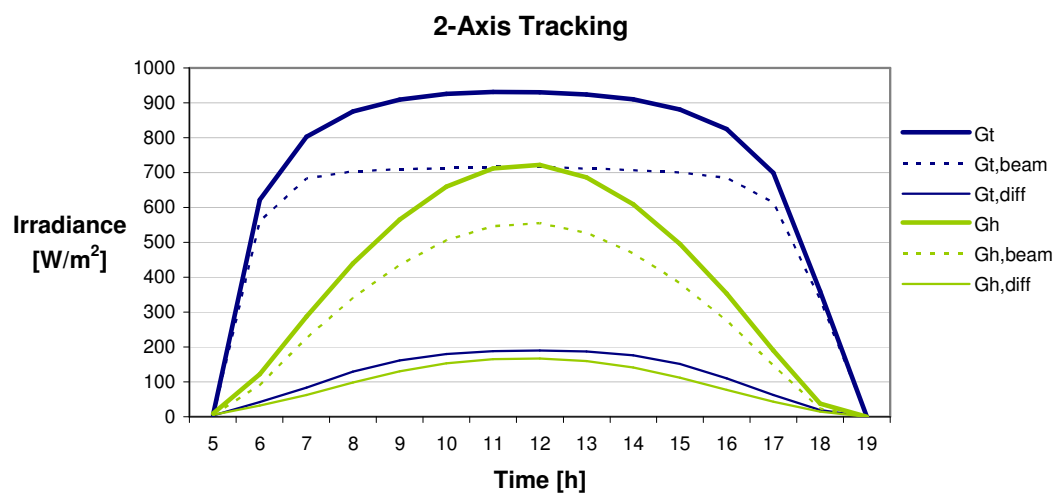
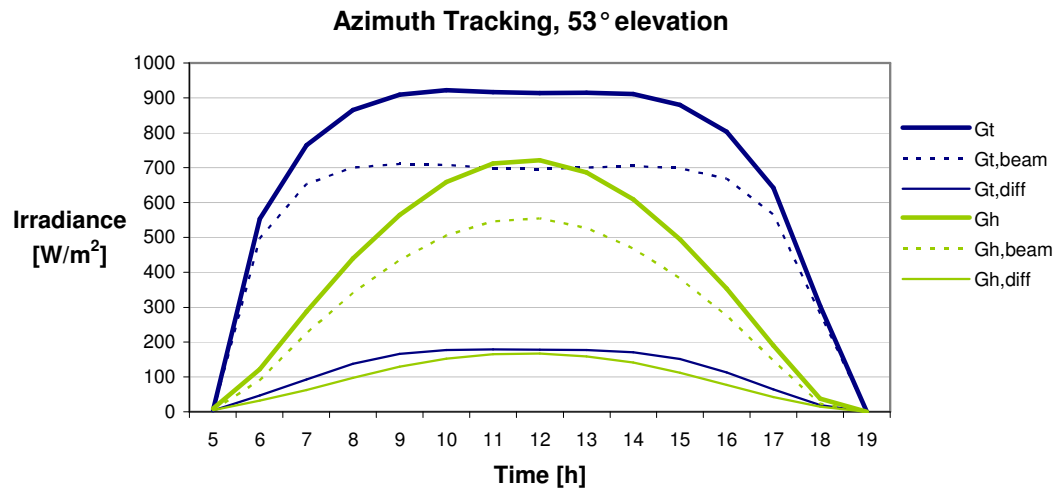
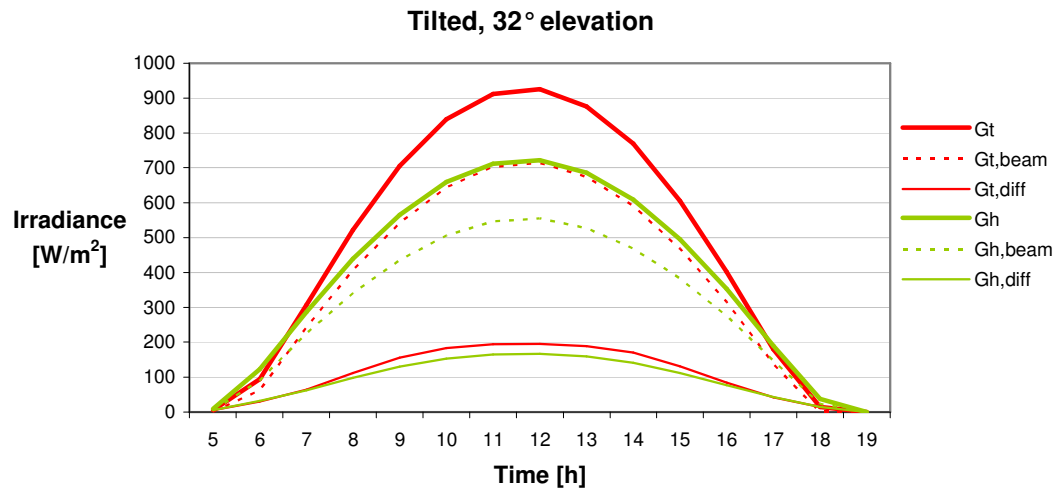


Figure 4-28: Irradiance profiles for September 1st using the SRY.

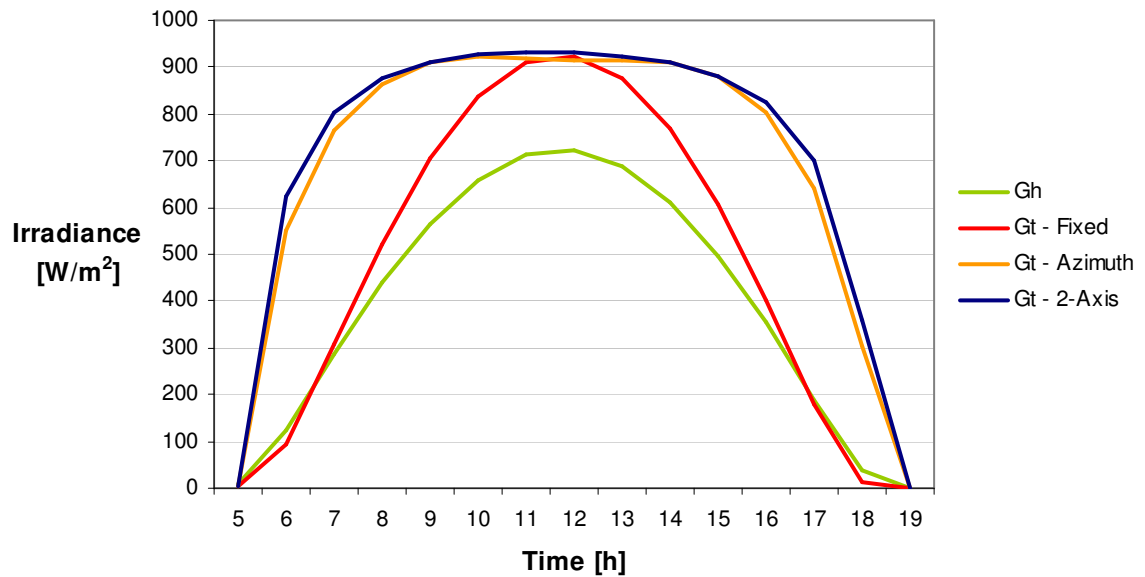


Figure 4-29: Comparing irradiance profiles for September 1st using the SRY.

It can be observed on Figure 4-29 that the 2-Axis tracking system reaches a slightly higher irradiation than the azimuth tracking system over the day. Some values quantifying this relation are presented on Table 4-10.

Table 4-10: Simulated irradiation and irradiance values for September 1st.

	Irradiance at noon W/m2	Daily Yield kWh/m ²	Irradiation Gain (compared to fixed surface)
Horizontal Surface	722	5.89	
Fixed Surface ($\beta = 32^\circ$)	925	7.16	
Azimuth tracked ($\beta = 53^\circ$)	914	10.31	44.01%
2-Axis tracked	930	10.60	48.12%

Until here we have compared the performance of the different solar tracking systems over one specific day. The objective however, is to compare the performance of the different systems over a complete year, in order to have results that could help decide which system is more appropriate, since this can not be decided just by considering the results over one day. Figure 4-30 compares the monthly irradiation of the different tracking systems. It can be observed, that the azimuth tracking system is a significant improvement compared to the fixed system. The 2-Axis tracked system is again a little bit better than the azimuth tracker. The energy consumption of the tracker will not be considered in this comparison, since it lays around 1 kWh/year and is thus not significant.

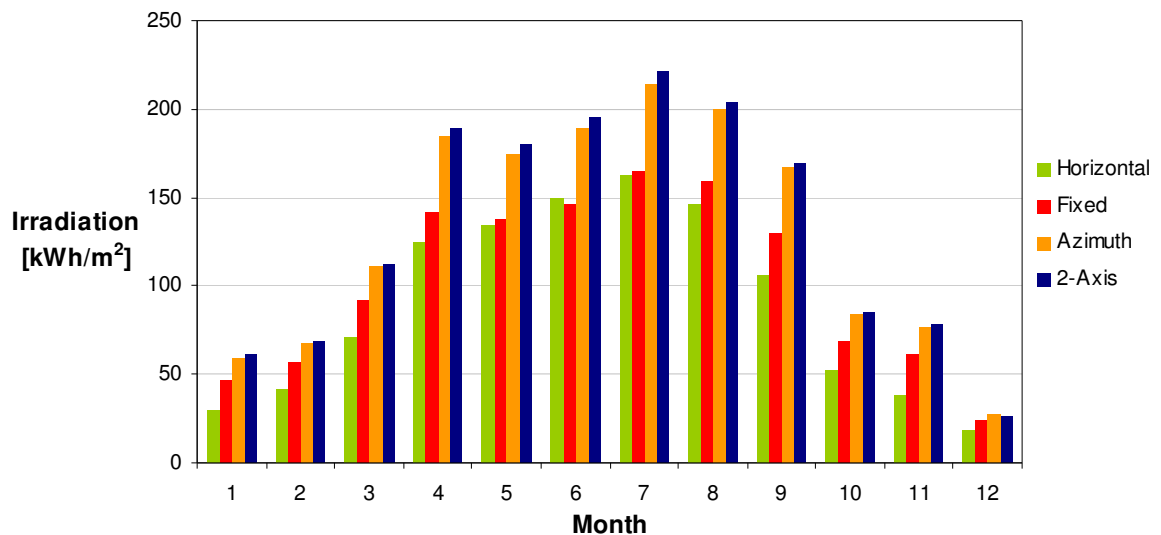


Figure 4-30: Monthly yields of the different tracking systems.

An additional configuration of a solar tracking system is also included in the assessment, the seasonal tracking. Here the optimum number of tracking steps per year has to be determined for the year. The results are shown in Figure 4-31. Since the gain between two and four seasonal tracking steps is lower than 0.1%, two steps seem to be a good compromise between yield and elevation adjustments.

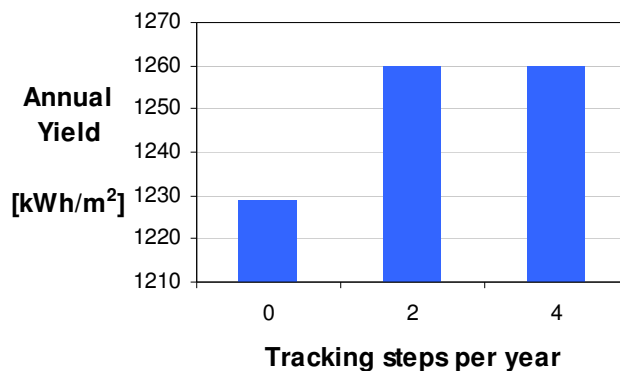


Figure 4-31: Comparing the annual yield according to the seasonal tracking steps.

Comparing now the annual yield of the different tracking systems seen up to here, the results are shown in Figure 4-32. In the graph, we can see that the seasonal tracking increases the annual yield in relation to the fixed system, but not significantly. The azimuth tracking, on the other hand, allows a gain of over 26%, which means at first, that this would be an option to be considered. Also the 2-Axis tracking system reaches almost 30% more irradiation over the year than the fixed system and becomes an attractive solar tracking option.

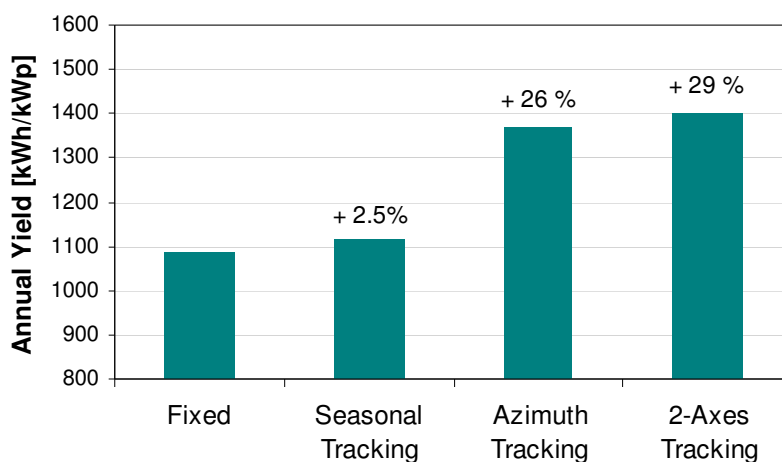


Figure 4-32: Comparing the annual yield of different tracking systems.

Table 4-11: Yields of the different tracking systems and gains on irradiation and AC energy.

	Irradiation		Energy	
	kWh/m ² a	Gain	kWh/kW _p *a	Gain
Horizontal	1072.6			
Fixed	1229.1	0.00%	1086.4	0.00%
Seasonal Tracking	1259.6	2.48%	1114.7	2.60%
Azimuth Tracking	1553.7	26.41%	1368.7	25.98%
2-Axes Tracking	1592.0	29.53%	1399.4	28.81%

Some exact values related to the gain in irradiation over the year are shown in Table 4-11. It is possible to see that the gain in AC-energy decays in relation to the irradiance gain. Considering the simulation models, this can be attributed to the efficiency of the inverters and the effect of the temperature on the solar panels.

To finish this section, one more important issue has to be discussed. These are the results considering the new SRY of Munich compared to the results with the older SRY. A comparison can be seen in Figure 4-33. Exact values of the simulation results with the new SRY are listed in Table 4-12. The annual irradiation on a horizontal surface has increased 6.83% in the last 20 years. This affects the tracking systems as well: Fixed, 7.64%; Azimuth, 5.56%; 2-Axis tracking 5.55%. As we see on Table 4-12, considering the data of the new SRY, the irradiation gain of a 2-Axis tracking system over the fixed system is 27%, more than 2% less than with the old data. This also affects the gain in AC-energy over the complete year. These changes in relation might be related to the pattern of the new STR. The 6.83% increase in the average global radiation comes from a 12.73% increase in the average diffuse radiation of the data. The direct or beam radiation has not changed from the old to the new SRY. As we have seen before (for example in section 4.1, experimental results), the diffuse radiation favors tilted surfaces on sunny days and

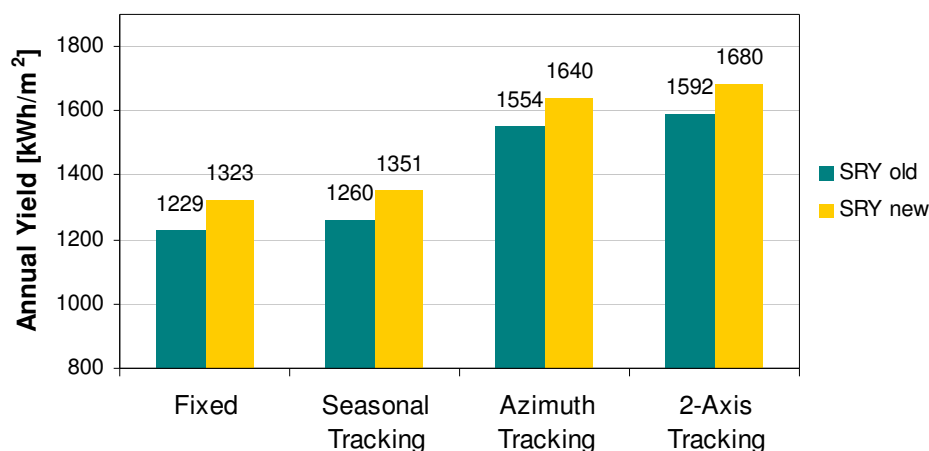


Figure 4-33: Comparing the annual yield of different tracking systems with the old and the new Standard Reference Years.

horizontal surfaces on cloudy days. This would mean that we have more cloudy days in the new SRY. This actually happens, since we passed from having 68.64% to 73.11% of hours in which the irradiance level of the diffuse radiation is higher the irradiance level of the beam radiation. If this tendency maintains in the following years, the use of tracked systems will become less attractive.

Table 4-12: Yields of the different tracking systems and gains on irradiation and AC energy, new STR.

	Irradiation		Energy	
	kWh/m²a	Gain	kWh/kWp*a	Gain
Horizontal	1145.8			
Fixed	1323.0	0.00%	1193.7	0.00%
Seasonal Tracking	1351.1	2.12%	1220.3	2.23%
Azimuth Tracking	1640.1	23.97%	1480.6	24.03%
2-Axes Tracking	1680.3	27.01%	1514.5	26.87%

4.5 More results related to the Simulations

As seen on Section 2.4.2 of this work, some problems have come into view when simulating some individual days and will be discussed here. These problems deal with the unexpected peaks appeared on the irradiance profiles.

4.5.1 The Batman Effect

When simulating with statistical meteorological data like the Standard Reference Years, some peaks tended to appear in the morning hours. The problem seems to be a timing problem with the INSEL simulations. It has been concluded, that if the simulation solar time does not fit the timeframe of the meteorological data, the conversion of horizontal beam radiation to beam radiation on a tilted surface leads to strongly deformed irradiation profiles, which can appear in the form of a morning peak or an evening peak. An example can be seen at Figure 4-34.

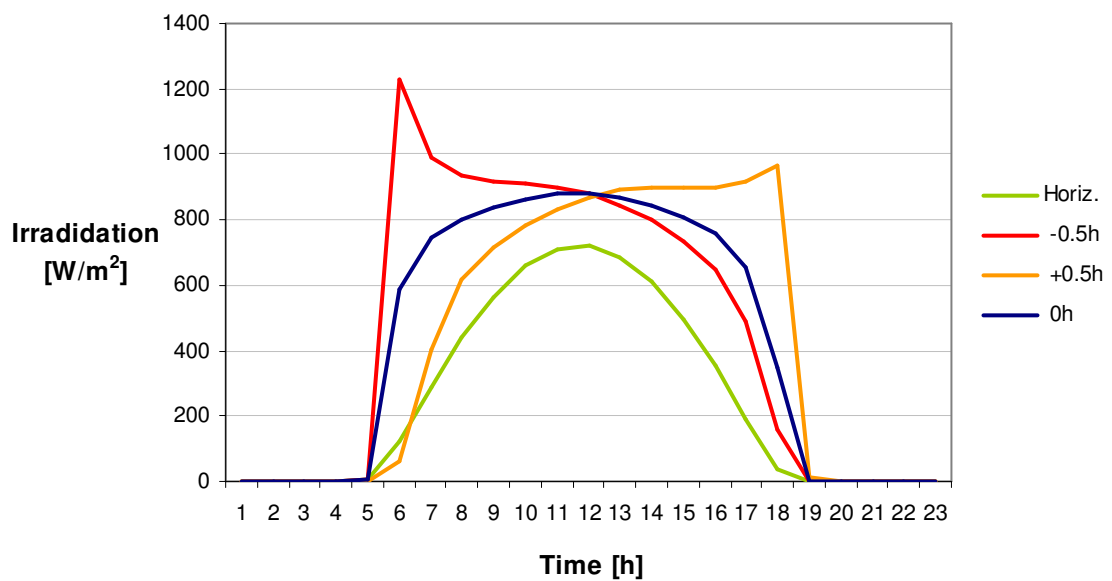


Figure 4-34: Daily profile of the global irradiation on tracked surfaces with different time shifts causing the “Batman-Effect”.

The problem is that the first term of the right hand side of Equation 2.2, representing the beam radiation on a tilted surface tends to higher values than expected during sunrise or sunset. What happens in the morning, for example, is that at sunrise the elevation angle of the sun is very small, thus $\theta_z \rightarrow 90^\circ$ and $\cos(\theta_z) \rightarrow 0$. It is also possible that the irradiance has reached some significant level. If at one simulation step, both conditions match simultaneously, the division will lead to a disproportional strong amplification factor, affecting the horizontal beam radiation. The “Batman-effect” appears due to a time shift, which tries to assign the high amplification factor from for example 6.00 a.m. to the already elevated horizontal irradiation value at that time, causing a peak. This peak represents very high irradiation values, either in the morning or in the evening, depending whether the time shift is positive or negative. The amplitude of the peak will depend on how well the conditions match at the simulation step.

In simulations these computer deviations lead to a misinterpretation of yearly irradiation energy on tracked surfaces. The impact of shifts in solar time on the annual yield can be seen in Figure 4-35. Depending on the time shift, this can lead to either higher or lower values.

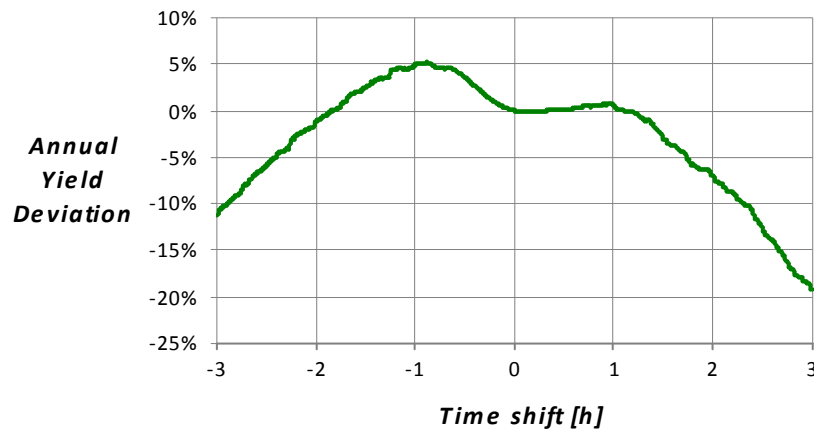


Figure 4-35: Influence of the time shift on the annual yield.

4.6 Application Options in Chile

Considering the existing simulation models used with the German weather databases, these can be used also to get similar results for other locations around the world with available meteorological data. At this point, to get an idea of the Chilean situation related to the efficiency of solar tracking systems, some local data is used in order to get a few representative results. The comparison of the main tracking systems for Santiago ($33^{\circ}26'15''\text{S}$ and $70^{\circ}39'00''\text{W}$, 573 m over the sea level) and Punta Arenas ($53^{\circ}08'00''\text{S}$ and $70^{\circ}54'00''\text{W}$, 2 m over the sea level) can be observed in Figure 4-36. The elevation angles of the surface used for the fixed and the azimuth tracking system at Santiago were 20° and 44° . For Punta Arenas the angles used were 37° and 55° . It can be seen that the annual yield in the Chilean cities is significantly greater than in Munich. The reason for this is the higher available annual irradiation. The gain on energy, using solar tracking systems, is also slightly higher than in Munich. Exact values of the results for the simulations at Chilean locations can be seen at Table 4-13. The data used for the simulations correspond to measured data of the year 1995 and not to statistical data as used for the German case.

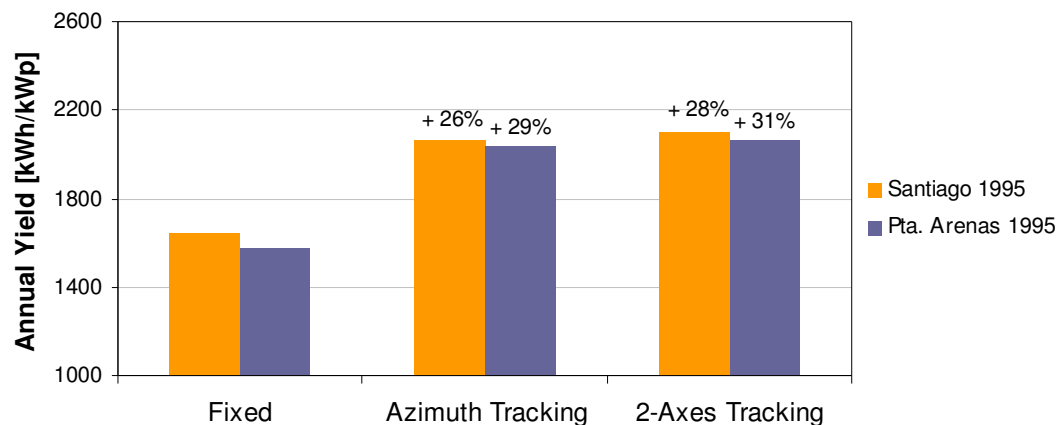


Figure 4-36: Comparison of the simulated annual yield of different solar tracking systems for Santiago and Punta Arenas, Chile. Average data 1995-2005.

Table 4-13: Simulated yields of the different tracking systems and gains on irradiation and AC energy for Santiago and Punta Arenas, Chile. Avg. Data 1995-2005.

		Irradiation		Energy	
		kWh/m ² a	Gain	kWh/kWp*a	Gain
Santiago	Horizontal	1801.0			
	Fixed	1933.7	0.00%	1638.7	0.00%
	Azimuth Tracking	2491.0	28.82%	2063.8	25.94%
	2-Axes Tracking	2545.4	31.63%	2102.4	28.30%
Pta. Arenas	Horizontal	1423.8			
	Fixed	1797.1	0.00%	1582.9	0.00%
	Azimuth Tracking	2349.8	30.76%	2039.5	28.85%
	2-Axes Tracking	2384.2	32.67%	2066.7	30.56%

In general, the results shown in this section should be considered as a tendency for the behavior of the solar tracking systems in Chile. The horizontal radiation values however, are correct, since they correspond to the used data. The results for fixed systems should be a little bit higher. The values of a few simulated days were truncated by the simulation software (happens when the irradiance level is higher than 1230 W/m²). The results for azimuth tracking and 2-Axis tracking systems are apparently higher than they should be. The simulations were affected by a variation of the Batman-Effect and could not be adjusted using the method applied in the German case.

In general however, the solar tracking systems can be recommended in Chile from an energy point of view.

4.7 Economic Evaluation

A brief economical evaluation will be presented here, in order to have an idea on how the energy gain using a solar tracking system might influence the decision of the investors. Some assumptions and values, considered for the evaluation of a grid-connected solar power plant in Munich are the following:

- Discount rate 2 %
- Credit rate 5.15 %
- Installed capacity 5 kW
- Sale price for solar kWh 0.3549 € (Field plants in Germany, 2008)
- Evaluation period 20 Years
- Efficiency losses of the modules 1 %/year
- Enough capital available to finance the complete plant
- Annual maintenance costs: 0.3 % for fixed plants and 0.5 % for trackers
- No ground investment necessary. Field or roof available for the project.

Even when the installed capacity was set to 5 kW, it should be considered that a higher installed capacity is needed to reach the investment prices shown here. For the fixed power plant, a standard value for the German market is used, 4000 €/kWp. For the 1-axis plant, the cost of a power plant manufactured by Conectavol, the Lybra, is used. The cost of the 2-axis tracking power plant is represented by the cost of a Soltec power plant, the 10K. The values were obtained by the author in the InterSolar 2008 and the PVSEC 2008. The costs of the VIAX power plant are obtained from Bauer et al. (2005).

As we can observe in Table 4-14, from the economical point of view there is no large variation between the investments on the different power plants. Using a fixed power plant, a 1-axis tracking plant or a 2-axis tracking power plant won't make much of a difference, since the larger energy yield reached with a tracker compensates with the higher cost of the power plant. The Internal Return Rate and the Payback Period are quite

similar for the three main options. The VIAX, instead, diverges a bit from the 2-axis tracker since the investment cost is somewhat higher. Anyways, if a capital of 25000 € is available for investment, a 2-axis tracking power plant would be the right decision according to the assumptions made here since it has a higher NPV.

In addition, if we consider that the different power plants cost the same, the power plants with a higher generation capacity should be chosen. That is obvious from an energy point of view.

Table 4-14: Economical Evaluation of the different power plants.

	Power Plant Cost	Total Investment	Energy / year	Energy	NPV	IRR	Payback period
	€/kWp	€	kWh/kWp (New SRY)	kWh*a	€		Years
Fixed	4,000 €	20,000 €	1193.7	5969	12,123 €	7.64%	9.95
1-Axis	4,850 €	24,250 €	1480.6	7403	14,828 €	7.69%	9.91
2-Axis	5,000 €	25,000 €	1514.5	7573	14,957 €	7.58%	9.99
VIAX	5,309 €	26,545 €	1514.5	7573	13,286 €	6.74%	10.66

At present, in Germany however, the fixed power plant would probably be the one chosen for smaller and mid-size projects, as it can be seen in the German landscape, since they can be easily installed on top of the roof of houses and other buildings and thus receive 0.4675 € per generated kW instead of 0.3549 €. In this case the fixed power plant would be paid for in 7.44 years and have a Net Present Value of 22627 €.

Summary

This chapter contains a complete description of the experimental results going through days with sunny, cloudy and mixed weather conditions, despite problems during the measurement period. It also presents the results of the simulations for these measured days and compares them, showing a clear association between results related to irradiance levels, unexpected results for simulated temperature and changing results for the power generation performance. Thus, the tendency is clear and the simulation results could be validated. Some other tracking options were analyzed along with the implemented ones in order to calculate annual yields and compare the tracking systems over longer periods of time. In addition, the Batman-Effect was commented. Finally, some results for the Chilean case were shown, as well as a brief economic evaluation for the tracking options in Germany not showing important differences.

5 CONCLUSIONS AND FURTHER WORK

5.1 *Main Conclusions*

After having success repairing the solar power plants and creating simulation models, in order to get experimental data and computer results, the validation of the simulations were possible. The behavior tendencies are clearly similar, when comparing experimental and simulation values. For the fixed solar power plant system represented by the MW-5 plant, the validation is completely satisfactory. For the 2-axis tracking system, represented by the VIAX, there is a small disparity when quantifying the results.

Best results when comparing experimental and simulation results are reached on irradiance levels. The power level results show higher divergences, which are however still in the acceptable inaccuracy range. The module temperature results evidence with greater differences which could be objected from a strict numerical point of view, even when the behavior tendencies are visibly related. Nevertheless, these differences seem not to have a significant influence in the analysis of the power performance of the plants. In general, the simulation values are quite higher than the measured ones.

Solar tracking mechanisms improve the energy gain of solar power plants. A double-axis tracking system is generally the one that reaches the highest energy gain in every region. It is therefore the most versatile system, since it can be installed anywhere, guaranteeing a high energy gain. Single-axis tracking systems can come very close in performance to double-axis systems in some regions when well designed and when the right system has been chosen. Polar tracking systems show high efficiency levels in lower latitudes of Europe, like Spain. Azimuth tracking systems, on the other hand, are recommended for higher European latitudes, like northern Scandinavia.

Solar trackers are recommended everywhere from an energetic point of view, since they always increase the amount of collected energy. The highest energy gains are reached

in regions where the solar beam radiation prevails compared to the diffuse solar radiation. Thus regions in central Europe with a high diffuse radiation share, like Germany and the British Isles, have the lowest energy increase amounts using solar trackers.

The energy gain offered by the solar industry could be reached depending on the region. Even up to 50% more energy is possible, for example in northern Scandinavia. For Munich the increased energy amount lies clearly under 30% with any tracking system.

From an economic point of view, the decision related to the installation, or not, of solar trackers and which solar tracker system should be chosen, will depend on several point in time dependant parameters like the cost and efficiency of the solar modules, the cost of the other components and the sales price of photovoltaic generated power. This last factor depends again on the energetic policies of the countries' governments. Countries like Germany and Spain are good examples of this idea.

The decision on installing solar trackers will depend mainly on the irradiation level and type of radiation available at the studied location and on an economical assessment that has to be done at the decision moment considering the time changing parameters. Thus this decision can't be taken in advance and neither as a general case. Following steps could guide the decision process:

1. Serious irradiance studies for the evaluated location have to be considered.
There are a variety of results that do not seem to be always representative.
2. If possible, evaluate the different tracking systems at the chosen location using computer simulations to get more precise values.
3. Inform the government policies on solar generated power.
4. Economic evaluation.

If the economical issue is not important, solar tracking systems should always be prioritized.

5.2 *Additional Comments*

The energy gain, using solar tracking systems, will depend mainly on the system used and the location of the power plant, since this is the main variable for determining the available irradiation. Latitude alone is not sufficient as a unique variable for the determining the irradiance levels. The solar radiation has no linear behavior as a function of the latitude as some authors have stated.

On cloudy days which have only a diffuse radiation component, the tracking systems are not increasing the amount of energy collected. It could even be a disadvantage using a tracking mechanism, due to the distribution of the diffuse radiation (on cloudy days the optimum orientation is towards the zenith). If the weather forecast is good enough, on deep cloudy days the plant could be oriented in fixed position towards the zenith. For days with changing weather conditions it is recommended to follow the sun path as planned.

Secondary effects like the wind speed affecting the module temperature and the power generation are not significant compared to the influence of the solar radiation.

The sensors used at the power plants seem not to be the right ones for scientific work. The photovoltaic detectors are not precise enough and can be easily affected by other factors like reflection. Pyranometers are quite more precise and should be used. The diffuse radiation sensors used measure wrong values during cloudy days. At this work this had to be adjusted afterwards.

The new weather data base for Munich shows an increase in hours where the diffuse radiation predominates, thus making it less interesting for solar tracking systems. This should be analyzed throughout the years to determine a possible tendency that could discourage the use of tracking systems.

The irradiation levels are much higher in Chile than in Germany. The use of solar tracking systems in Chile can be highly recommended from an energetic point of view.

5.3 Recommendations for Further Research

There is a huge variety of studies concerning solar tracking systems. However, there are still enough research fields available. On the one hand, the simulations could be validated in more places, using the right methods and power plants. In addition, there are enough aspects of the simulations that could be improved.

Considering the situation at the Technical University of Munich, there are still many areas that can be enhanced, in order to make a deeper study of solar tracking systems. The new solar power plant that is already operational by now, named “Heliostat” which is located at the roof of the MW-7 building, and might get also that name in the future, is a 2-axis tracking systems with independent axis control. It can thus be used as a standard 2-axis tracking system or as an azimuth tracking system without any modifications in order to validate this simulation models. Moreover, it is located only 50 m away from the MW-5 power plant and installed with the same roof conditions. Thus, it has ground reflectance, temperature and wind conditions closer to the MW-5 plant than the VIAX plant would have.

In order to keep doing measurements for scientific purposes with the power plants located at the faculty of mechanical engineering, there are still some adjustments that have to be done. The PLC of the VIAX power plant needs to be reprogrammed to avoid the tracking distortions that happen in the evening hours, every once in a while. A modification could also be made to the system, in order to extend the tracking range of the VIAX plant in the early morning and late evening hours. The data logger of the VIAX could also be replaced to facilitate retrieving the data from it with unfavorable weather conditions (low temperatures and rain makes this difficult).

The radiation sensors should also be replaced installing the adequate instruments like pyranometers instead of the photovoltaic detectors. This would help with the reflectance problem of the PV-cells and probably with the influence of high temperature, among other disadvantages that are present at the PV-detectors. The diffuse radiation sensor should also be replaced at the VIAX. It is not only a problem on cloudy days, when the diffuse radiation is underestimated, but also on days when the seasonal angle set at the VIAX is not the optimum one, which causes some beam radiation to reach the sensor. A series of radiation and temperature sensors could be installed independently of the power plants at the Solar Research Center of the faculty.

Once the hardware upgrades have been fulfilled, new measurement activities could take place. Measurements in other seasons of the year would help validate the simulations with other weather conditions. During April and May, some perfect sunny days with mild temperatures offer the best conditions for radiation analysis. Also, warm days in summer should be included in the new measurements to analyze the temperature influence of the solar modules in the performance of the power plant. Longer measurement periods, like a month or a complete year, would be useful to validate simulations with more accuracy. It would also allow getting the real energy gain using a solar tracker over a year. Finally the analysis of days with changing weather conditions will remain as a little challenge, since most of the measurement and simulation problems converge on those days, making it extremely difficult getting precise results.

The simulation models can also be improved. For the conversion of horizontal to tilted radiation the Perez et al. model could be used and compared to the existing results. To simulate the solar power plants of the TUM with real PV modules and inverters is also an outstanding issue that could be worked out. Some additional tracking mechanisms like the polar tracking option could be developed for the INSEL software.

The Batman-Effect has been solved for the German case. However it is still present in the Chilean results. This could also be studied more in depth. Despite having INSEL an

internal control process that restricts the amplification factor, causing the Batman-Effect to to 20, this seems to not be good enough as seen here and could be also enhanced.

With solid simulation models and plenty of working solar power plants, some other factors could be analyzed in detail and quantified. The reflection on the solar modules, the module temperature dependence of the power performance and the wind incidence could be studied.

In the future the study of solar tracking systems could be extended to other methods used to capture the sun's radiation like multijunction PV cells, solar thermal systems and photovoltaic concentrators. More than studying the tracking systems itself, like it was done at this work, an efficiency comparison could be made between different technologies under optimized conditions, to determine the most efficient solar power systems. An example could be a PV tracker with multijunction PV cells compared to a photovoltaic collector systems.

REFERENCES

- Bauer, M., Flurl, B. y Schulze J. (2005). *Entwicklung, Konstruktion und Bau einer Zweiachsigen Nachführung von Solarzellen mit dem VIAX-Getriebe*. Not published academic research, Technical University of Munich, Munich, Germany. Available under request at the Chair of Thermodynamic, Faculty of Mechanical Engineering.
- Bernal, E. (2007). *Detailed analysis and optimization of the energy yield of SunThink solar active sunscreen systems*. Not published master thesis, Technical University of Munich, Munich, Germany.
- BMU (2008). *Erneuerbare Energien in Zahlen - nationale und internationale Entwicklung*. KI III 1. Bundesministerium für Umwelt, Naturschutz und Reaktorsicherheit, Berlin, Germany.
- Canova, A., Giaccone, L. y Spertino F. (2007, September). *Sun tracking for capture improvement: Simulation and experimental results on operating systems*. Document presented at the 22nd European Photovoltaic Solar Energy Conference (PVSEC), Milan, Italy.
- Doppelintegral (2006). *Block Reference for INSEL*. Doppelintegral GmbH, Stuttgart, Germany. www.insel.eu.
- Doppelintegral (2006). *INSEL Tutorial*. Doppelintegral GmbH, Stuttgart, Germany. www.insel.eu.
- Duffie, J. & Beckman W. (2006). *Solar engineering of thermal processes*. (3a.ed.). Hoboken, New Jersey: John Wiley & Sons, Inc.
- Hoffmann, A., Frindt, H., Spinnler, M., Wolf, J., Sattelmayer, T. y Hartkopf, T. (2008, September). *A systematic study on potentials of PV tracking modes*. Document presented at the 23rd European Photovoltaic Solar Energy Conference (PVSEC), Valencia, Spain.
- Huld, T., Sári, M., Cebecauer, T. y Dunlop E. (2008, September). *Optimal mounting strategy for single-axis tracking non-concentrating PV in Europe*. Document presented at the 23rd European Photovoltaic Solar Energy Conference (PVSEC), Valencia, Spain.
- Kaltschmitt, M., Streicher W. y Wiese A. (2006). *Erneuerbare Energien*. (4a.ed.). Berlin: Springer-Verlag.
- Keller, A. (1989). *Konstruktion eines Solargenerators mit VIAX-Nachführung*. Not published academic research, Technical University of Munich, Munich, Germany. Available under request at the Chair of Thermodynamic, Faculty of Mechanical Engineering.

Mie, G. (1908). *Beiträge zur Optik trüber Medien, speziell kolloidaler Metallösungen*. *Annalen der Physik*, Vierte Folge, Band 25, 1908, No. 3, p 377-445.

Mohring, H., Klotz, F. y Gabler, H. (2006, Septiembre). *Energy Yield of PV tracking systems – Claims and reality*. Document presented at the 22nd European Photovoltaic Solar Energy Conference (PVSEC), Dresden, Germany.

Narvarte, L., Lorenzo, E. (2007, September). *Tracking gains and ground cover ratio*. Document presented at the 22nd European Photovoltaic Solar Energy Conference (PVSEC), Milan, Italy.

Patel, M. (1999). *Wind and Solar Power Systems*. Boca Raton, Florida: CRC Press.

Pelzl, M. (1988). *Grundlagen zur Konstruktion einer VIAX-Nachführungseinrichtung eines Solargenerators*. Not published academic research, Technical University of Munich, Munich, Germany. Available under request at the Chair of Thermodynamic, Faculty of Mechanical Engineering.

Pichard (1999). *Secador Solar para Plantas y Hierbas Medicinales*. Not published master thesis, Pontificia Universidad Católica de Chile, Santiago, Chile.

REN21 (2009). *Renewables Global Status Report: 2009 Update*. Renewable Energy Policy Network for the 21st Century (REN21), Paris.

Seifert, D. (1983). *Europäische Patentanmeldung*. European Bureau of Patents, Munich, Germany.

Sorichetti, R., Perpiñán, O. (2007, September). *PV solar tracking systems analysis*. Document presented at the 22nd European Photovoltaic Solar Energy Conference (PVSEC), Milan, Italy.

WBGU (2003). *Welt im Wandel: Energiewende zur Nachhaltigkeit*. Wissenschaftlicher Beirat der Bundesregierung Globale Umweltveränderungen (WBGU), Berlin: Springer-Verlag.

Wolf, J., Böll, M., Hartkopf, T. y Khanh, T. (2008, September). *Analysis and characterization of sloped irradiated solar modules*. Document presented at the 23rd European Photovoltaic Solar Energy Conference (PVSEC), Valencia, Spain.

Websites:

Climate at Munich	www.synopvis.co.uk/weather/munclim.html www.wordtravels.com/Cities/Germany/Munich/Climate www.synopvis.co.uk/weather/munclim.html
Inverters information	www.sma.de
Loster (2006).	www.ez2c.de/ml/solar_land_area/index.html

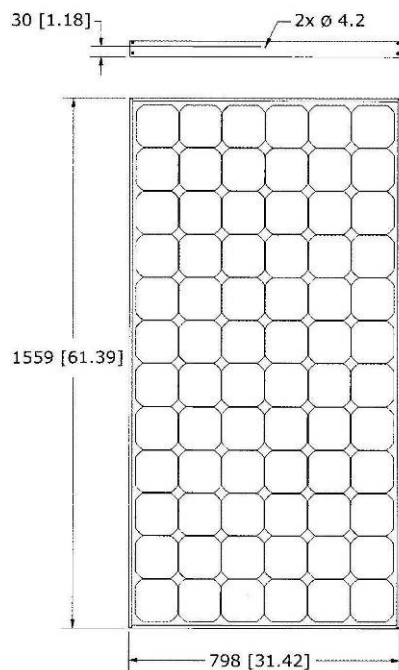
APPENDIXES

**APPENDIX A: DATA SHEET OF THE SOLAR MODULES INSTALLED AT
THE MW-5 AND VIAX POWER PLANTS**

- 210/220 Wp Nennspitzenleistung bei STC
- +/- 3 % Leistungstoleranz
- 20 % Zelleffizienz Minimum
- 25 Jahre Garantie auf 80 % der Nennleistung
- 10 Jahre Produktgarantie
- 72 monokristalline Rückseitenkontakt-Zellen
- Multi-Contact-Stecker
- Rahmen: Aluminium schwarz-eloxiert
- Abmessungen: 1559 x 798 x 46 mm (L/B/T)
- Gewicht: 16,5 kg
- Schutzart Anschlussdose: IP 65
- Zertifikate: IEC 61215, Schutzklasse II bis maximal 1000 V

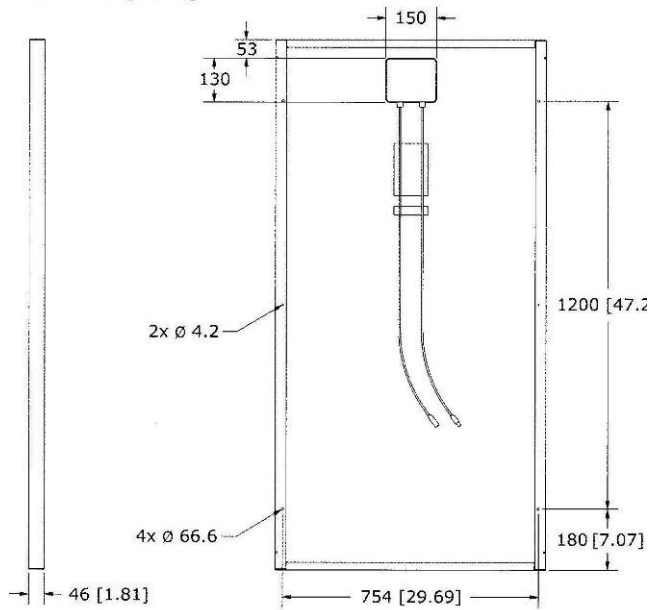
**STM 210 und STM 220 –
exklusiv von SunTechnics.**

	STM 210 FBS	STM 210 FWS	STM 220 FWS
Bei 1000 W/m² (STC)			
P _{max}	210 W	210 W	220 W
I _{sc}	5,85 A	5,75 A	5,95 A
U _{oc}	47,65 V	47,7 V	47,75 V
U _{mpp}	40,0 V	40,0 V	40,0 V
I _{mpp}	5,25 A	5,25 A	5,5 A
Bei 800 W/m² (NOCT, AM 1,5)			
P _{max}	150 W	150 W	163,4 W
I _{sc}	4,5 A	4,5 A	4,8 A
U _{oc}	43,8 V	43,8 V	44,5 V
U _{mpp}	36,2 V	36,2 V	36,8 V
I _{mpp}	4,15 A	4,15 A	4,4 A
NOCT	50,5 °C	48,5 °C	48,5 °C
Temperaturkoeffizienten für I _{sc}	2,27 mA/°C	2,27 mA/°C	2,27 mA/°C
Temperaturkoeffizienten für U _{oc}	-0,1368 V/°C	-0,1368 V/°C	-0,1368 V/°C
P _{max} (bei 200 W/m ² , 25 °C, AM 1,5)	40 W	40 W	N/A
Max. zulässige Systemspannung	1000 V	1000 V	1000 V



Die Vorderansicht des STM 210 / 220

Alle Angaben in Millimeter [Inches]



Die Seitenansicht des STM 210 / 220

Die Rückansicht des STM 210 / 220

Technische Änderungen vorbehalten.
Stand 04/2006

SunTechnics GmbH
Anckelmannsplatz 1 | D-20537 Hamburg
Tel. +49-40-23 62 08 0 | Fax +49-40-23 62 08 222
info@SunTechnics.com | www.SunTechnics.com



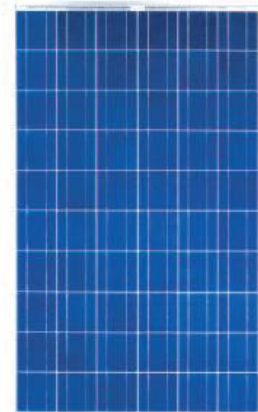
Geprüfte Qualität für
• Beratung
• Planung
• Komponentenauswahl
• Installation
• Serviceleistungen
von netzgekoppelten
Solarstromanlagen



SOLON P220/6+

Mechanische Daten

Länge:	1.660 mm
Breite:	990 mm
Höhe:	42 mm
Gewicht:	26 kg
Anschlussdose:	1 SOLON Dose mit Bypassdioden
Kabel:	Solkabel 1100 mm Länge, 4 mm ² , vorkonfektioniert mit MC-Stecker
Frontglas:	ESG Weißglas 4 mm
Zellen:	60 Stk. polykristallin Si 6,2" (156 x 156 mm)
Zelleinbettung:	EVA (Ethylen-Vinyl-Acetat)
Rückseite:	Tedlar-Verbundfolie
Rahmen:	eloxiertes Aluminiumprofil
Maße des Laminats ohne Rahmen:	1653 x 983 x 5 mm (L x B x H)



Elektrische Daten (typisch)

Modulkategorie P _{max} (±3%):	235 W _p	230 W _p	225 W _p	220 W _p	215 W _p	210 W _p	205 W _p	200 W _p
Nennspannung U _{mp} :	29,0 V	28,9 V	28,8 V	28,7 V	28,5 V	28,2 V	28,0 V	27,75 V
Nennstrom I _{mp} :	8,1 A	7,95 A	7,8 A	7,65 A	7,55 A	7,45 A	7,3 A	7,2 A
Leerlaufspannung U _{oc} :	36,9 V	36,8 V	36,5 V	36,4 V	36,3 V	36,1 V	35,9 V	35,5 V
Kurzschlussstrom I _{sc} :	8,7 A	8,6 A	8,5 A	8,3 A	8,2 A	8,1 A	8,05 A	7,8 A
Max. Systemspannung:	860 V	860 V	860 V	860 V	860 V	860 V	860 V	860 V
Modulwirkungsgrad:	14,3 %	14,0 %	13,7 %	13,4 %	13,1 %	12,8 %	12,5 %	12,2 %

Temperaturkoeffizient der Leerlaufspannung: -0,35 %/K

Temperaturkoeffizient des Kurzschlussstroms: 0,05 %/K

Temperaturkoeffizient der Leistung: -0,44 %/K

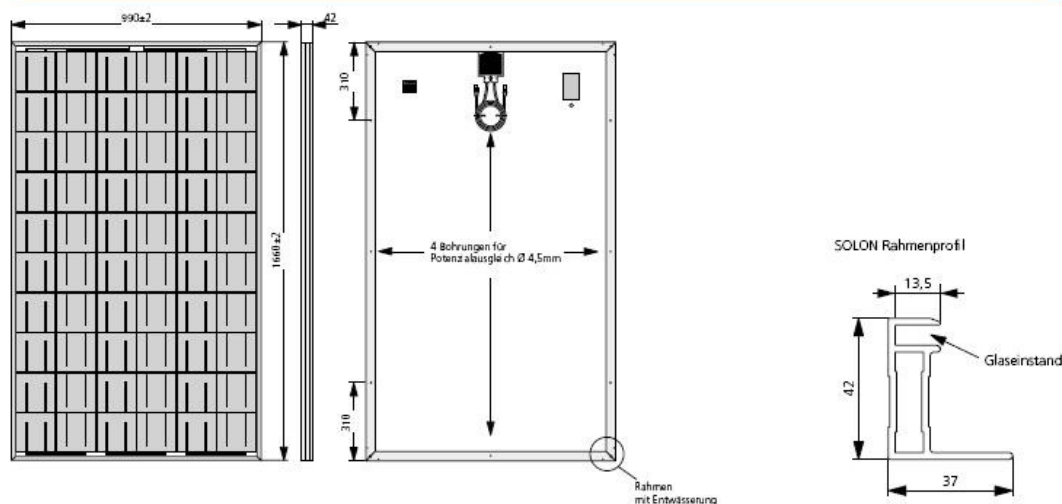
Die oben genannten Werte gelten für eine Einstrahlung von 1.000 W/m², AM 1,5 und eine Zelltemperatur von 25 °C (Standard Testbedingungen). Auf Anfrage werden die Module mit den dazugehörigen Messprotokollen ausgeliefert.

Zulässige Betriebsbedingungen

Temperaturbereich: -40 °C bis +85 °C

Hagel: bis 28 mm Korndurchmesser und 86 km/h Aufschlaggeschwindigkeit

Prüfbelastung: geprüft bis 5400 Pa nach IEC 61215 (erweiterter Test)

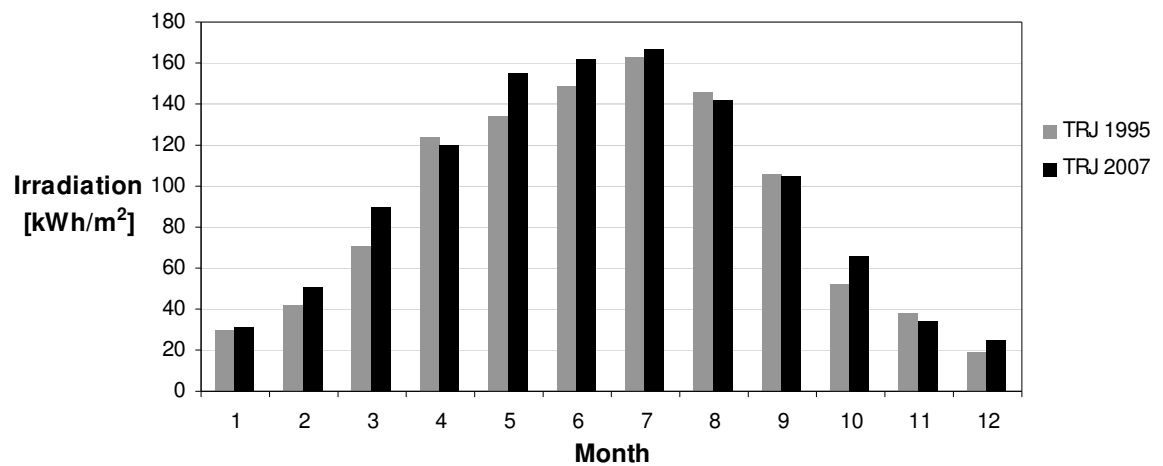


Genaue Details entnehmen Sie bitte unseren Montagehinweisen, die Sie auf unserer Homepage www.solon-pv.com finden.
Stand 11/2006. Änderungen vorbehalten, elektrische Daten ohne Gewähr

**APPENDIX B: SUMMARY OF THE RADIATION DATA USED FOR THE
SIMULATIONS**

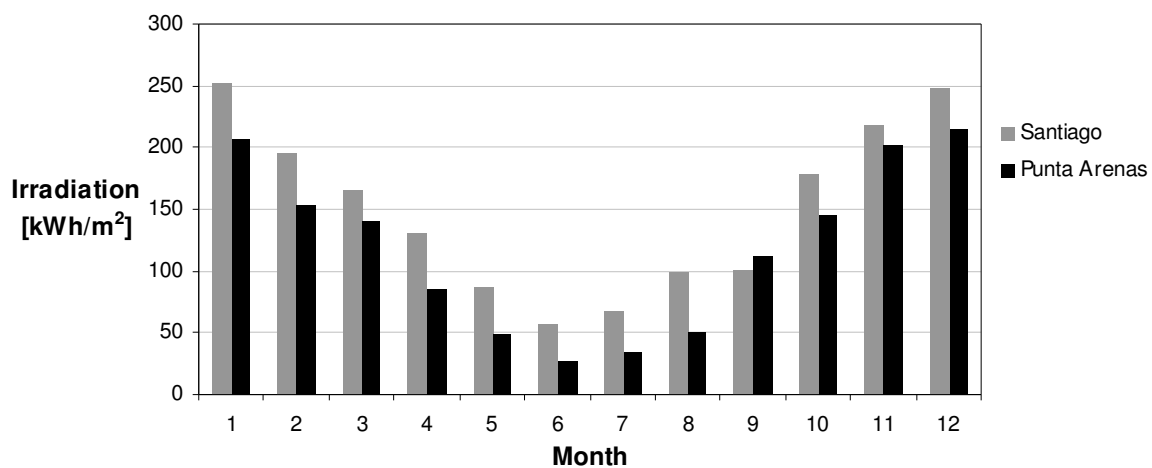
Statistical Monthly Irradiation for Munich, Germany		
	kWh/m ²	
	TRJ 1995	TRJ 2007
1	29.33	31.86
2	41.62	50.26
3	70.91	89.07
4	123.95	119.91
5	134.24	155.48
6	149.04	161.54
7	163.18	166.21
8	146.03	141.94
9	105.4	104.97
10	51.95	66.15
11	37.99	33.87
12	18.91	24.53
Total	1072.55	1145.79

Montly Irradiation for Munich



Measured Monthly Irradiation for Chilean locations, Avg. 1995-2005		
	kWh/m ²	
	Santiago	Punta Arenas
1	253.21	207.63
2	195.85	153.83
3	166.45	141.23
4	131.52	85.47
5	86.64	48.2
6	56.56	27.42
7	67.57	35.3
8	98.69	51.23
9	100.98	111.85
10	178.37	144.88
11	217.64	202.63
12	247.54	214.17
Total	1801.02	1423.84

Montly Irradiation for Chilean locations



APPENDIX C: SENSORS DESCRIPTION

Sensor	Model	Serial Nr.	Manufacturer
Pyranometer 1 (Nr. 955711)	CM11	955711	Kipp & Zonen
Pyranometer 2 (Nr. 924241)	CM11	924241	Kipp & Zonen
Pyranometer 3 (Nr. 830194)	CM11	830194	Kipp & Zonen
Pyranometer 4 (Nr. 7468)	N.A.	7468	N.A.
PV-Detector (Nr. 1211)	SOZ-03	1211	N.A.
PV-Detector (Nr. 1016)	SOZ-03	1016	N.A.
PV-Detector (Nr. 1018)	SOZ-03	1018	N.A.
PV-Detector SensorBox MW-5	N.A.	N.A.	SMA

Sensor	Calibration Factor	Sensibility original set up mV / 1000 W/m ²	Sensibility at data logger since 20.10.2008 mV / 1000 W/m ²
Pyranometer 1 (Nr. 955711)	1	5.17	
Pyranometer 2 (Nr. 924241)	0.997	4.44	
Pyranometer 3 (Nr. 830194)	1.014	4.63	
Pyranometer 4 (Nr. 7468)	Faulty	Faulty	
PV-Detector (Nr. 1211)	1.133	91.00	80.31
PV-Detector (Nr. 1016)	1.075	83.30	77.47
PV-Detector (Nr. 1018)	1.056	83.30	78.89
PV-Detector SensorBox MW-5	1.14	N.A.	

Sensor	Calibration Factor	Model
T-Sensor VIAX-module	0.734	PT100
T-Sensor VIAX-air	0.867	PT100
T-Sensor MW-5-module	1.1	PT100

APPENDIX D: SIMULATION DESCRIPTION

Simulation Blocks and Network

The main simulation blocks used in the models of this work are presented here in order to get an idea of the simulation procedure and available simulation options. The information presented here is complementary to the description of Section 3.4.2. Some information like parameters are just presented as example values.

Block READD

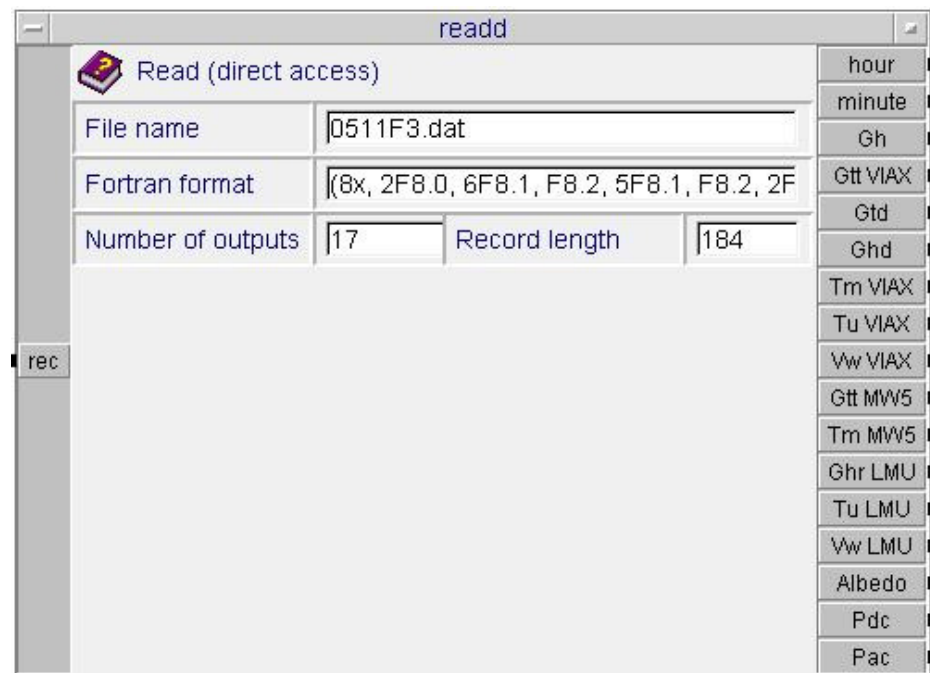


Figure D-1: The *readd* block

The *readd* block reads the information from a file with direct access. The inputs correspond to the information from the counter block of the simulation which indicates the simulation step being simulated. The outputs represented by the terminals on the left of Figure D-1 relate to the meteorological information required by the simulation model at each step. The parameters of this block relate to the reading procedure.

Block SUNAE

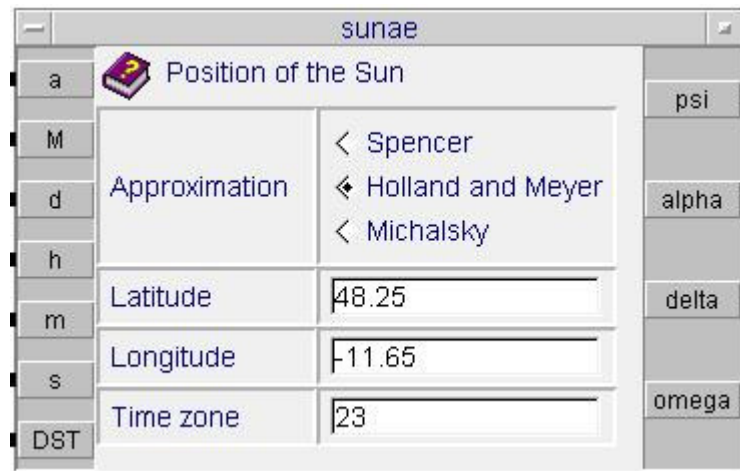


Figure D-2: The *sunae* block

The *sunae* block calculates the position of the sun in horizon and equator coordinates. The inputs correspond to data and time information. The outputs are the sun coordinates like azimuth, elevation, declination and hour angle. The parameters relate to approximations used to calculate the exact position of the sun and the location for which the desired values have to be calculated.

Block GH2GT


The *gh2gt* block calculates the radiation on a tilted surface from horizontal data. The inputs are the values for the horizontal radiation, the orientation of the surface according to sun coordinates and the calculation time. The outputs are the radiation values on the tilted surface. The parameters relate to the location of the surface and the calculation model used to convert the horizontal into tilted radiation.

Figure D-3: The *gh2gt* block

Block PVI and PVV

The *pvi* block calculates the output current and the temperature of a crystalline photovoltaic generator, depending on PV generator voltage, global radiation on the generator plane, ambient temperature, and wind speed. The parameters relate to the configuration of the PV-generator and can be seen on Figure D-4. It has to be said, that for the simulation of each different solar module type, a different *pvi* block has to be used. Other alternative is to simulate introducing all the solar module parameters required by the simulation program as shown in Figure D-5, when using the *pvv* block instead.


pvi

 SOLON P220/6+ (230 Wp) Solon Photovt

V	Cells in series per module	60	I
Gt	Cells in parallel per module	1	
Ta	Modules in series	12	Tm
	Modules in parallel	2	
Vw	NOCT temperature	45.7	
t	Initial value cell temperature	25	
Temperature mode		Tm = f(NOCT) ▾	

Figure D-4: The *pvi* block

PVV

 Photovoltaic generator voltage

Cells in series per module	36	Band gap	1.14
Cells in parallel per module	1	Short-circuit-current parameter	0.2841
Modules in series	1	Isc temperature coefficient	0.000164
Modules in parallel	1	Shockley saturation current	14589
Single cell area	0.01	Recombination saturation current	1.189
Module area	0.494	Series resistance	0.00013041
Characteristic module length	0.459	Parallel resistance	0.0899
Module mass	6.65	Shockley diode quality	1
		Recombination diode quality	2
Absorption coefficient	0.7	Bishop parameter-1	0
Emission coefficient	0.85	Bishop parameter-2	0
Specific module heat capacity	900	Bishop parameter-3	0
NOCT temperature	47		
Initial value cell temperature	25	Voltage error tolerance	0.0001
Temperature mode	Tm = ln(3) ▾	Maximum number of iterations	100
Module tolerance plus	5	Module tolerance minus	-5

Figure D-5: The *pvv* block

Block PVI and PVV

The *ivp* block simulates inverter losses. The first option is to use a block from the INSEL library containing almost all available inverters of the solar industry. The second option is to indicate the inverters efficiency using the available parameters input. Both options are shown in Figure D-6 and Figure D-7.



Figure D-6: The *ivp* block for a SB 6000 inverter

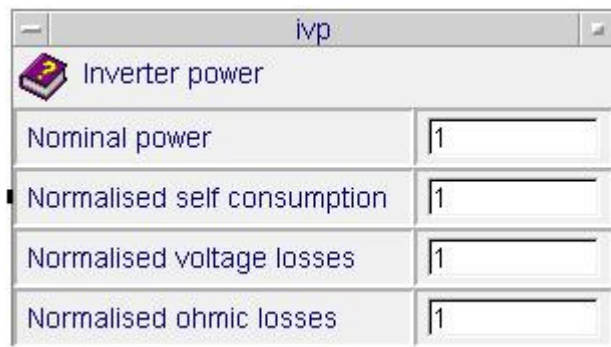
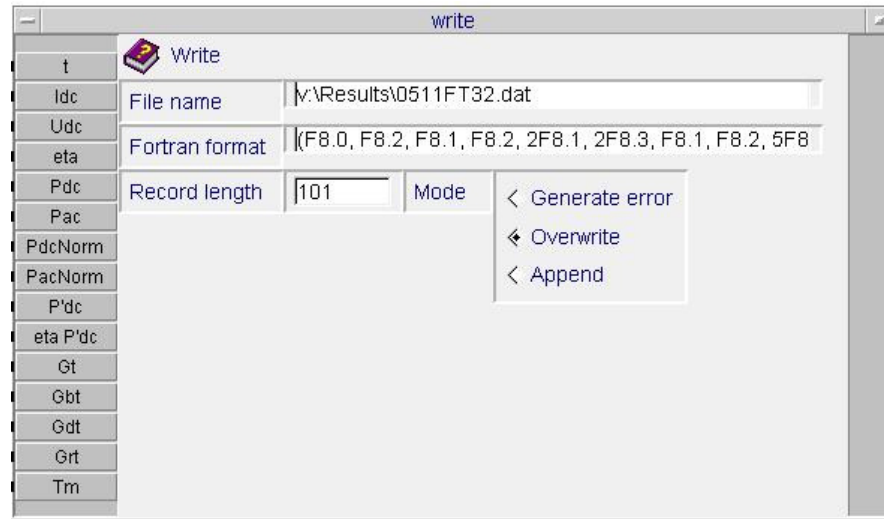


Figure D-7: The *ivp* block

Block WRITE

The *write* block writes data to a file with sequential access. The parameters are related to the file name and configuration.

Figure D-8: The *write* block

Other blocks

Other mathematical blocks are used to calculate the tracking system, the efficiency of the solar power plant, the radiation sets and more simulation details. An example of a simulation model is shown in Figure D-9.

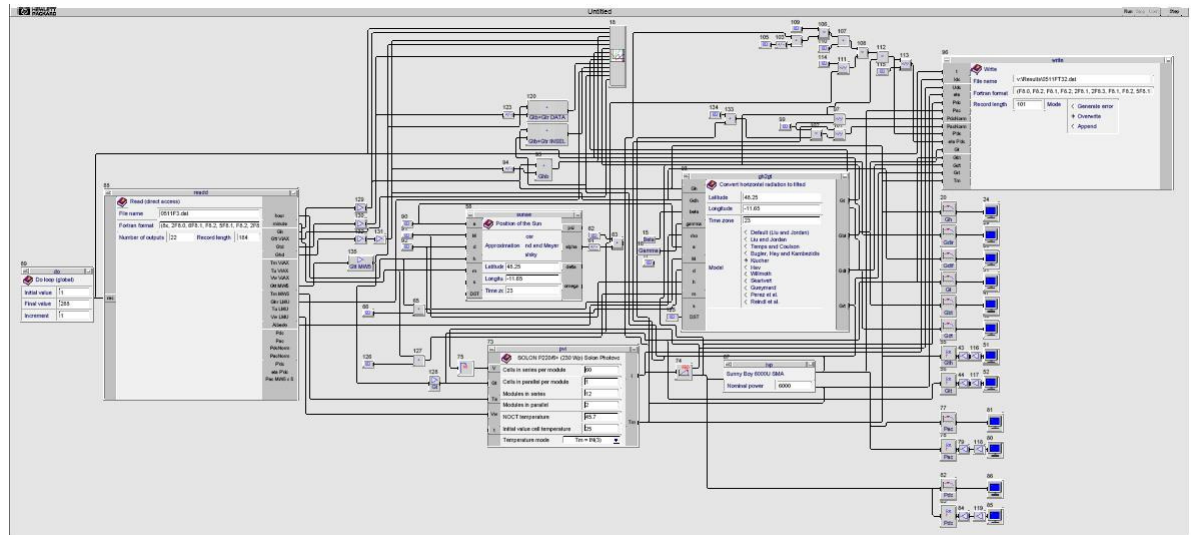


Figure D-9: Example of a simulation network

APPENDIX E: EXPERIMENTAL ASSEMBLY



Figure E-1: Radiation sensors for global tilted and diffuse tilted radiation installed at the VIAX power plant, following the sun together with the solar power panels

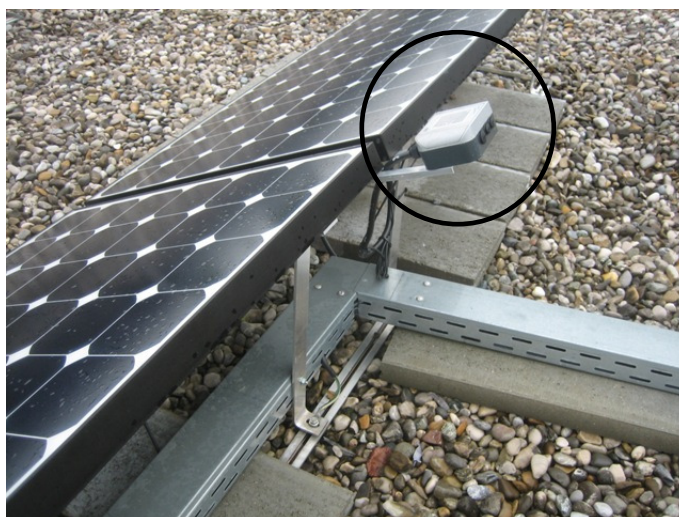


Figure E-2: Radiation sensors installed at the MW-5 power plant fixed to the solar power panels



Figure E-3: Temperature sensor installed at the back of the solar panels to measure the module temperature



Figure E-4: Wind speed and direction sensors installed at the VIAX power plant, along with the air temperature sensor protected from the sun's radiation.



Figure E-4: Radiation sensors set for calibration on an inclined surface

